

dc\_230\_11

**ANALYSIS OF TRIBOLOGICAL PHENOMENA  
IN VISCOUS FLUID FLOWS OVER SOLID SURFACES**

by  
Gabriella Vadászné Bognár



University of Miskolc  
Faculty of Mechanical Engineering and Informatics

Submitted for the degree of  
“Doctor of the Hungarian Academy of Sciences”  
Category:  
“Technical Science”

2013

## CONTENTS

<b>1</b>	INTRODUCTION	1
1.1	LUBRICATION AND MATERIALS PROCESSING . . . . .	2
1.2	THE BASIC EQUATIONS IN RECTANGULAR COORDINATE SYSTEM . . . . .	4
1.3	BOUNDARY CONDITIONS . . . . .	7
1.4	VISCOSITY VARIATION . . . . .	8
1.5	INVESTIGATIONS . . . . .	11
<b>2</b>	BOUNDARY LAYER FLOW ON A FLAT PLATE	15
2.1	NEWTONIAN FLUID FLOW . . . . .	15
2.1.1	BASIC EQUATIONS . . . . .	15
2.1.2	SIMILARITY SOLUTION . . . . .	16
2.1.3	TÖPFER TRANSFORMATION . . . . .	19
2.1.4	POWER SERIES SOLUTIONS . . . . .	20
2.2	NON-NEWTONIAN FLUID FLOW WITH CONSTANT MAIN STREAM VELOCITY . . . . .	21
2.2.1	BOUNDARY LAYER GOVERNING EQUATIONS . . . . .	22
2.2.2	TÖPFER-LIKE TRANSFORMATION . . . . .	24
2.2.3	POWER SERIES SOLUTIONS . . . . .	30
2.3	NON-NEWTONIAN FLUID FLOW DRIVEN BY POWER-LAW VE- LOCITY PROFILE . . . . .	34
2.3.1	DERIVATION OF THE PROBLEM . . . . .	35
2.3.2	ANALYTIC SOLUTIONS . . . . .	37
2.3.3	SOME SPECIAL CASES . . . . .	38
<b>3</b>	BOUNDARY LAYER FLOWS DUE TO A MOVING FLAT PLATE IN AN OTHERWISE QUIESCENT FLUID	43
3.1	NEWTONIAN FLUID FLOW . . . . .	45
3.1.1	GOVERNING EQUATIONS FOR BOUNDARY LAYERS . . . . .	45
3.1.2	EXACT SOLUTIONS . . . . .	47
3.1.3	THE EXPONENTIAL SERIES SOLUTION . . . . .	48
3.2	NON-NEWTONIAN FLUID FLOW . . . . .	51
3.2.1	BOUNDARY LAYER EQUATIONS . . . . .	52
3.2.2	SIMILARITY SOLUTION . . . . .	52
3.2.3	NUMERICAL RESULTS . . . . .	53

<b>4</b>	<b>BOUNDARY LAYER FLOWS ON A MOVING SURFACE</b>	<b>55</b>
4.1	NEWTONIAN FLUID FLOW . . . . .	55
4.2	NON-NEWTONIAN FLUID FLOW . . . . .	56
4.2.1	BOUNDARY LAYER EQUATION . . . . .	56
4.2.2	PROPERTIES OF THE SOLUTION $g$ . . . . .	65
4.2.3	UPPER BOUND ON $\lambda_c$ . . . . .	66
4.2.4	THE ANALYTIC SOLUTION . . . . .	68
4.3	COMPARISON OF SIMILARITY SOLUTIONS WITH NUMERICAL SOLUTIONS . . . . .	68
<b>5</b>	<b>SIMILARITY SOLUTIONS TO HYDRODYNAMIC AND THERMAL BOUNDARY LAYER</b>	<b>75</b>
5.1	MARANGONI EFFECT . . . . .	75
5.1.1	BOUNDARY LAYER EQUATIONS . . . . .	77
5.1.2	EXPONENTIAL SERIES SOLUTION . . . . .	79
5.2	CONVECTIVE BOUNDARY CONDITION . . . . .	90
5.2.1	BASIC EQUATIONS . . . . .	91
5.2.2	NUMERICAL RESULTS . . . . .	94
<b>6</b>	<b>CONCLUSIONS</b>	<b>98</b>
<b>7</b>	<b>ACKNOWLEDGEMENT</b>	<b>102</b>
	<b>BIBLIOGRAPHY</b>	<b>103</b>

## List of Abbreviations

$a, b, d$	.....	constants
$a_i$	.....	coefficients of the power series $i = 0, 1, 2, \dots$
$\bar{a}$	.....	constant defined by (5.38)
$A, B$	.....	constants defined by (2.8)
$\bar{A}$	.....	temperature gradient coefficient
$A_i, B_i$	.....	coefficients of the exponential series $i = 0, 1, 2, \dots$
$\tilde{A}, \tilde{B}$	.....	constants for the power-law velocity profile
$C_{D,\tau}$	.....	non-dimensional drag coefficient
$f$	.....	dimensionless stream function defined by (2.8)
$f_w$	.....	transpiration rate at the surface
$F, G$	.....	functions
$h_f$	.....	heat transfer coefficient defined in (5.28)
$k$	.....	fluid thermal conductivity
$K$	.....	consistency index in the power-law model (1.11)
$L$	.....	characteristic length
$m$	.....	parameter relating to the power-law exponent
$M$	.....	constant defined by (2.55)
$n$	.....	power-law exponent in the power-law model (1.11)
Pr	.....	the Prandtl number
Re	.....	the Reynolds number
$Re_x$	.....	local Reynolds number
$T$	.....	temperature across the boundary layer
$T_f$	.....	fluid temperature at the bottom of the surface
$T_w$	.....	temperature at the surface
$T_\infty$	.....	temperature across the boundary layer
$x$	.....	distance along the surface from the leading edge
$y$	.....	distance normal to the surface
$u$	.....	dimensionless velocity component along $x$ direction
$v$	.....	dimensionless velocity component along $y$ direction
$U_e$	.....	power-law velocity profile
$U_\infty$	.....	uniform main stream velocity
$U_w$	.....	wall velocity
$v_w$	.....	mass transfer velocity
$Z$	.....	variable

**Greek symbols**

$\alpha_t$	.....	thermal diffusivity defined by (5.35)
$\alpha, \beta$	.....	constants
$\gamma$	.....	curvature of $f$ at the origin $f''(0)$
$\delta$	.....	power index
$\delta_{bl}$	.....	boundary layer thickness
$\epsilon$	.....	parameter defined in (2.30)
$\eta$	.....	dimensionless similarity variable
$\eta_c$	.....	radius of convergence
$\lambda$	.....	velocity ratio
$\lambda_c$	.....	critical velocity parameter
$\kappa$	.....	parameter defined in (2.30)
$\Theta$	.....	dimensionless temperature
$\mu$	.....	dynamic viscosity
$\mu_c$	.....	kinematic viscosity defined in (2.7)
$\mu_{cn}$	.....	defined in (2.20)
$\nu$	.....	kinematic viscosity
$\rho$	.....	fluid density
$\sigma$	.....	power exponent
$\bar{\sigma}$	.....	surface tension
$\sigma_T$	.....	derivative of surface tension with respect to temperature
$\tau_{..}$	.....	components of the stress tensor
$\tau_w$	.....	wall shear stress
$\phi$	.....	function
$\psi$	.....	stream function
$\omega$	.....	positive parameter
$\Phi, \Psi, \Omega$	.....	functions

## 1 INTRODUCTION

In the 1800s, applying the basic principles of mass conservation and Newton's second law, Leonhard Euler described the fluid flow in terms of spatially varying three-dimensional pressure and velocity fields by two coupled nonlinear partial differential equations. Euler did not account for the effect of friction acting on the motion of the fluid elements. In 1822 Claude-Louis Navier [158] and independently in 1845 George Stokes [192] took the viscous forces into considerations and derived the mathematical description of a viscous fluid flow by a system of more complex nonlinear partial differential equations called Navier-Stokes equations. No one has given a general analytic solution to them. In 1904 Ludwig Prandtl introduced the concept of the boundary layer in a fluid flow. From that time the modern aerodynamics and fluid dynamics have been dominated by Prandtl's idea. Prandtl has given the first description of the *boundary layer* concept in his paper [168] entitled "Über Flüssigkeitsbewegung bei sehr kleiner Reibung" ("On the motion of fluids with very little friction"). In his theory an effect of friction was to cause the fluid adjacent to the solid surface to stick to the solid surface of the body submerged in the fluid flow (i.e., no-slip condition at the surface) and the frictional effect was experienced in a thin region near the surface. That boundary layer is very thin in comparison with the size of the body of the object. Prandtl concluded that if the viscosity is small, the velocity changes substantially in a very short distance normal to the solid surface. Within the boundary layer the velocity gradient is very large. With the Newton's shear-stress law (i.e. the shear stress is proportional to the velocity gradient and viscosity) the local shear stress can also be very large. Near the solid surface in the thin boundary layer the friction is dominant while in the outer inviscid flow external to the boundary layer the friction is negligible. The outer flow generates the boundary conditions at the edge of the layer.

With Prandtl's idea it became available to reduce the Navier-Stokes equations to differential equations of simpler form called boundary layer equations [13]. While the Navier-Stokes equations are elliptic and the complete flow field must be solved simultaneously, the boundary layer equations are parabolic for which simplifications are available (see e.g., [10], [13], [74], [76], [177], [178]). In 1908 Heinrich Blasius [30] gave solutions for two-dimensional boundary layer flows over a flat plate and a circular cylinder. For constant pressure along the flat plate oriented parallel to the flow, the coupled nonlinear partial differential equations were reduced to a nonlinear ordinary differential equation called Blasius equation [30].

In 1921 von Kármán [119] and Pohlhausen [165] provided an approximate method, which has been used with considerable success for the analysis of

boundary layer flows. The method is based on an integral formulation of the problem and its result, the calculated flow field, usually satisfies the equations of continuity and momentum. The boundary conditions for the flow are expanded to polynomial functions as an approach for the velocity profiles in the laminar boundary layer.

Exact solutions to problems involving the motion of fluids are very difficult, or even impossible to obtain, even when the geometry is simple and the fluid's physical properties are constant. Numerical solutions are usually good options but, when an analytical description is required, approximate methods of formulation and solution are often useful.

## 1.1 LUBRICATION AND MATERIALS PROCESSING

Lubrication, spreading, polymer coating and processing, and thin film casting are important applications of the flow near a solid wall in engineering. Computational analysis of flow near solid surfaces is performed to complement the experimental observations. The advantage of the theoretical investigations over experiments is that one can control the conditions and parameters in the analyzed problem to predict velocity profiles and shear stress, and it can be used also for assessing the error of numerical simulations of the problem.

The first paper on fluid-film lubrication of journal bearings was published in 1883. The hydrodynamic effect has been shown experimentally by Tower [204]. In 1886, Reynolds developed on the base of Tower's results his theory of hydrodynamic lubrication by assuming the fluid as viscous and Newtonian. However, in real situations, non-Newtonian fluids are used in order to increase the viscosity of the lubricants by adding additives to base oils. The addition of polymers to mineral oils has spread in practice [198], [24]. To predict the mechanical behavior of these lubricants is much more complicated than of mineral oil lubricants which are considered Newtonian fluids. The resulting lubricants, e.g., silicone fluids and polymer solutions are described by non-Newtonian power-law model due to the model's simplicity ([154], [181], [182], [183], [184]). The non-Newtonian lubricants are encountered in various processes of lubrication. Recently, considerable effect has been expanded for solving problems in tribology regarding the non-Newtonian influence on lubrication flow characteristics of squeeze films ([154], [181], [182]), externally pressured bearings ([183], [184]), journal bearings ([198], [173], [211]) and roller bearings ([186], [187]).

Because of the importance of tribology and materials processing, considerable research effort has been directed at the transport phenomena in such processes in recent years. Many books are available on the area of lubrication, manufacturing and materials processing (see e.g., [9], [75], [87], [108], [126],

[149], [145], [195], [196], [198]). Fluids engineering research can impact on the field of tribology and materials processing only if significant effort is also directed at understanding the basic mechanisms. In the last four decades the demand in materials processing of composites, ceramics and advanced polymers has been increasing.

An intense research of fluid flow mechanism arising in many materials processing applications is necessitated to improve product quality, reduce costs and achieve custom-made material properties. Fluid flow appears in a lot of material processing operations e.g., in crystal growth for semiconductor fabrication, polymer extrusion, casting or continuous processing of thin films. Due to the importance of fluid flow in materials processing, extensive research is being done in this field. Jaluria [117] gave a review on the main aspects that must be considered in material processing, on the fluid flow phenomena involved in different areas, such as drying, heat treatments, metal forming, casting, crystal growing, polymer extrusion, food processing, coating and microgravity materials processing. He emphasized that relatively little information can be found in the literature on the link between the diverse processing techniques and the basic mechanisms of the govern flow; and the quantitative dependence of the product quality on the fluid flow. Fluid flow properties are important in many manufacturing processes as they effect on the transport mechanisms, on the impurities and defects, on the time spent by the material in the system, on the properties and characteristics of the final product and on the product quality [209]. It is important to understand the basic flow mechanisms involved in these processes so that high quality coatings can be achieved at relatively large speeds of the coated material (see Kistler and Schweizer [122] ). The casting processes have been reviewed by Ruschak [172]. Weinstein and Ruschak [209] have pointed out that predictive analysis is usually not available for the coating methods. Therefore, it is advantageous to describe the mechanical details for the fluid flow components and then combine this knowledge for the applications. The main interest is the achievable coating thickness and the uniformity, the attainable speed together with the rheological requirements.

The production and use of polymers have grown increasingly. The extrusion process is one of the most important polymer processing techniques today. The extruders produce a tremendous variety of products. For example, in the plasticating extruder the solid polymer is melted, homogenized and pumped through the die at high pressure and temperature (see and [27], [87], [149], [153]).

The processing of sheet-like materials is a necessary operation in the production of paper, linoleum, polymeric sheets, roofing shingles, insulating materials, and fine-fiber matts. Virtually, in all such processing operations,

the sheet moves parallel to its own plane [9]. The moving sheet may induce motion in the neighboring fluid or, alternatively, the fluid may have an independent forced-convection motion that is parallel to that of the sheet.

## 1.2 THE BASIC EQUATIONS IN RECTANGULAR COORDINATE SYSTEM

We shall consider laminar fluid flows with constant density  $\rho$  over a thin flat plate in a uniform stream with velocity  $U_\infty$ . The kinematic and dynamic viscosity are denoted by  $\nu$  and  $\mu$ , respectively. Consider the plate of length  $L$ . We assume that the Reynolds number  $Re = \rho U_\infty L / \mu$  expressing the quotient from inertial and viscous forces is small, the flows considered in this study are laminar. The fluid flows in parallel layers next to the solid surface.

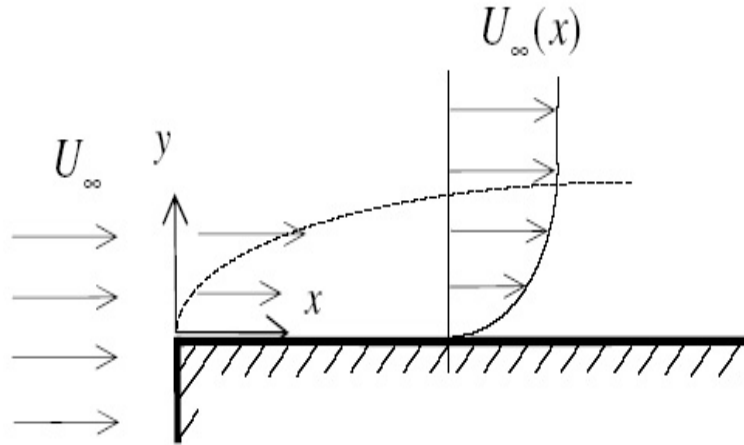


Fig. 1.1 Boundary layer flow along a plate

The  $x > 0$  and  $y > 0$  are the Cartesian coordinates along and normal to the plate with  $y = 0$  is the plate and the coordinate  $x$  is as taken positive in the direction of the mainstream. The plate origin is located at  $x = y = 0$ , and  $u, v$  represent the components of the fluid velocity in the direction of increasing  $x$  and  $y$ , respectively (see Fig. 1.3).

The governing equations for fluid flow and the associated heat transfer in materials processing are derived from the basic conservation principles for mass, momentum and energy. *The continuity equation* for an incompressible fluid can be formulated as

$$(1.1) \quad \frac{\partial u}{\partial x} + \frac{\partial v}{\partial y} = 0.$$

The equation of motion is a vectorial equation. For steady, a two-dimensional fluid flow it can be formulated under the assumptions that the flow is independent of time, laminar and the gravity forces are neglected [26], [149], [210]:

$$(1.2) \quad \rho \left( u \frac{\partial u}{\partial x} + v \frac{\partial u}{\partial y} \right) = -\frac{\partial p}{\partial x} + \left( \frac{\partial \tau_{xx}}{\partial x} + \frac{\partial \tau_{yx}}{\partial y} \right),$$

$$(1.3) \quad \rho \left( u \frac{\partial v}{\partial x} + v \frac{\partial v}{\partial y} \right) = -\frac{\partial p}{\partial y} + \left( \frac{\partial \tau_{xy}}{\partial x} + \frac{\partial \tau_{yy}}{\partial y} \right),$$

where  $\tau_{xx}$ ,  $\tau_{yy}$ ,  $\tau_{xy}$ ,  $\tau_{yx}$  are the components of the stress tensor.

Taking into consideration the components of the stress tensor in rectangular coordinates [26] equations (1.2) and (1.3) are reduced to

$$(1.4) \quad \rho \left( u \frac{\partial u}{\partial x} + v \frac{\partial u}{\partial y} \right) = -\frac{\partial p}{\partial x} + 2 \frac{\partial}{\partial x} \left[ \mu \left( \frac{\partial u}{\partial x} \right) \right] + \frac{\partial}{\partial y} \left[ \mu \left( \frac{\partial u}{\partial y} + \frac{\partial v}{\partial x} \right) \right],$$

$$(1.5) \quad \rho \left( u \frac{\partial v}{\partial x} + v \frac{\partial v}{\partial y} \right) = -\frac{\partial p}{\partial y} + \frac{\partial}{\partial x} \left[ \mu \left( \frac{\partial u}{\partial y} + \frac{\partial v}{\partial x} \right) \right] + 2 \frac{\partial}{\partial y} \left[ \mu \left( \frac{\partial v}{\partial y} \right) \right],$$

where  $\mu$  denotes dynamic viscosity.

The velocity in the boundary layer increases until it reaches the outer flow velocity  $U_\infty$ . As all fluid flows must be zero at a solid boundary, the velocity must increase rapidly to  $U_\infty$  in a boundary layer. The region of velocity change is called a hydrodynamic boundary layer. The boundary layer thickness  $\delta_{bl}$  is defined as the distance required for the flow to reach  $U_\infty$ .

Prandtl's boundary layer theory applies to flows where there are extensive inviscid regions separated by thin shear layers of boundary layer thickness  $\delta_{bl} \ll L$ . It is satisfied if  $Re \gg 1$ . Except this close neighborhood of the solid surface, the flow velocity is comparable to the free stream velocity  $U_\infty$ . Outside the boundary layer the velocity gradients are negligibly small and the influence of the viscosity is unimportant. In the flow of the region near the solid surface there is friction. In the normal direction  $y$  inside the thin layer the gradient  $\partial u / \partial y$  is very large compared with gradients in the streamwise direction  $\partial u / \partial x$ . Although the viscosity was meant to be very small in this flow, the shear stress can be large. For steady flows the approximations used by Prandtl (1904) in deriving the boundary layer equations are the following:

$$Re \gg 1, \quad \delta_{bl} \ll L, \quad v \ll u, \quad \partial u / \partial x \ll \partial u / \partial y, \quad \partial v / \partial x \ll \partial v / \partial y.$$

moreover,  $\partial p / \partial y \approx 0$ , then  $p = p(x)$  only, and if the free stream outside the boundary layer is  $U_\infty(x)$ , then

$$\frac{\partial p}{\partial x} = -\rho U_\infty \frac{dU_\infty}{dx}.$$

Within the framework of these assumptions the governing equations of motion (1.2) and (1.3) for a flow of constant property fluid neglecting the buoyancy and the body forces can be substituted by ([171], [178], [225]):

$$(1.6) \quad \rho \left( u \frac{\partial u}{\partial x} + v \frac{\partial u}{\partial y} \right) = \rho U_\infty \frac{dU_\infty}{dx} + \frac{\partial \tau_{yx}}{\partial y}.$$

If the temperature of the wall is different from that of the free stream, there is a thermal boundary layer thickness different from the flow boundary layer thickness. To predict the temperature variation we need an equation for the temperature field in the boundary layer.

*The equation of energy* for a steady two-dimensional boundary layer without heat sources in rectangular coordinates takes the form ([171], [178], [201], [202], [225]):

$$(1.7) \quad u \frac{\partial T}{\partial x} + v \frac{\partial T}{\partial y} = \frac{\partial}{\partial y} \left( \alpha_t \frac{\partial T}{\partial y} \right),$$

where  $T$  is the temperature of the fluid in the boundary layer and  $\alpha_t$  is the thermal diffusivity. Equation (1.7) includes the following approximations

- i.) the pressure variations in the flow are not enough to affect the thermodynamic properties,
- ii.) the viscous stresses do not dissipate enough energy to warm the fluid significantly and
- iii.) in the boundary layer  $\partial^2 T / \partial x^2 \ll \partial^2 T / \partial y^2$ .

It should be noted that the boundary layer equations are not exact but are asymptotic forms of the basic hydrodynamic equations when the Reynolds number is large. The experimental flows at large Reynolds numbers are turbulent, yet useful comparisons with laminar flow experiments at moderate large Reynolds numbers can sometimes be made with large Reynolds number asymptotic theories [71]. We restrict ourself for studying only the laminar boundary layer flow.

In the following sections we study the possibility of reducing the system of equations (1.1), (1.6) and (1.7) to ordinary differential equations by similarity transformation. The term "similarity solution" in fluid mechanics was first introduced by Blasius [30] when he found a solution to a problem of Prandtl's boundary layer theory. Generally, a *similarity solution* is one in which the number of variables can be reduced by some analytical techniques, e.g. by a coordinate transformation. The theory of similarity in physical problems has been investigated in several books from mathematical approaches by Ames [10], or from physical viewpoint by Sedov [180] and Hansen [99].

The similarity method is a technique which reduces a set of partial differential equations into ordinary differential equation(s) involving only a single

variable. A systematic approach to provide solutions to partial differential equations by the solution of ordinary differential equations which were obtained by special transformations of the dependent/independent variables. It is the use of specific combinations of variables which enables a conversion of the partial differential equation to an ordinary differential equation.

Similarity analysis is applicable to certain problems in which the characteristic lengths are determined by rate processes rather than by the geometric or physical dimensions. Such problems generally involve regions which are regarded as being semi-infinite. The field variable of velocity attained through similarity method has profiles which are identical in shape for all positions or times, differing only by the scale over which the variations occur and described by a variable of similarity. The benefit of the similarity analysis is that a set of partial differential equations can be reduced to ordinary differential equations. This mathematical gain is accompanied by a loss in generality. Similarity solutions are limited to certain geometries and certain boundary conditions.

In sum, a primary advantage of the similarity method is that it is one of the few general techniques for obtaining exact (nonlinear) solutions of partial differential equations. A primary disadvantage of the similarity method is that the solution found may satisfy only a very restricted set of initial and boundary conditions.

### 1.3 BOUNDARY CONDITIONS

We must specify the boundary conditions to the set of differential equations (1.1), (1.6) and (1.7). Many of the boundary conditions are the usual no-slip conditions for velocity and the appropriate thermal or mass transfer conditions at the boundaries. In general, boundary conditions are divided into three types: initial conditions, surface boundary conditions and field boundary conditions.

*Initial conditions* are specified at an initial position on the surfaces, e.g. at the leading edge of a semi-infinite flat plate.

*Surface boundary conditions* are specified at the solid surface of the body. Usually, it gives conditions on the velocity components and on the temperature or heat transfer rate at the surface. The no-slip condition means that the velocity of the fluid at the solid surface is assumed equal to the velocity of the surface. Similarly, the temperature of the fluid at the solid surface is assumed equal to the surface temperature. Instead of giving the temperature at the surface, the heat transfer rate can also be given, i.e., the temperature gradient at the solid surface can be specified. Surface tension effects are important in many materials processing flows. Examples include flows in

welding, Czochralski and the floating-zone crystal growing methods, wave soldering, and continuous casting. Surface tension can also have a significant effect on the flow near the free surface. Large surface tension gradients can arise along the interface due to temperature and concentration gradients. Such surface tension gradients can generate significant shear stresses and resulting flow along the interface. This flow, known as thermocapillary or Marangoni convection, is important in many material processing flows [126]. Furthermore, the mass flow rate through the surface can be specified. If the mass flow rate through the surface is zero the velocity component normal to the surface is zero. Positive mass flow rates are referred to as blowing or injection and negative mass flow rates as suction.

The *field boundary conditions* are given at some point in the flow field usually at a large distance from the surface. The velocity components and/or thermodynamic variables can be required to approach a constant or some specific functional form.

#### 1.4 VISCOSITY VARIATION

The properties of the material undergoing thermal processing play a very important role in the mathematical and numerical modeling of the process.

The variation of dynamic viscosity  $\mu$  requires special consideration for materials such as lubricants, plastics, polymers, food materials and several oils, that are of interest in a variety of manufacturing processes. Most of these materials are non-Newtonian in behavior, implying that the shear stress is not proportional to the shear rate. The viscosity  $\mu$  is a function of the shear rate. For Newtonian fluids like air and water, the viscosity is independent of the shear rate, but increases or decreases with the shear rate for shear thickening or thinning fluids, respectively. These are viscoelastic fluids, which may be time-independent or time-dependent.

The mechanical behavior of a material and its mechanical or rheological properties can be characterized in terms how the shear stress and shear rate are related. If the properties of the fluid are such that the shear stress and shear rate are proportional, the material is known as a *Newtonian fluid*. This relationship in the boundary layer is expressed by

$$(1.8) \quad \tau_{yx} = \mu \frac{\partial u}{\partial y}$$

called Newton's law of viscosity. For materials which do not obey this law, i.e., the shear stress and shear rate are not directly proportional but are related by some function, the fluid is called non-Newtonian [213]. Many of industrial liquids show non-Newtonian behavior, see for example [22],

[27]-[29], [213]. The physical origin of a non-Newtonian behavior relates to the microstructure of the material. Materials such as slurries, pastes, gels, drilling mud, paints, foams, polymer melts or solutions are examples of non-Newtonian fluids. For such fluids the viscosity is not constant, it is a function of either the shear rate or the shear stress.

Many papers have concentrated on the prediction of rheological properties under shear using molecular dynamics computations ([89], [90], [226]). The observations of these simulations greatly assist us in understanding the behavior of lubricant properties. Various models are employed to represent the viscous or rheological behavior of fluids of practical interest. Frequently, the fluid is treated with the non-Newtonian viscosity function given in terms of the shear rate.

A chief difficulty in the theoretical study of non-Newtonian fluid mechanics is to define this relationship. The apparent viscosity  $\mu_{app}$  is the ratio of shear stress and shear rate, then

$$\tau_{yx} = \mu_{app} \frac{\partial u}{\partial y}$$

holds. We shall investigate boundary layer problems for non-Newtonian fluids whose apparent viscosity depends only on the rate of strain. The actual mathematical form of  $\mu_{app}$  for these materials will depend on the nature of the particular material. The flow behavior of fluids determined by their rheological properties is described by the relationship between the shear stress and shear rate. This relationship is determined experimentally. The time-independent viscoelastic fluids are often represented by

$$(1.9) \quad \mu_{app} = K \phi \left( \frac{\partial u}{\partial y} \right),$$

where  $\phi$  is an empirically determined function.

The most common flow model is the so-called power-law model or the Ostwald-de Waele power-law model, given by [195]. Throughout this work we apply this model when the flow behavior of the non-Newtonian fluid is described by

$$(1.10) \quad \mu_{app} = K \left| \frac{\partial u}{\partial y} \right|^{n-1}.$$

This provides an adequate representation of many non-Newtonian fluids over the most important range of shear. The shear stress is related to the strain rate  $\partial u/\partial y$  by the expression

$$(1.11) \quad \tau_{yx} = K \left| \frac{\partial u}{\partial y} \right|^{n-1} \frac{\partial u}{\partial y},$$

where  $K$  and  $n > 0$  are a positive constants called consistency and power-law index, respectively, and defined by Bird [26]. The case  $0 < n < 1$  corresponds to pseudoplastic fluids (or shear-thinning fluids), the case  $n > 1$  is known as dilatant or shear-thickening fluids. For  $n = 1$ , one recovers a Newtonian fluid. The deviation of  $n$  from a unity indicates the degree of deviation from Newtonian behavior [13].

It should be noted that without the above boundary layer simplifications the dynamic viscosity  $\mu$  in (1.4) and (1.5) for power-law fluids is calculated by the following relationship

$$(1.12) \quad \mu = K \left\{ 2 \left[ \left( \frac{\partial u}{\partial x} \right)^2 + \left( \frac{\partial v}{\partial y} \right)^2 \right] + \left( \frac{\partial u}{\partial y} + \frac{\partial v}{\partial x} \right)^2 \right\}^{(n-1)/2}.$$

The two-parameter relations (1.11) or (1.12) have been useful in fitting rheological data for a large variety of fluids (see [153], [179]). Parameters  $K$  and  $n$  are determined empirically. Relation (1.11) may fail to fit the total range of experimental data for some materials. However, the formula can be fitted well to measured data over a restricted range of shear rate. The properties of the material undergoing thermal processing must be known and appropriately modeled to accurately predict the resulting flow and transport, as well as the characteristics of the final product. Some of the values of  $n$  are shown in Table 1.1 ([57], [63], [161]). In process industries most non-Newtonian fluids are pseudoplastic ( $n < 1$ ).

The "functionalization" of solid and fluid materials by addition of chemical compound is a process that is going back to Maxwell [147], [148] and Rayleigh [170]. The effective viscosity was characterized by Einstein [80], [81]. Due to measurements for crude oil and experiments with various liquids ranging from simple molecular liquids to polymer melts it was shown that the apparent viscosity dependent on the shear rate. On the base of measurements the authors observed for the apparent viscosity a power law of the form (1.10). The dependence of the power  $n$  on many factors (e.g. the pressure, the temperature and the film thickness) was confirmed by simulations ([2], [133], [134], [79]). Application of molecular dynamics to rheology has helped to understand the behavior of non-Newtonian fluids to predict quantitative rheological properties such as the viscosity of lubricants [116]. Some lubricants, e.g. silicone fluids and polymer solutions are described by the non-Newtonian power-law model due to the model's simplicity (see [154], [181], [182], [183], [184]).

<b>Material</b>	$n$
clay suspension	0.1
suspensions (kaolin in water, bentonite in water)	$\approx 0.1-0.15$
cosmetic cream	$\approx 0.1-0.4$
toothpaste	0.3
molten polymers	$\approx 0.3-0.7$
drilling fluid (oil based mud), paper pulp, latex paint	$\approx 0.4-0.6$
lubricants	$\approx 0.4-1.1$
water, glycerin	1
slurry (sand-water mixture)	$\approx 1.1-1.4$
saturated honey	$\approx 1.5$

**Table 1.1**

Thompson et al. [199] showed that at high shear rates the viscosity of glassy films obeys a power law in the form (1.10) with  $n = 2/3$ . In [41] and [52] the power exponent  $n$  was determined for a polyethylene and  $n \approx 0.3$  was obtained in the range of temperature  $160^\circ\text{C}-180^\circ\text{C}$ . It was shown that both  $K$  and  $n$  depend on the temperature. In case of sand-bentonite-water mixtures for different sand volumetric concentrations the experiments gave  $n \approx 1.4$  and here the rheological parameters  $K$ ,  $n$  do depend on the volumetric concentration [49].

For simplicity, in our calculations we assume that the power-law exponent  $n$  and the consistency  $K$  are constants. Even if the main advantage of the power-law model is its relative simplicity, the non-Newtonian behavior of the material complicates the viscous terms in the momentum equation.

**Remark.** Due to the wide range of applications a large number of articles has been devoted to different mathematical aspects of the so-called  $p$ -Laplacian operator  $\Delta_p u = \nabla(|\nabla u|^{p-2} \nabla u)$ . Here, instead  $n$  the  $p$  parameter is applied. On the mathematical examinations of the solutions to the equations involving  $\Delta_p$  we mention the book by Dořlý and Rehák [77], Drábek and Milota [78] and also some of my papers [31]-[37]. That type of nonlinearity appears also in nonlinear diffusion equations arising from a variety of diffusion phenomena ([36], [216]).

## 1.5 INVESTIGATIONS

Analytical and numerical techniques can be applied to investigate flow characteristics and how the fluid flow affects the process and the product. In general, predictive modeling of complex processes is not yet known. The practice remains largely empirical. However, physical insights and mathematical models are greatly beneficial to explore the effect of the fluid flow on

the lubricated machine elements or on the final product. Due to the practical necessity, it is important to study the influence of the viscosity on the lubrication velocity and temperature fields. Within the thin boundary layer, the wall shear stress and the friction drag of the solid surface can also be estimated. It is important to understand the fluid flow mechanisms determined by the governing equations and boundary conditions along with important parameters to minimize and control their effects.

Due to the complexity of the governing equations and boundary conditions that analytical methods can be used to obtain the solution in very few practical circumstances. However, numerical approaches are extensively used to obtain the flow characteristics, analytical solutions are very valuable since they can be used for verifying numerical models, they provide information about the basic mechanisms and give quantitative results for some components. Analytical solutions can be obtained for simplified and idealized models of certain processes.

The main topic of this dissertation is to introduce, review and discuss several models which can be investigated by similarity analysis. Our results are given for some boundary layer problems of Newtonian or non-Newtonian fluid flows over horizontal solid surfaces.

In Section 2.1, the boundary layer problem for an idealized Newtonian viscous fluid past a semi-infinite flat plate is one of the best known problems in fluid mechanics, as its first analytic solution for the laminar case dates back to the beginning of the last century with Blasius [30]. The classic book by Schlichting and Gersten [177] describes the similarity approach of Newtonian fluid flow problem called the Blasius problem. The similarity solution and Töpfer's transformation [203] are reviewed.

The first analysis of the boundary-layer equations for a power-law fluid is due to Schowalter [179] and Acrivos et al. [4] in 1960. In Section 2.2, we deal with the analysis of similarity solutions of the two-dimensional boundary layer flow of a power-law non-Newtonian fluid past a semi-infinite flat plate. The boundary value problem of the momentum equation is converted into initial value problem by applying proper similarity variables and the partial differential equations are transformed into the so called generalized Blasius equation. For this we apply a Töpfer-like transformation to determine the dimensionless wall gradient numerically. The power series expansion of the solution is also presented for  $n > 0$  ([38], [47]).

In Section 2.3, the similarity solutions to the Prandtl boundary layer equations describing a non-Newtonian power law fluid past an impermeable flat plate, driven by a power law velocity profile  $U_e = \tilde{B}y^\sigma$  ( $\tilde{B} > 0$ ) are investigated. We give that there are analytical solutions for any  $n > 0$ ,  $n \neq 2$  and any  $-1/2 \leq \sigma < 0$  and examine the effect of parameters  $\sigma$ , and  $n$  on the

velocity profiles [46].

Boundary layer behavior on a moving continuous solid surface occurs in a number of materials processes, an example is a polymer sheet or filament extruded continuously from a die. The flow behavior was theoretically studied by Sakiadis [175] and experimentally by Tsou et al. [205]. Since some polymers are flexible materials, the filament surface may stretch during the production and therefore the surface velocity deviates from being uniform. Sakiadis studied the flow induced by the uniform motion of a continuous solid surface. Crane [72] gave an exact boundary layer solution, which is an exact solution of the Navier-Stokes equations, for continuous sheet when the sheet velocity is proportional to distance from the extrusion origin. In Section 3.1, the boundary layer equations are considered for two-dimensional boundary layer flows of Newtonian fluids over a moving flat surface moving at a speed of  $U_w(x)$  in an otherwise quiescent Newtonian fluid medium. We give a generalization of Crane's solution for stretching wall with power law stretching velocity [43]. The shear stress at the solid surface and the interval of convergence are also discussed.

A technologically important source of the boundary layer phenomenon is the non-Newtonian fluid flow over a continuously moving solid surface. For example, hot rolling, glass-fiber production and conveyor belt are included in the applications. In Section 3.2 we provide a theoretical analysis of the boundary layer flow on a flat solid surface moving in an otherwise quiescent non-Newtonian fluid medium. A special emphasis is given to the formulation of boundary layer equations, which provide similarity solutions for the velocity profiles. We give numerical results on the velocity profiles and represent the effect of the power exponent on the shape of the velocity distribution [39].

After Blasius' pioneering work in 1908, more than three decades later the uniqueness of Blasius' famous velocity boundary layer solution was rigorously proved by Weyl [212]. On this background it was quite surprising that further three decades later, Steinheuer [191] and Klemp and Acrivos [123], [124] reported that in the Blasius-problem non-unique solutions may occur when the plate is not at rest, but moves with a constant velocity  $U_w$ , opposite in direction to the free stream of velocity  $U_\infty$ . It means that for positive values of the velocity ratio  $\lambda = -U_w/U_\infty$  dual solutions exist as long as  $\lambda$  is smaller than the critical value  $\lambda_c = 0.3541\dots$ , after which no similarity solutions exist. For  $\lambda < 0$ , Callegari and Nachman [62] have found unique solutions. The aim of Section 4.1 is to give an introduction to the results on the development of the doubly-driven Blasius flows reported by Klemp and Acrivos in their Journal of Fluid Mechanics papers [123], [124] and by Steinheuer [191]. In Section 4.2, our purpose is to give a theoretical analysis

of similarity solutions for the boundary layer of a non-Newtonian fluid on a flat plate moving opposite to the stream. The generalized Blasius boundary value problem is considered with non-homogeneous lower boundary conditions  $f(0) = 0$ ,  $f'(0) = -\lambda$ , where  $\lambda$  is the velocity ratio. The numerical calculations indicate that for non-Newtonian fluids there is a critical value  $\lambda_c$  such that solution to the boundary layer problem exists only if  $\lambda < \lambda_c$ . For Newtonian fluid ( $n = 1$ ) this phenomena was shown by Hussaini and Lakin [110] and  $\lambda_c$  was found to be 0.3541... We give estimation analytically for the critical velocity ratio  $\lambda_c$  depending on the power-law exponent  $n$  and show the dependence of  $\lambda_c$  on the power exponent  $n$  [44].

When a free liquid surface is present, the surface tension variation resulting from the temperature gradient along the surface can also induce motion in the fluid called thermal Marangoni convection. Marangoni convection is mass transfer along a liquid surface and it appears in many engineering problems. e.g., in highly stressed lubricated ball or friction bearings [125], and in crystal growth melts [67]. These phenomena have also been investigated by similarity analysis (see [14], [16], [65]-[67], [164]). In Section 5.1, we present the derivation of the equations and show how the boundary layer approximation leads to the two points boundary value problem and the similarity solutions for Newtonian fluids. The new model, written in terms of stream function and temperature, consists of two strongly coupled ordinary differential equations. Its analytical approximate solutions are represented in terms of exponential series. The influence of various physical parameters on the flow and heat transfer characteristics are discussed [48].

Many principal past studies concerning natural convection flows over a semi-infinite vertical plate immersed in an ambient fluid have been found in the literature ([141], [225]). In many cases, these problems may admit similarity solutions. The idea of using a convective boundary condition for Newtonian fluids was recently introduced by Aziz [18], while Magyari [143] revisited this work, and obtained an exact solution for the temperature boundary layer in a compact integral form. The effects of suction and injection have been studied by the similarity analysis by Ishak [115] and a couple of recent papers have been devoted to the subject of boundary layer flow with convective boundary conditions (see e.g., [11], [45], [97], [100], [101], [144], [162], [169], [193], [194], [217], [218]). Motivated by the above mentioned studies, in Section 5.2 we investigate the steady laminar boundary layer flow of a non-Newtonian fluid over a permeable flat plate in a uniform free stream, when the bottom surface of the plate is heated by convection from a hot fluid. We examine the heat and velocity distributions of a viscous and incompressible power-law non-Newtonian fluid over a permeable steady sheet in a uniform shear flow with a convective surface boundary condition ([45], [50]).

## 2 BOUNDARY LAYER FLOW ON A FLAT PLATE

The simplest example of application of boundary layer equations is the fluid flow along a stationary solid surface. Although experimental studies of such flows are important, it is crucial that the fluid mechanical properties are determined. Theoretical understanding of the flow behavior is necessary. We predict the boundary layer flow field by solving the equations that express conservation of mass and momentum in the boundary layer for Newtonian and non-Newtonian media. The geometry allows the governing partial differential equations to be reduced to ordinary differential equations using a similarity transformation.

### 2.1 NEWTONIAN FLUID FLOW

The problem of Newtonian fluid flow along a stationary, horizontal, infinite, plate situated in a fluid stream moving with constant velocity  $U_\infty$  is a classical problem of fluid mechanics. In this problem, the fluid motion is produced by the free stream. The Blasius flow is the result of the interaction of a flow that is spatially uniform for large  $x$  with a solid plate, which is idealized as being infinitely thin and extending infinitely far to the right as  $x \rightarrow \infty$ . The simplifications in the Navier-Stokes equations are valid for very high Reynolds numbers

$$(2.1) \quad \text{Re} = \frac{\rho U_\infty L}{\mu}.$$

Although the geometry is idealized, all flows past a solid body have thin boundary layers similar to the Blasius flow. Air rushing past a bird or an airplane, ocean currents streaming past an undersea mountain - all have boundary layers. The Blasius problem has developed a vast bibliography with the most well-known book written by Schlichting and Gersten [177].

#### 2.1.1 BASIC EQUATIONS

We review the steady-state classical problem of a fluid flow along a horizontal, stationary surface located in a uniform free stream  $U_\infty$ . This problem has been solved first by Blasius [30].

Let us consider the boundary layer governing equations (1.1), (1.6) for the two-dimensional steady flow of an incompressible fluid parallel to the  $x$  axis (see Fig. 2.1). In this case the velocity of the potential flow is constant, and  $\partial p / \partial x = 0$ . For Newtonian fluids the shear stress and shear rate relationship

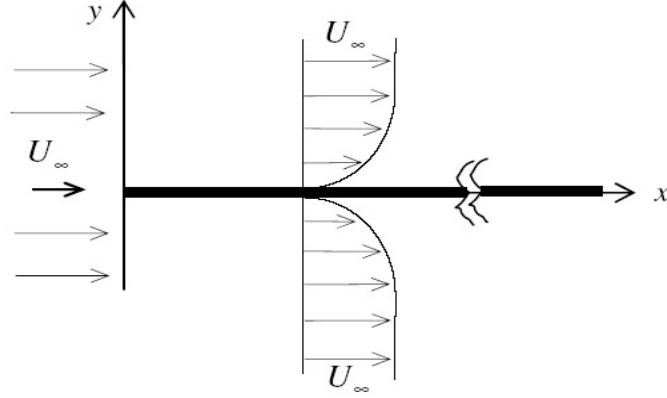


**Fig. 2.1** Boundary layer on a flat surface at zero incidence

given by (1.8). The boundary layer equations (1.1) and (1.6) become

$$(2.2) \quad \frac{\partial u}{\partial x} + \frac{\partial v}{\partial y} = 0,$$

$$(2.3) \quad \rho \left( u \frac{\partial u}{\partial x} + v \frac{\partial u}{\partial y} \right) = \mu \frac{\partial^2 u}{\partial y^2}.$$

To solve these equations three boundary conditions are needed:

(i.) at the solid surface there is neither slip nor mass transfer:

$$(2.4) \quad u(x, 0) = 0, \quad v(x, 0) = 0,$$

(ii.) outside the viscous boundary layer the streamwise velocity component  $u$  should approach the main stream velocity  $U_\infty$ :

$$(2.5) \quad \lim_{y \rightarrow \infty} u(x, y) = U_\infty.$$

### 2.1.2 SIMILARITY SOLUTION

In order to study this problem it is convenient to introduce the stream function  $\psi$  defined by

$$(2.6) \quad u = \frac{\partial \psi}{\partial y}, \quad v = -\frac{\partial \psi}{\partial x}.$$

Then, the continuity equation (2.2) is satisfied automatically and the equation (2.3) becomes

$$(2.7) \quad \frac{\partial \psi}{\partial y} \frac{\partial^2 \psi}{\partial y \partial x} - \frac{\partial \psi}{\partial x} \frac{\partial^2 \psi}{\partial y^2} = \mu_c \frac{\partial^3 \psi}{\partial y^3}, \quad \mu_c = \mu/\rho.$$

The boundary conditions (2.4), (2.5) can be written as

$$\frac{\partial\psi}{\partial y}(x,0) = 0, \quad \frac{\partial\psi}{\partial x}(x,0) = 0, \quad \lim_{y \rightarrow \infty} \frac{\partial\psi}{\partial y}(x,0) = U_\infty.$$

Now, we have a single unknown function  $\psi$  in the partial differential equation (2.7). We look for similarity solutions using the linear transformation  $x \rightarrow \omega x$ ,  $y \rightarrow \omega^{-\beta}y$ ,  $\psi \rightarrow \omega^{-\alpha}\psi$  with a positive parameter  $\omega$ . Equation (2.7) is invariant under this transformation for all  $\omega > 0$  when the scaling relation  $\alpha - \beta = 1$  holds. Then one can write

$$(2.8) \quad \psi = Ax^\alpha f(\eta), \quad \eta = Bx^\beta y,$$

where  $A, B, \alpha$  and  $\beta$  are constants to be determined (see [20]). Research on this subject dates back to the pioneering works by Blasius [30], Falkner and Skan [83].

In order to fulfill the differential equation and the boundary conditions, the real numbers  $A, B > 0$  are such that  $\mu_c B/A = 1$  and  $AB = U_\infty$ , that means

$$(2.9) \quad A = (\mu_c U_\infty)^{\frac{1}{2}}, \quad B = \left( \frac{U_\infty}{\mu_c} \right)^{\frac{1}{2}},$$

and equation (2.7) with (2.9) leads to the following third order differential equation

$$f''' + \alpha f f'' = (\alpha + \beta) f'^2,$$

where the prime on the  $f$  implies differentiation with respect to  $\eta$ . The condition at infinity gives  $\alpha + \beta = 0$ . Hence,  $\alpha = 1/2$ ,  $\beta = -1/2$  and we arrive at the Blasius problem

$$(2.10) \quad f''' + \frac{1}{2} f f'' = 0,$$

$$(2.11) \quad f(0) = 0, \quad f'(0) = 0, \quad \lim_{\eta \rightarrow \infty} f'(\eta) = 1.$$

Therefore

$$\psi(x, y) = (\mu_c U_\infty x)^{\frac{1}{2}} f(\eta), \quad \eta = \left( \frac{U_\infty}{\mu_c} \right)^{\frac{1}{2}} \frac{y}{x^{\frac{1}{2}}}$$

and important characteristics of the flow, that the non-dimensional velocity components can be given by  $f$  and  $\eta$ :

$$(2.12) \quad u(x, y) = U_\infty f'(\eta),$$

$$v(x, y) = v^*(x) [\eta f'(\eta) - f(\eta)],$$

where

$$v^*(x) = \frac{U_\infty}{2} \text{Re}_x^{-\frac{1}{2}} \quad \text{and} \quad \text{Re}_x = \frac{\rho U_\infty x}{\mu},$$

$\text{Re}_x$  denotes the local Reynolds number. The exact solution for  $u(x, y)$  reveals a most useful fact that  $u$  can be expressed as a function of a single variable  $\eta$ .

The solution  $f$  is called the shape function or the dimensionless stream-function and its first derivative, after suitable normalization, represents the velocity parallel to the plate. We point out that the function  $f(\eta)$  gives all information about the flow in the boundary layer.

One of our main aim is to determine the value of  $f''(0)$  which is the velocity gradient at the wall. It has an important physical meaning. It appears in drag force due to wall shear stress. For a solid object moving in a fluid, the drag force is a hydrodynamic force acting in the direction of the movement to oppose the motion. The drag force is proportional to the drag coefficient  $C_{D,\tau}$ , the density and the velocity square. In general,  $C_{D,\tau}$  is not an absolute constant. The drag coefficient is a non-dimensional quantity and it varies with the speed (or more generally with Reynolds number), the flow direction, the fluid density and fluid viscosity. The value  $f''(0)$  is used to call the skin friction parameter and it is involved in the drag coefficient

$$C_{D,\tau} = (2)^{\frac{1}{2}} \text{Re}^{-\frac{1}{2}} f''(0),$$

and in the wall shear stress

$$\tau_w = \left[ \frac{\rho \mu U_\infty^3}{x} \right]^{\frac{1}{2}} f''(0).$$

The velocity profiles measured at different distances  $x$  from the leading edge when represented in coordinate system  $u(x, y)/U_\infty$  and  $y/x^{\frac{1}{2}}$  collapse into one. So, the velocity profiles are similar to one another, the boundary layer is self-similar, i.e. they can be mapped onto one another by choosing suitable scaling factors.

Applying the similarity method, the two independent variables  $x$  and  $y$  are combined to form a new variable  $\eta$  in order to transform the partial differential equation (2.7) into an ordinary differential equation (2.10). In [212] Weyl has proved that there is a unique solution to the Blasius problem (2.10), (2.11).

### 2.1.3 TÖPFER TRANSFORMATION

In this section instead of the Blasius problem (2.10), (2.11) we consider the initial value problem

$$f''' + \frac{1}{2}ff'' = 0,$$

$$f(0) = 0, \quad f'(0) = 0, \quad f''(0) = \gamma.$$

The task is to determine  $\gamma$  such that the corresponding solution satisfies (2.10) and (2.11). Töpfer [203] realized for the Blasius problem (2.10), (2.11) that the knowledge of  $\gamma$  is in fact unnecessary. The reason is that there is a second group invariance such that if  $g(\eta^*)$  denotes the solution to the Blasius equation (2.10) with initial conditions  $g(0) = 0$ ,  $g'(0) = 0$ , and for its second derivative  $g''(0) = 1$ , then the solution  $f$  with initial conditions  $f(0) = 0$ ,  $f'(0) = 0$ ,  $f''(0) = \gamma$  can be obtained as

$$(2.13) \quad f(\eta) = \gamma^{1/3}g(\gamma^{1/3}\eta)$$

(see [203]). It therefore suffices to compute  $g(\eta^*)$  and then rescale of  $g(\eta^*)$  so that the rescaled function has the desired asymptotic behavior at large  $\eta$ , namely,  $f'(\infty) = 1$ . The true value of the second derivative at the origin is then

$$\gamma = \lim_{\eta^* \rightarrow \infty} [g'(\eta^*)]^{-3/2}.$$

With Töpfer's transformation, it is only necessary to solve the differential equation as an initial value problem.

This scaling invariance has both analytical and numerical interest. From numerical viewpoint this transformation allows us to find non-iterative numerical solutions by the related initial value problem. From a numerical point of view to calculate  $\lim_{\eta^* \rightarrow \infty} g'(\eta^*)$  is not simple. The most widely used numerical technique to boundary value problems on infinite domains is to introduce a suitable truncated boundary  $\eta_t^*$  instead of  $+\infty$ . Töpfer [203] solved the initial value problem obtained for the Blasius equation (2.10) for a large but finite  $\eta_j^*$ , ordered such that  $\eta_j^* < \eta_{j+1}^*$ . He computed the corresponding values of  $\gamma_j$ . If  $\gamma_j$  and  $\gamma_{j+1}$  agree with a specified accuracy, then  $\gamma$  is approximated by the common value of  $\gamma_j$  and  $\gamma_{j+1}$ . Töpfer kept repeating his calculations with a larger value of  $\eta^*$ .

Weyl [212] noted that the Blasius problem "was the first boundary-layer problem to be numerically integrated . . . [in] 1907."

### 2.1.4 POWER SERIES SOLUTIONS

The Blasius function is defined as the unique solution to the boundary value problem (2.10), (2.11). Blasius [30] derived power series expansion which begins

$$(2.14) \quad f(\eta) \approx \frac{1}{2}\gamma\eta^2 - \frac{1}{240}\gamma^2\eta^5 + \frac{11}{161280}\gamma^3\eta^8 - \frac{5}{4257792}\gamma^4\eta^{11} + \dots,$$

where  $\gamma = f''(0)$  is the curvature of the function at the origin. A closed form for the coefficients is not known. However, the coefficients can be computed for

$$f(\eta) = \eta^2 \sum_{k=0}^{\infty} \left(-\frac{1}{2}\right)^k \frac{A_k \gamma^{k+1}}{(3k+2)!} \eta^{3k},$$

from the recurrence

$$A_k = \sum_{j=0}^{k-1} \binom{3k-1}{3j} A_j A_{k-j-1}, \quad \text{if } k \geq 2,$$

with  $A_0 = A_1 = 1$ . Here  $\gamma$  must be numerically given. Howarth [109] obtained a numerical result  $\gamma \approx 0.332057$ . Recently, Abbasbandy [1] proposed an Adomian's decomposition method to the Blasius's problem and obtained  $\gamma = 0.333329$  with a 0.383% relative error of the initial slope, and Tajvidi et al. [197] has used a modified rational Legendre method, to show that  $\gamma = 0.33209$  with a 0.009% relative error. By the fourth-order Runge-Kutta method  $\gamma$  is determined  $\gamma \approx 0.33205733621519630$ , where all the sixteen decimal places are believed correct [56]. A fully analytical solution (i.e. not relying on any approximation) of the Blasius problem has been found by Liao [128] using the homotopy analysis method. He's homotopy perturbation method has been successfully applied in fluid mechanics (see e.g. [15], [150], [219], [220]).

It should be noted that Blasius' series has only a finite radius of convergence:

$$(2.15) \quad \rho = \lim_{k \rightarrow \infty} \left( \frac{(3k)(3k+1)(3k+2)A_{k-1}}{A_k \gamma} \right)^{\frac{1}{3}} = 5.688.$$

The limitation of a finite radius of convergence can be overcome by constructing power series by Padé approximants or an Euler-accelerated series, which both apparently converge for all positive real  $x$  [55].

Although the Blasius problem is almost a century old, it is still a topic of active current research (see e.g. [1], [5], [6], [55], [69], [84], [102], [103], [128], [206]).

A brief history of the numerical determination of  $\gamma$ :

- (1912)  $\gamma = 0.332$ , Töpfer [203]
- (1938)  $\gamma = 0.332057$ , Howarth [109]
- (1941) Weyl [212]
- (1941) John von Neumann
- (1948) Ostrowski [163]
- (1956) Meksyn [151]
- (1998) Fazio [86]
- (1999) Liao [128]
- (2006)  $\gamma = 0.33209$ , Tajvidi et al. [197]
- (2007)  $\gamma = 0.333293$ , Abbasbandy [1]
- (2008)  $\gamma = 0.33205733621519630$ , Boyd [56]
- (2011) Peker, Karaoğlu, Oturanc [166]

## 2.2 NON-NEWTONIAN FLUID FLOW WITH CONSTANT MAIN STREAM VELOCITY

Fluids such as molten plastics, pulps, slurries and emulsions, which do not obey the Newtonian law of viscosity are increasingly produced in the industry. By analogy with the Blasius description [30] for Newtonian fluid flows, similarity solutions can be studied and investigated to the model arising for a laminar boundary layer with power-law viscosity. The first analysis of the boundary layer approximations to power-law pseudoplastic fluids was given by Schowalter [179] in 1960. The author derived the equations governing the similarity flow. The numerical solutions were presented of the laminar flow of non-Newtonian power-law model past a two-dimensional horizontal surface by Acrivos, Shah and Petersen [4]. When the geometry of the surface is simple the system of differential equations can be examined in details and can be obtained fundamental information about the behavior of non-Newtonian fluids in motion (e.g., to predict the drag). The existence of a unique solution was proved in [25]. We show that a Töpfer-like transformation can be applied for the determination of the dimensionless wall gradient and we provide power series solution near the wall [38]. Moreover, we can give a method for the determination of the power series approximation similar to Blasius's form (2.14) for  $n > 0$ .

### 2.2.1 BOUNDARY LAYER GOVERNING EQUATIONS

We consider two-dimensional steady flow of a viscous fluid with constant velocity  $U_\infty$ . The problem is a model for the the laminar incompressible flow of a non-Newtonian power-law fluid past a flat surface. The surface is located at  $y = 0$ .

The analysis is restricted to the cases when the usual boundary layer approximations can be made, for large Reynolds numbers, defined for power-law fluids by

$$(2.16) \quad \text{Re} = \frac{\rho U_\infty^{2-n} L^n}{K}.$$

This allows to simplify the basic equations of conservation of momentum and mass. The problem is deduced from the boundary layer approximation (1.1), (1.6), where the shear stress  $\tau_{yx}$  is given by the power-law expression (1.11):

$$(2.17) \quad \frac{\partial u}{\partial x} + \frac{\partial v}{\partial y} = 0,$$

$$(2.18) \quad \rho \left( u \frac{\partial u}{\partial x} + v \frac{\partial u}{\partial y} \right) = K \frac{\partial}{\partial y} \left( \left| \frac{\partial u}{\partial y} \right|^{n-1} \frac{\partial u}{\partial y} \right).$$

At the solid surface the usual impermeability and no-slip are applied and outside the viscous boundary layer the streamwise velocity component  $u$  should approach the exterior streaming speed  $U_\infty$ :

$$(2.19) \quad u(x, 0) = 0, \quad v(x, 0) = 0, \quad \lim_{y \rightarrow \infty} u(x, y) = U_\infty.$$

The boundary layer equations (2.17) and (2.18) are nonlinear and have boundary conditions at 0 and at  $+\infty$ .

Introducing the stream function  $\psi$  defined in (2.6), the continuity equation (1.1) is automatically satisfied and (2.18) can be written as

$$(2.20) \quad \frac{\partial \psi}{\partial y} \frac{\partial^2 \psi}{\partial y \partial x} - \frac{\partial \psi}{\partial x} \frac{\partial^2 \psi}{\partial y^2} = \mu_{cn} \frac{\partial}{\partial y} \left[ \left| \frac{\partial^2 \psi}{\partial y^2} \right|^{n-1} \frac{\partial^2 \psi}{\partial y^2} \right], \quad \mu_{cn} = K/\rho.$$

Boundary conditions in (2.19) can be formulated as

$$(2.21) \quad \frac{\partial \psi}{\partial y}(x, 0) = 0, \quad \frac{\partial \psi}{\partial x}(x, 0) = 0,$$

and

$$(2.22) \quad \lim_{y \rightarrow \infty} \frac{\partial \psi}{\partial y}(x, 0) = U_\infty,$$

where the unknown function is the stream function  $\psi$ .

Let us define the stream function  $\psi$  and similarity variable  $\eta$  such as

$$\psi = Ax^\alpha f(\eta), \quad \eta = Bx^\beta y,$$

where  $A, B, \alpha$  and  $\beta$  are constants to be determined, and  $f(\eta)$  denotes the dimensionless stream function. Choosing  $\beta = -\alpha$  and  $AB = U_\infty$ , the boundary value problem (2.20)-(2.22) is transformed by means of dimensionless variables ([4], [25], [38],[179])

$$(2.23) \quad \psi(x, y) = \mu_{cn}^{\frac{1}{n+1}} U_\infty^{\frac{2n-1}{n+1}} x^{\frac{1}{n+1}} f(\eta),$$

$$(2.24) \quad \eta = \mu_{cn}^{-\frac{1}{n+1}} U_\infty^{\frac{2-n}{n+1}} \frac{y}{x^{\frac{1}{n+1}}}$$

into the so-called generalized Blasius problem

$$(2.25) \quad \left( |f''|^{n-1} f'' \right)' + \frac{1}{n+1} f f'' = 0,$$

$$(2.26) \quad f(0) = 0, \quad f'(0) = 0, \quad \lim_{\eta \rightarrow \infty} f'(\eta) = 1,$$

where the prime denotes the differentiation with respect to the similarity variable  $\eta$  and the non-dimensional velocity components are obtained by  $f$  as follows:

$$u(x, y) = U_\infty f'(\eta),$$

$$v(x, y) = v^*(x) [\eta f'(\eta) - f(\eta)],$$

with

$$v^*(x) = \frac{U_\infty}{n+1} \text{Re}_x^{-\frac{1}{n+1}},$$

when for power-law non-Newtonian fluids the local Reynolds number  $\text{Re}_x$  is defined by

$$\text{Re}_x = \frac{\rho U_\infty^{2-n} x^n}{K}.$$

If  $n = 1$ , equation (2.25) is the same as the famous Blasius equation (2.10). Equation (2.25) is nonlinear except in the case  $n = 2$ , when explicit solution exists. For detailed analysis we refer to the paper by Liao [129].

Since the boundary layer equations are valid when the Reynolds number is large, it is worth to examine under what conditions laminar boundary layer flows would be expected to occur. In [4] the following conclusions were

deduced:

(i.) If  $U_\infty$  is sufficiently small and the inertia terms of the equations of motion may be neglected, all fluids approach Newtonian behavior.

(ii.) If  $n < 2$ , boundary layer type flow can be obtained when  $U_\infty$  is large and therefore the Reynolds number is sufficiently large.

(iii.) If  $n > 2$ , boundary layer type flow can be obtained for moderate values of  $U_\infty$  when the Reynolds number is large. If  $U_\infty$  is too large then  $Re$  will be small. So, if  $U_\infty$  is sufficiently large the boundary layer flow is not an asymptotic state of laminar motion. If  $U_\infty$  tends to zero then  $Re$  tends to  $\infty$  and the characteristic velocity is small as the model (1.11) is valid when  $\partial u/\partial y$  is relatively large. When  $U_\infty$  and therefore  $\partial u/\partial y$  is small non-Newtonian boundary layer flow do not occur. So, for  $n > 2$ , the laminar boundary layer flows are probably not of interest because their range of validity is rather limited.

For the numerical solution to (2.25), (2.26) we refer to the paper by Acrivos et al. [4] when the Polhausen-type momentum integral method was applied for the determination of the velocity distribution and the shear stress at the wall. It should be noted that when  $n \geq 2$  there is no solution  $f$  to (2.25), (2.26). Then, the boundary condition at infinity in (2.26) has to be changed

$$(2.27) \quad f(0) = 0, \quad f'(0) = 0, \quad f'(\eta) = 1, \quad \text{for } \eta \geq \eta_0,$$

where  $\eta_0 = \infty$  for  $n < 2$  and  $\eta_0$  is finite for  $n \geq 2$ . The phenomenon of a finite  $\eta_0$  has not appeared in the case of laminar Newtonian boundary layer fluid flows.

### 2.2.2 TÖPFER-LIKE TRANSFORMATION

Here we want to provide a transformation similar to Töpfer's transformation for power-law type viscosity. We replace the condition at infinity by one at  $\eta = 0$ . Therefore, the generalized Blasius problem (2.25), (2.26) is converted into the initial value problem

$$(2.28) \quad \left( |f''|^{n-1} f'' \right)' + \frac{1}{n+1} f f'' = 0,$$

$$(2.29) \quad f(0) = 0, \quad f'(0) = 0, \quad f''(0) = \gamma.$$

The solution can be obtained if only  $\gamma = f''(0)$  were known such that the corresponding solution satisfies (2.25), (2.26).

We present a modified version of Töpfer-method for non-Newtonian fluid flows [38]. In order to transform the boundary value problem (2.25), (2.26) into an initial value problem let us introduce the scaling transformation

$$(2.30) \quad g = \lambda^\kappa f, \quad \eta^* = \lambda^\epsilon \eta,$$

where  $\kappa$  and  $\epsilon$  are real, non-zero parameters. Our aim is to determine  $\kappa$  and  $\epsilon$  such that the boundary conditions are substituted by suitable initial conditions. After simple calculations we have

$$\frac{df}{d\eta} = \lambda^{\kappa-\epsilon} \frac{dg}{d\eta^*}, \quad \frac{d^2f}{d\eta^2} = \lambda^{\kappa-2\epsilon} \frac{d^2g}{d\eta^{*2}}, \quad \frac{d^3f}{d\eta^3} = \lambda^{\kappa-3\epsilon} \frac{d^3g}{d\eta^{*3}}.$$

The governing differential equation is left invariant by the new variables  $g$  and  $\eta^*$

$$(2.31) \quad \left( |g''|^{n-1} g'' \right)' + \frac{1}{n+1} g g'' = 0,$$

where the prime for  $g$  denotes the derivatives with respect to  $\eta^*$ , when

$$\kappa(2-n) = (1-2n)\epsilon.$$

The initial conditions in (2.29) correspond to

$$(2.32) \quad g(0) = 0, \quad g'(0) = 0,$$

moreover, with the choice of  $\lambda = \gamma$ , one gets

$$g''(0) = \gamma^{\kappa-2\epsilon} f''(0) = \gamma^{\kappa-2\epsilon+1}.$$

So, with  $\kappa = \frac{1-2n}{3}$  and  $\epsilon = \frac{2-n}{3}$ , i.e.,  $g = \gamma^{\frac{1-2n}{3}} f$ ,  $\eta^* = \gamma^{\frac{2-n}{3}} \eta$ , we obtain

$$(2.33) \quad g''(0) = 1.$$

Then

$$f(\eta) = \gamma^{(2n-1)/3} g(\gamma^{(2-n)/3} \eta),$$

which is reduced to Töpfer's form (2.13) for Newtonian fluid ( $n = 1$ ). Value  $\gamma$  will be determined by the boundary condition at  $+\infty$  in (2.29) such as

$$1 = \lim_{\eta \rightarrow \infty} f'(\eta) = \lim_{\eta^* \rightarrow \infty} \gamma^{\kappa-\epsilon} g'(\eta^*) = \lim_{\eta^* \rightarrow \infty} \gamma^{\frac{n+1}{3}} g'(\eta^*),$$

that is

$$\lim_{\eta^* \rightarrow \infty} g'(\eta^*) = \gamma^{-\frac{n+1}{3}},$$

and hence

$$\gamma = \lim_{\eta^* \rightarrow \infty} [g'(\eta^*)]^{-\frac{n+1}{3}}.$$

Table 2.1 shows numerical results for  $\eta_t^*$  of the solutions to (2.31)-(2.33) for  $n$ -values between 0.1 and 5. Here we represent suitable truncated boundaries  $\eta_t^*$  instead of  $+\infty$ .

The classical fourth-order Runge-Kutta method is applied and a local error of the order of  $10^{-6}$  is maintained. Table 2.1 also contains the corresponding values,  $g'(\eta_t^*)$ , and the values of  $\gamma$  for  $n$ -values between 0.1 and 5 such that  $\gamma = [f''(\eta_t^*)]^{-3/(n+1)}$  with the present numerical techniques. These values give approximations for the dimensionless wall gradient, with  $f''(0)$  represented for  $n$ -values between 0.1 and 25 in Fig. 2.5.

$n$	$g'(\eta_t^*)$	$\eta_t^*$	$\gamma$
0.1	1.082888	1580	0.8047872846
0.2	1.338859	980	0.4821258779
0.3	1.507245	450	0.3879770360
0.4	1.634506	180	0.3489340836
0.5	1.737550	60	0.3312265785
0.6	1.824658	40	0.3238052732
0.7	1.900523	21	0.3220110529
0.8	1.968071	11	0.3235427888
0.9	2.029252	8.6	0.3271391413
1	2.085409	6.8	0.3320574397
1.1	2.137511	5.01	0.3378333248
1.2	2.186271	4.44	0.3441653539
1.4	2.275793	3.83	0.3577535406
1.6	2.356978	3.562	0.3718424054
1.8	2.431724	3.431	0.3859405042
2	2.501222	3.362	0.3997908558
2.5	2.657653	3.29999	0.4326575477
3	2.796410	3.33381	0.4624333153
4	3.035898	3.44260	0.5136031483
5	3.241207	3.57487	0.5554521362

**Table 2.1.**

Since the pioneering work by Acrivos et al. [4], different approaches have been investigated for  $\gamma$  in the case of non-Newtonian fluids. It has a physical meaning. It appears in drag force due to wall shear stress which is a fluid dynamic force. The skin friction parameter  $\gamma$  originates from the wall shear

stress

$$(2.34) \quad \tau_w(x) = \left[ \frac{\rho^n K U_\infty^{3n}}{x^n} \right]^{\frac{1}{n+1}} |\gamma|^{n-1} \gamma,$$

and it gives the non-dimensional drag coefficient

$$C_{D,\tau} = (n+1)^{\frac{1}{n+1}} \text{Re}^{\frac{-n}{n+1}} |\gamma|^{n-1} \gamma.$$

The solutions to the generalized Blasius equation (2.28), displayed in Figs. 2.2-2.4, were found by rescaling. Fig. 2.2 shows the dimensionless velocity components  $f'(\eta)$  parallel to the wall, for some different values of the power law index  $n$  ( $n = 0.5; 1; 3$ ). It is observed that the form of the velocity profiles changes dramatically as  $n$  is varied. The slope of the profiles is strongly dependent on  $n$ . This dependency is also represented by  $f'''(0)$  in Fig. 2.5 The transverse components of the dimensionless velocity are demonstrated in Fig. 2.3 by plotting  $v(x, y)/v^*(x)$  for some different values of  $n$ .

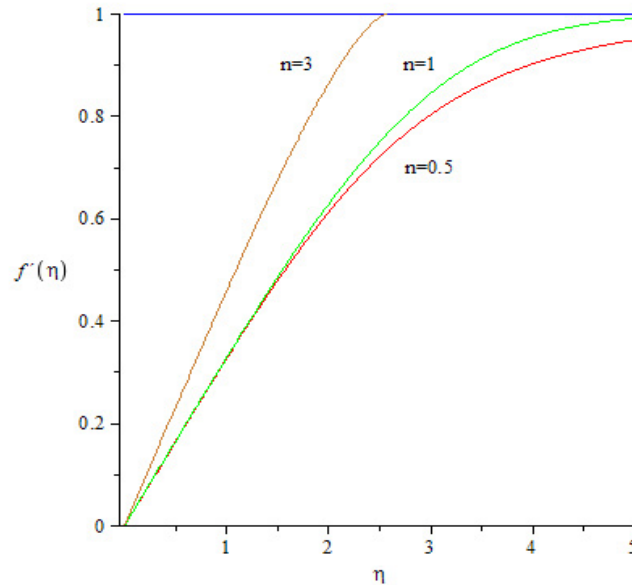


**Fig. 2.2** Similarity velocity profiles  $f' = u(x, y)/U_\infty$

The cross-stream variation of the dimensionless velocity gradient  $f''(\eta)$  is shown in Fig. 2.4 for some different  $n$ -values. The solutions are monotonically decreasing from  $f''(0)$  at the wall to zero outside the viscous boundary layer.

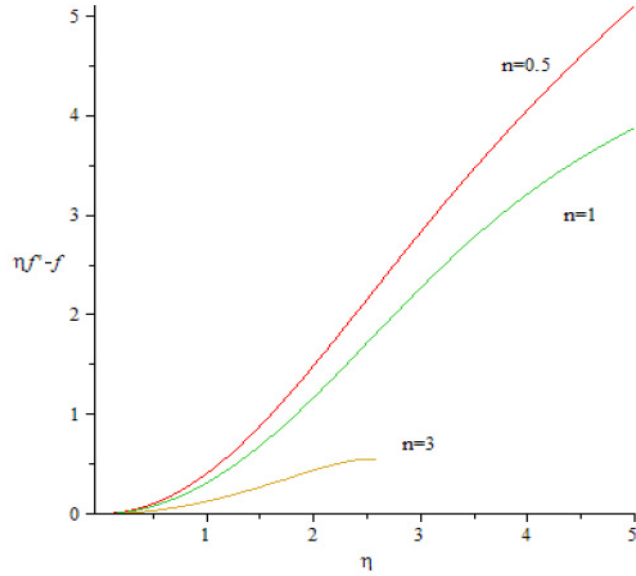


Fig. 2.3 Similarity velocity profiles  $\frac{v(x,y)}{v^*(x)} = \eta f'(\eta) - f(\eta)$

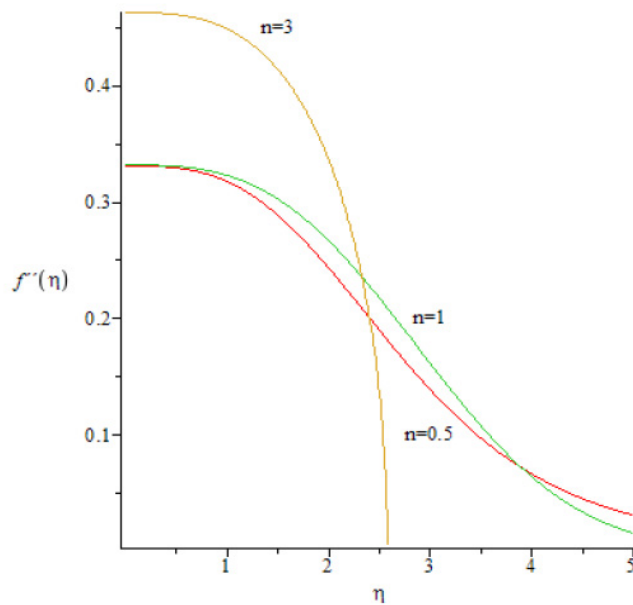


Fig. 2.4 The cross-stream variation of the dimensionless velocity gradient  $f''(\eta)$

$n$	0.1	0.2	0.3	0.4	0.5	0.6	0.7	0.8
$\eta_t = \gamma^{\frac{n-2}{3}} \eta_t^*$	1813	1518	769	315	104	67	34	17
$n$	0.9	1	1.1	1.2	1.4	1.6	1.8	2
$\eta_t = \gamma^{\frac{n-2}{3}} \eta_t^*$	12.9	9.7729	6.9379	5.9008	4.7042	4.0642	3.6554	3.362

Table 2.2

Table 2.2 shows the rescaled values  $\eta_t$ , and the results suggest that the thickness  $\eta_t$  is a rapidly decreasing function of  $n$  until  $n = 2$ .

Using numerical techniques in [4], the authors noted that for  $n > 1$ , the boundary layer has a finite thickness; that is  $f''(\eta) = 0$  for  $\eta \geq \eta_0 > 0$ . This phenomena is also represented on Fig. 2.4 for  $n = 3$ . However, for  $n \neq 1$ , differential equation in (2.29) can be either degenerate or singular at the point  $\eta_0$ , where  $f''(\eta_0) = 0$ . In the case  $0 < n \leq 1$ ,  $f''$  is strictly positive, so the equation is not degenerate [224].

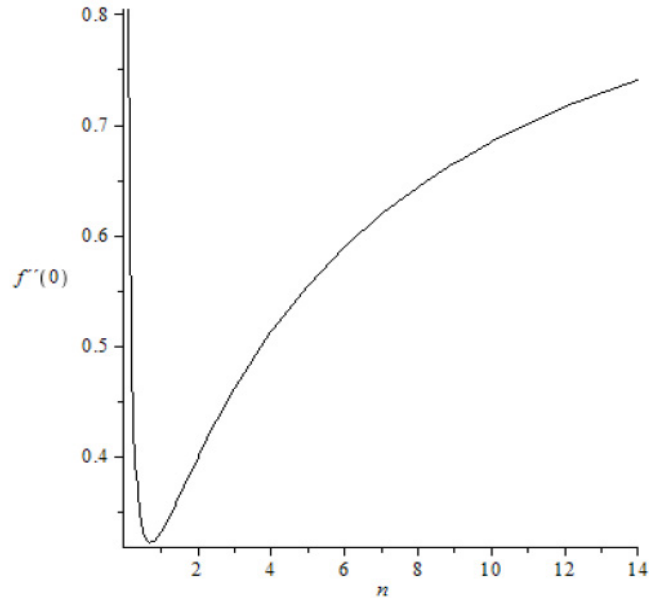


Fig. 2.5 Dimensionless wall gradient parameter  $f''(0)$  with power exponent  $n$

**Remark.** The scaling invariant property remains valid, when the flow behavior of the non-Newtonian fluid is characterized by (1.9) and function  $\phi$  satisfies some prescribed properties. Then equation (2.25) is substituted by

$$(2.35) \quad [\phi(f'')] + f f'' = 0,$$

and the solution to (2.35)-(2.26) has similar properties to solution of (2.25)-(2.26) (see Bognár [47]).

### 2.2.3 POWER SERIES SOLUTIONS

It is obvious from the complexity of the equations and boundary conditions that analytical methods can be used to obtain exact solution in very few practical circumstances. Approximate analytic solutions are very valuable because they provide physical insight into the basic mechanisms. The numerical studies of such boundary value problems involve more than one integration process. The use of different type of series presents an attractive alternative approach. The series solution is very useful in analyzing some of the boundary layer problems. It is more efficient in its implementation on a computer than a purely numerical method. The numerical and analytic methods of these nonlinear problems have their own advantages and limitations.

The object of this section is to determine an approximate local solution  $f(\eta)$  to the initial value problem (2.28), (2.29). Let us suppose that  $0 < n < 2$ , and  $f''$  is positive in the neighborhood of zero. In this case, (2.28), (2.29) can be written as

$$(2.36) \quad f''' + \frac{1}{n(n+1)} f (f'')^{2-n} = 0, \quad f(0) = 0, \quad f'(0) = 0, \quad f''(0) = \gamma$$

for appropriate values of  $\gamma$ . In [38] we considered the equation in (2.36) as a system of certain differential equations, namely, the special Briot-Bouquet differential equations [59]. For this type of differential equations we refer to the book by Hille [105], Ince [112]. We showed that there exists a formal solution to (2.36) in the form

$$(2.37) \quad f(\eta) = \eta^2 \sum_{k=0}^{\infty} a_k \eta^{3k},$$

where the first three coefficients are given by

$$(2.38) \quad a_0 = \frac{\gamma}{2},$$

$$(2.39) \quad a_1 = -\frac{\gamma^{3-n}}{5!n(n+1)},$$

$$(2.40) \quad a_2 = \frac{\gamma^{5-2n}(21-10n)}{8!n^2(n+1)^2}.$$

The Briot-Bouquet theorem ensures the convergence of formal solutions. We note that this theorem has been successfully applied to the determination of local analytic solutions of different nonlinear initial value problems [35], [37].

For the determination of coefficients  $a_k$ ,  $k > 2$ , one can use the J.C.P. Miller formula [91], [104], namely:

$$(2.41) \quad \left[ \sum_{k=0}^L c_k x^k \right]^{p+1} = \sum_{k=0}^{(p+1)L} d_k(p) x^k,$$

for a polynomial with coefficients  $c_k$ ; moreover,  $d_0(p) = 1$  for  $c_0 = 1$ , and

$$(2.42) \quad d_k(p) = \frac{1}{k} \sum_{j=0}^{k-1} [(p+1)(k-j) - j] d_j(p) c_{k-j}, \quad (k \geq 1).$$

From (2.37)

$$\begin{aligned} f''(\eta) &= \sum_{k=0}^{\infty} (3a_k + 2)(3a_k + 1) \eta^{3k}, \\ f'''(\eta) &= \eta^2 \sum_{k=0}^{\infty} (3a_k + 5)(3a_k + 4)(3a_k + 3) \eta^{3k}, \end{aligned}$$

and

$$[f''(\eta)]^{2-n} = \left[ \sum_{k=0}^{\infty} (3a_k + 2)(3a_k + 1) \eta^{3k} \right]^{2-n} = \sum_{k=0}^{\infty} A_k \eta^{3k},$$

where coefficients  $A_k$  can be expressed in terms of  $a_k$  ( $k = 0, 1, \dots$ ) by applying the J.C.P. Miller formula. Substituting them into the differential equation (2.36) we get

$$(2.43) \quad \sum_{k=0}^{\infty} (3a_k + 5)(3a_k + 4)(3a_k + 3) \eta^{3k} + \frac{1}{n(n+1)} \sum_{k=0}^{\infty} a_k \eta^{3k} \sum_{k=0}^{\infty} A_k \eta^{3k} = 0.$$

Applying the recursion formula (2.42) for the determination of  $A_k$  and the comparison of the proper coefficients in (2.43) one can have

$$\begin{aligned} a_3 &= -\frac{\gamma^{7-3n} b_3(n)}{11! n^3 (n+1)^3}, \\ b_3(n) &= 560n^2 - 2054n + 1869, \end{aligned}$$

$$a_4 = -\frac{\gamma^{9-4n}b_4(n)}{14!n^4(n+1)^4},$$

$$b_4(n) = 92400n^3 - 467840n^2 + 784616n - 437073,$$

$$a_5 = -\frac{\gamma^{11-5n}b_5(n)}{17!n^5(n+1)^5},$$

$$b_5(n) = 33633600n^4 - 214361000n^3 + 509689280n^2 - 536861976n + 211717233,$$

$$a_6 = -\frac{\gamma^{13-6n}b_6(n)}{20!n^6(n+1)^6},$$

$$b_6(n) = 22870848000n^5 - 174571028800n^4 + 530727289280n^3 - 804421691584n^2 + 608609067906n - 1840803558917.$$

We note that our computations indicate that all the coefficients obtained from (2.43) can be written in the form

$$(2.44) \quad a_k = \gamma^{1-k(n-2)} \frac{b_k(n)}{(3k+2)!n^k(n+1)^k},$$

where  $b_k$  is a polynomial of  $n$  of order  $(k-1)$ .

One can calculate coefficients  $a_k$  for the determination of  $f'(\eta)$  for any  $n$ . We present an example where the coefficients have been evaluated by using the symbolic algebra software Maple 12:

**2.1. Example** For  $n = 0.5$  the initial value problem (2.36)

$$f''' + \frac{1}{0.75} f (f'')^{1.5} = 0$$

$$f(0) = 0, \quad f'(0) = 0, \quad f''(0) = 0.3312265785$$

has power series solution near zero in the form:

$$f(\eta) \approx \eta^2 (0.165613 - 0.000702\eta^3 + 0.84913710^{-5}\eta^6 - 0.13380110^{-6}\eta^9 + 0.23813310^{-8}\eta^{12} - 0.45456310^{-10}\eta^{15} + 0.90801810^{-12}\eta^{18} - 0.18724610^{-13}\eta^{21} + 0.39530710^{-15}\eta^{24} - 0.84977010^{-17}\eta^{27} + 0.18530210^{-18}\eta^{30}).$$

The series expansion of  $f(\eta)$  is presented above for  $0 < n < 2$ . Numerical results for the case  $n = 2$  were obtained by Kim et al. [121] and Liao [129]. In this case equation (2.25) becomes

$$\left(f''' + \frac{1}{6}f\right) f'' = 0$$

subject to the boundary conditions (2.26). The above equation gives either

$$f'''(\eta) + \frac{1}{6}f(\eta) = 0$$

or  $f''(\eta) = 0$ . In [129] it was shown that this boundary value problem has infinite number of analytic solutions.

Fig. 2.6 reports the approximations obtained by the partial sums (thin lines) compared to the numerical solution (thick line) obtained by the fourth-order Runge-Kutta method for the case  $n = 0.5$ .

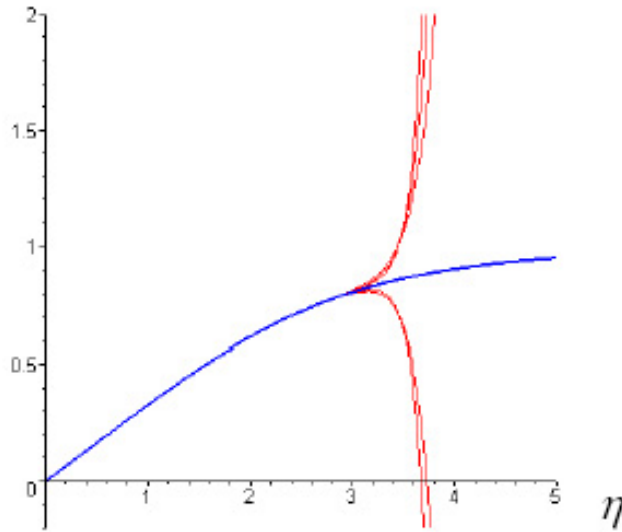


**Fig. 2.6** Velocity profiles for  $n = 0.5$

The convergence radius for the series (2.37) can be found by applying the ratio test, expressed with (2.44) in the form:

$$(2.45) \quad \eta_c = 3\gamma^{\frac{n-2}{3}} [n(n+1)]^{\frac{1}{3}} \lim_{k \rightarrow \infty} k \left| \frac{b_k(n)}{b_{k+1}(n)} \right|^{\frac{1}{3}}.$$

The numerical results for  $\eta_c$  using the first ten terms from the series are presented in Table 2.3. We point out that our result for  $n = 1$  is the same as the Blasius result (2.15).

$n$	0.3	0.5	0.7	1	1.1	1.3	1.5
$\eta_c$	2.612	3.579	4.355	5.688	6.261	7.735	10.225

**Table 2.3**

### 2.3 NON-NEWTONIAN FLUID FLOW DRIVEN BY POWER-LAW VELOCITY PROFILE

The problems of heat and mass transfer in two-dimensional boundary layers on continuous stretching surfaces, moving in a fluid medium, have attracted considerable attention for the last few decades. There are numerous applications in industrial manufacturing processes, such as rolling, wire drawing, glass-fiber and paper production, drawing of plastic films, metal and polymer extrusion and metal spinning.

For Newtonian fluids, the laminar boundary layer to an exterior power law velocity profile of the form  $U_e = \tilde{B}y^\sigma$  was investigated by Weidman et al. [207] for a large range of the power law parameter  $\sigma$ . An analytical solution of the momentum equation in terms of Airy function was proposed for the case  $\sigma = -1/2$ . The power law velocity profile form  $U_e = \tilde{B}y^\sigma$  was proposed by Barenblatt [20] for the mean velocity to fully developed turbulent shear flows, and in [21] Barenblatt and Protokishin proved that  $\sigma = 3/(2 \ln \text{Re})$ . Recently, Magyari et al. [139] have examined the effect of a lateral suction/injection of the fluid for the existence of similarity solutions in the Newtonian case. It was shown that while for  $\sigma = -2/3$  the flow over an impermeable plate to power law shear is not possible, the presence of suction allows for a family of boundary layer solutions. In the case  $\sigma = -1/2$ , the solutions were found both for suction and injection, and the skin friction parameter is independent of the suction/injection parameter.

For both Newtonian fluids [94] and non-Newtonian fluids [95] Guedda has given a theoretical analysis of the existence of the boundary layer similarity flows for a range of exponents  $\sigma$  and  $\tilde{B}$ .

For Newtonian fluid with  $\sigma = 0$  the problem of laminar boundary layer problem is described by the famous Blasius equation [30].

Our interest has been motivated by the work of Cossali [70]. In [46] the similarity flow over an impermeable flat plate driven by a power law velocity profile for Newtonian fluid has been considered, for which power series solutions were found for all the allowed range of the parameter  $\sigma$ .

In this section our aim is to present analysis for the steady-state laminar boundary layer flow, governed by the Ostwald-de Waele power law model of an incompressible non-Newtonian fluid driven by a power law velocity profile. A generalization of the usual Blasius similarity transformation is used to find similarity solutions. We establish the existence of analytic solutions, i.e., solutions are expandible in convergent power series to the momentum boundary layer equation under the general case of the power law velocity profile, thus extending the classical Blasius result for the shear driven case and Cossali's results for non-Newtonian fluid flow when  $n \neq 2$ . Some properties of the solutions are discussed depending on the viscosity power law index.

### 2.3.1 DERIVATION OF THE PROBLEM

Consider a steady two-dimensional laminar flow of an incompressible fluid of density  $\rho$ , past a semi-infinite flat plate. The continuity and momentum equations (2.17) and (2.18) are accompanied by the boundary conditions

$$(2.46) \quad u(x, 0) = 0, \quad v(x, 0) = 0 \quad \text{and} \quad \lim_{y \rightarrow \infty} u(x, y) = U_e,$$

where  $U_e = B_0 y^\sigma$  as  $y \rightarrow \infty$ . In term of the stream-function  $\psi$ , which satisfies (2.6) equations (2.17) and (2.18) can be reduced to the equation

$$(2.47) \quad \frac{\partial \psi}{\partial y} \frac{\partial^2 \psi}{\partial y \partial x} - \frac{\partial \psi}{\partial x} \frac{\partial^2 \psi}{\partial y^2} = \mu_{cn} \frac{\partial}{\partial y} \left[ \left| \frac{\partial^2 \psi}{\partial y^2} \right|^{n-1} \frac{\partial^2 \psi}{\partial y^2} \right],$$

where  $\mu_{cn} = K/\rho$ , with the boundary conditions

$$(2.48) \quad \frac{\partial \psi}{\partial y}(x, 0) = 0, \quad \frac{\partial \psi}{\partial x}(x, 0) = 0,$$

and

$$(2.49) \quad \lim_{y \rightarrow \infty} \frac{\partial \psi}{\partial y}(x, 0) = U_e.$$

To look for similarity solutions we define the stream function  $\psi$  and similarity variable  $\eta$  as

$$(2.50) \quad \psi = Ax^{-\alpha} f(\eta), \quad \eta = Bx^{-\beta} y,$$

where  $A, B, \alpha$  and  $\beta$  are constants to be determined, and  $f(\eta)$  denotes the dimensionless stream function. Using (2.47) and (2.50) we find that the

profile function  $f$  satisfies

$$(2.51) \quad \mu_{cn} B^{2n+1} A^{2n} x^{-(\alpha+2\beta)n-\beta} \left( |f''|^{n-1} f'' \right)' - \alpha B^2 A^2 x^{-2(\alpha+\beta)-1} f f'' + (\alpha + \beta) B^2 A^2 x^{-2(\alpha+\beta)-1} f'^2 = 0$$

Equation (2.51) is an ordinary differential equation if and only if

$$(2.52) \quad (2 - n) \alpha + (1 - 2n) \beta = 1,$$

and  $\alpha + \beta = M$ ; the scaling relation, i.e.,

$$(2.53) \quad \alpha = \frac{M(2n-1)-1}{n+1}, \quad \beta = \frac{M(2-n)+1}{n+1},$$

and the parameters  $A$  and  $B$  satisfy

$$(2.54) \quad \mu_{cn} B^{2n-1} A^{n-2} = 1.$$

Moreover,

$$(2.55) \quad M = -\frac{\sigma}{(2-n)\sigma + (n+1)}.$$

So, function  $f$  satisfies the following boundary value problem

$$(2.56) \quad \left( |f''|^{n-1} f'' \right)' - \alpha f f'' + M f'^2 = 0,$$

$$(2.57) \quad f(0) = 0, \quad f'(0) = 0, \quad \lim_{\eta \rightarrow \infty} f'(\eta) = \tilde{A} \eta^\sigma,$$

where the prime denotes the differentiation with respect to the similarity variable  $\eta$ , and

$$(2.58) \quad \tilde{A} = \tilde{B} / (AB^{1+\sigma}), \quad \sigma + 1 = -\alpha/\beta.$$

With the choice  $B = 1$  we get that

$$(2.59) \quad A = \mu_{cn}^{1/(2-n)}, \quad \tilde{A} = \tilde{B} \mu_{cn}^{-1/(2-n)}, \quad n \neq 2,$$

and the non-dimensional velocity components are obtained by  $f$  as follows:

$$(2.60) \quad u(x, y) = \mu_{cn}^{1/(2-n)} x^{-M} f'(\eta),$$

$$(2.61) \quad v(x, y) = x^{-(\alpha+1)} [\alpha f(\eta) + \beta \eta f'(\eta)].$$

For  $\sigma = 0$ , equation (2.56) is referred to as generalized Blasius equation [38] and for the Newtonian case, equation (2.56) coincides with the well-known Blasius equation (2.10). If  $\sigma = 0$ , then (2.57) is reduced to

$$(2.62) \quad f(0) = 0, \quad f'(0) = 0, \quad \lim_{\eta \rightarrow \infty} f'(\eta) = \tilde{A}.$$

We shall not consider the case  $n = 2$ . For that case with  $\sigma = 0$ ,  $n = 2$ , we refer to the numerical results obtained by Kim et al. [121] and Liao [129].

### 2.3.2 ANALYTIC SOLUTIONS

Our objective is to determine the approximate local solution  $f(\eta)$  to the boundary value problem (2.56), (2.57). We use the shooting method and replace the condition at infinity by one at  $\eta = 0$ . Therefore, (2.56), (2.57) is converted into an initial value problem of (2.56) with initial conditions

$$(2.63) \quad f(0) = 0, \quad f'(0) = 0, \quad f''(0) = \gamma.$$

We suppose that  $n > 0$ ,  $n \neq 2$  and  $f''$  is positive in the neighborhood of zero. We consider (2.56) as a system of the Briot-Bouquet differential equations [59].

In the paper [46], we showed that there exists a formal solution

$$(2.64) \quad f(\eta) = \eta^2 \sum_{k=0}^{\infty} a_k \eta^{3k},$$

where the first three coefficients are known

$$\begin{aligned} a_0 &= \frac{\gamma}{2}, \\ a_1 &= \frac{1}{5!} \left( \frac{\alpha}{n} \gamma^{3-n} - 2M\gamma^2 \right), \\ a_2 &= \frac{1}{8!} \left( \frac{\alpha(21-10n)}{n} \gamma^{2-n} - 10M\gamma \right) \left( \frac{\alpha}{n} \gamma^{3-n} - 2M\gamma^2 \right). \end{aligned}$$

For the determination of coefficients  $a_k$ ,  $k > 2$ , one can use the J.C.P. Miller formula (2.41). From (2.64)

$$(2.65) \quad [f''(\eta)]^{2-n} = \left[ \sum_{k=0}^{\infty} (3k+2)(3k+1)a_k \eta^{3k} \right]^{2-n} = \sum_{k=0}^{\infty} A_k \eta^{3k},$$

$$(2.66) \quad [f''(\eta)]^{1-n} = \left[ \sum_{k=0}^{\infty} (3k+2)(3k+1)a_k \eta^{3k} \right]^{1-n} = \sum_{k=0}^{\infty} C_k \eta^{3k},$$

where coefficients  $A_k$ ,  $C_k$  can be expressed in terms of  $a_k$  ( $k = 0, 1, \dots$ ). Substituting them into equation (2.56) we get

$$\sum_{k=0}^{\infty} (3k+5)(3k+4)(3k+3)a_{k+1} \eta^{3k} - \frac{\alpha}{n} \sum_{k=0}^{\infty} a_k \eta^{3k} \sum_{k=0}^{\infty} A_k \eta^{3k}$$

$$(2.67) \quad +\frac{M}{n} \left[ \eta \sum_{k=0}^{\infty} (3k+2)a_k \eta^{3k} \right]^2 \sum_{k=0}^{\infty} C_k \eta^{3k} = 0.$$

Applying the recursion formula (2.42) for the determination of  $A_k$  and comparing the proper coefficients in (2.67) one can have the necessary values of  $a_k$  for some given values of  $n$ ,  $M$ ,  $\alpha$ . We note that the coefficients obtained by this method for  $n = 1$ ,  $\sigma \neq 0$  are the same as the coefficients of the power series approximation given by Cossali [70] for Newtonian fluids. Moreover, if  $n \neq 1$  and  $\sigma = 0$ , coefficients  $a_k$  are fully consistent with the result obtained in [38]. If  $n = 1$ ,  $\sigma = 0$ , the coefficients coincide with the Blasius results given in (2.14).

### 2.3.3 SOME SPECIAL CASES

In this section we present numerical results obtained for  $\tilde{A} = 1$ , three different values of  $n$  (0.5; 1; 1.5) and three different values of  $\sigma$  ( $-1/2$ ;  $-1/3$ ; 0). Figs. 2.7-2.9 represent the effect of power-law index on  $f'(\eta)/\eta^\sigma$  for  $\sigma = -1/2$ ,  $\sigma = -1/3$ ,  $\sigma = 0$ . We note that Fig. 2.9 is the same as Fig. 2.2. Figs. 2.10-2.12 exhibit how the graph of  $f'(\eta)/\eta^\sigma$  changes for different values of  $n$  ( $n = 0.5$ ;  $n = 1$ ;  $n = 1.5$ ). Figs. 2.10-2.12 exhibit how the graph of  $f'(\eta)/\eta^\sigma$  changes for different values of  $n$  ( $n = 0.5$ ;  $n = 1$ ;  $n = 1.5$ ).

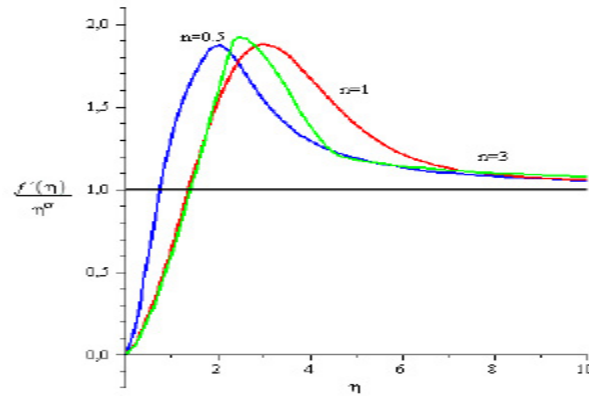


**Fig. 2.7**  $\sigma = -1/2$

For  $\sigma = 0$ , the numerical results for  $\gamma$  and the boundary layer thickness  $\eta_{bl}$  are exhibited in Table 2.4.

2. BOUNDARY LAYER FLOW ON A FLAT PLATE

---

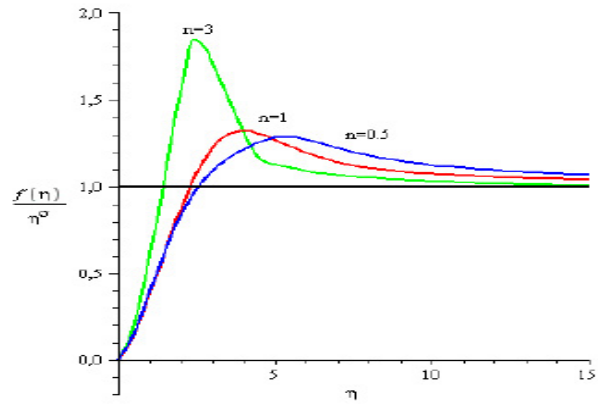


Fig. 2.8  $\sigma = -1/3$

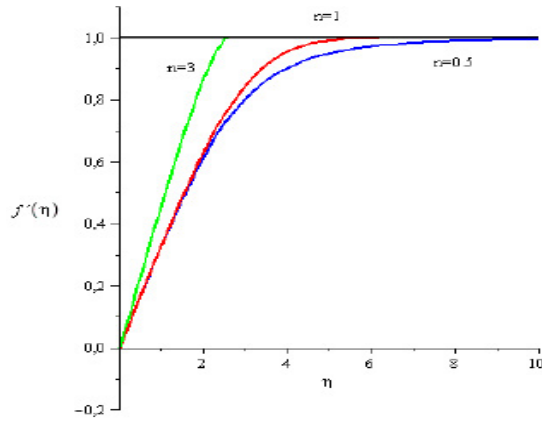


Fig. 2.9  $\sigma = 0$

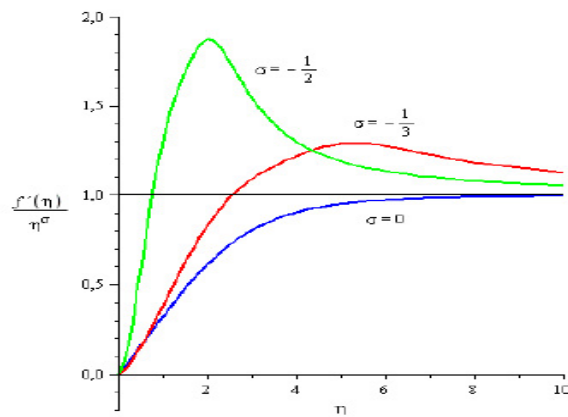


Fig. 2.10  $n = 0.5$

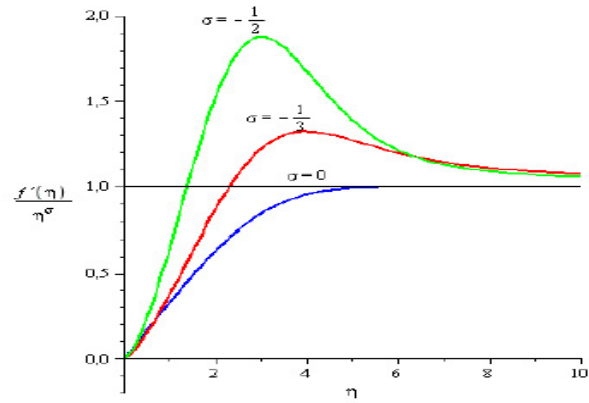


Fig. 2.11  $n = 1$

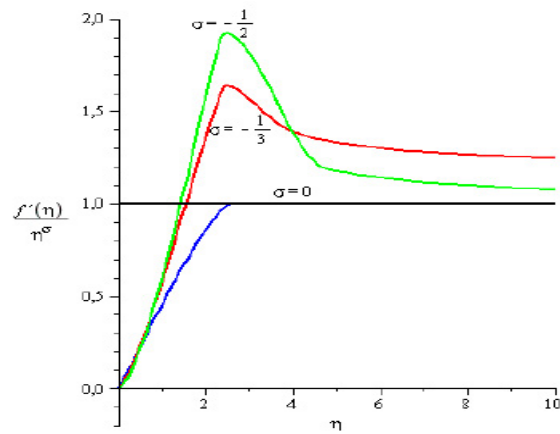


Fig. 2.12  $n = 1.5$

$n$	$\gamma$	$\gamma^n$	$\eta_{bl}$
0.5	0.331226	0.57552	3.579
1	0.332057	0.332057	5.688
1.5	0.364798	0.22033	10.225

Table 2.4 Case  $\sigma = 0$ 

In case of  $\sigma = -1/2$ , the value of  $f''(0)$  can be obtained as (see [95])

$$(2.68) \quad \gamma = \left( \frac{2}{3n} \right)^{\frac{1}{n}}.$$

Applying (2.68) for the determination of the coefficients  $a_k$  from (53) we obtain

$$\begin{aligned} a_0 &= \frac{\gamma}{2} \\ a_1 &= \frac{1}{3} \frac{1}{5!} \frac{1}{n} \left( \frac{\gamma^{3-n}}{n} + 2\gamma^2 \right) \\ a_2 &= \frac{1}{3^2} \frac{1}{8!} \frac{1}{n^2} \left( \frac{\gamma^{3-n}}{n} + 2\gamma^2 \right) \left( \frac{21-10n}{n} \gamma^{2-n} + 10\gamma \right) \\ &\vdots \end{aligned}$$

and for  $f(\eta)$  the following approximations are valid:

$$\mathbf{n=0.5:} \quad f(\eta) = \eta^2(0.888888888 - 0.819387287 \cdot 10^{-1}\eta^3 + 0.152220095 \cdot 10^{-1}\eta^6 - 0.335551670 \cdot 10^{-2}\eta^9 + 0.922430723 \cdot 10^{-3}\eta^{12} - 0.269036066 \cdot 10^{-3}\eta^{15})$$

$$\mathbf{n=1:} \quad f(\eta) = \eta^2(0.33333333 - 0.370370370 \cdot 10^{-2}\eta^3 + 0.514403292 \cdot 10^{-4}\eta^6 - 0.427226078 \cdot 10^{-6}\eta^9 + 0.464427254 \cdot 10^{-8}\eta^{12} - 0.521840015 \cdot 10^{-10}\eta^{15})$$

$$\mathbf{n=1.5:} \quad f(\eta) = \eta^2(0.291193488 - 0.180489903 \cdot 10^{-2}\eta^3 + 0.10595952 \cdot 10^{-4}\eta^6 - 0.856898347 \cdot 10^{-8}\eta^9 + 0.187290094 \cdot 10^{-10}\eta^{12} - 0.557628629 \cdot 10^{-13}\eta^{15})$$

$n$	$\gamma$	$\gamma^n$	$\eta_{bl}$
0.5	1.777778	1.333333	1.439
1	0.666667	0.666667	4.465
0.5	0.582387	0.444444	6.951

Table 2.5 Case  $\sigma = -1/2$ 

According to the numerical results in the two cases ( $\sigma = 0$ ;  $\sigma = -1/2$ ), increasing the power-law exponent leads to an increase in the thickness  $\eta_{bl}$ , or in  $\gamma$ .

We note that the power series formulation of the similarity solution of the Newtonian flow over an impermeable flat plate driven by a power law velocity profile obtained by Cossali [70] can be generalized to non-Newtonian fluid flow with Ostwald-de Waele power law nonlinearity when for the power

law index the condition  $n \neq 2$  holds. The coefficients of the more general problem coincide with the coefficients obtained for problems related to special values of the parameters.

### 3 BOUNDARY LAYER FLOW DUE TO A MOVING FLAT PLATE IN AN OTHERWISE QUIESCENT FLUID

The study of flow generated by a moving surface in an otherwise quiescent fluid plays a significant role in many material processing applications such as hot rolling, metal forming and continuous casting (see e.g., [9], [87], [196]). Boundary layer flow induced by the uniform motion of a continuous plate in a Newtonian fluid has been analytically studied by Sakiadis [176] and experimentally by Tsou et al. [205]. A polymer sheet extruded continuously from a die traveling between a feed roll and a wind-up roll was investigated by Sakiadis [175], [176]. He pointed out that the known solutions for the boundary layer on surfaces of finite length are not applicable to the boundary layer on continuous surfaces. In the case of a moving sheet of finite length, the boundary layer grows in a direction opposite to the direction of motion of the sheet. Figure 3.1 shows the model of a long continuous plane sheet which issues from a slot and moves steadily to the right through an otherwise quiescent fluid environment. Tsou et al. [205] showed in their analytical and experimental study that the obtained analytical results for the laminar velocity field is in excellent agreement with the measured data, therefore it validates that the mathematical model for boundary layer on a continuous moving surface describes a physically realizable flow.

In tribology it is important and useful to study the behavior of lubricants on solid surfaces and their role in friction. In tribological systems, lubricant reduces adhesion, friction and wear. Among the lubricant properties, viscosity and its dependence on shear rate are investigated in the literature ([108], [145], [214]). It is known that the relative velocity between the moving surface and each layer of the lubricant is affected by the lubricant viscosity. In a thin boundary layer, the wall shear stress and from this the friction drag caused by the shear next to the wall can be estimated. This drag depends on the fluid properties, and on the shape, size and speed of the solid object submerged in the fluid. Journal bearing is the most commonly used application of the hydrodynamic lubrication theory. The friction loss in the bearing is caused by shearing of the lubricant film. Journal bearings are designed such that during the operation the hydrodynamic lubrication is ensured when there is no solid-solid contact. In this case, the friction results entirely from the shear stress within the lubricant. Hydrodynamic lubrication is the most desired regime of lubrication since it is possible to achieve very low coefficients of friction, and there is no wear. The viscosity of the lubricant is an important factor as hydrodynamic friction increases

3. BOUNDARY LAYER FLOWS DUE TO A MOVING FLAT PLATE IN AN OTHERWISE  
QUIESCENT FLUID

---

with viscosity. The higher the viscosity, the higher the friction between the lubricant and the solid surface, but the thicker the hydrodynamic film. The heat generated by friction will reduce the viscosity and also the thickness of the film that makes the solid-solid contact more likely [214].

The flow of an incompressible fluid over a stretching surface has applications in the extrusion of a polymer sheet from a die or in the drawing of plastic film. During the manufacturing process of these sheets, the melt issues from a slit and is stretched to achieve the desired thickness. Material traveling between the feed roll and wind-up roll or on conveyor belts possess the characteristics of a moving continuous surface. The quality of the final product strictly depends on the stretching rate.

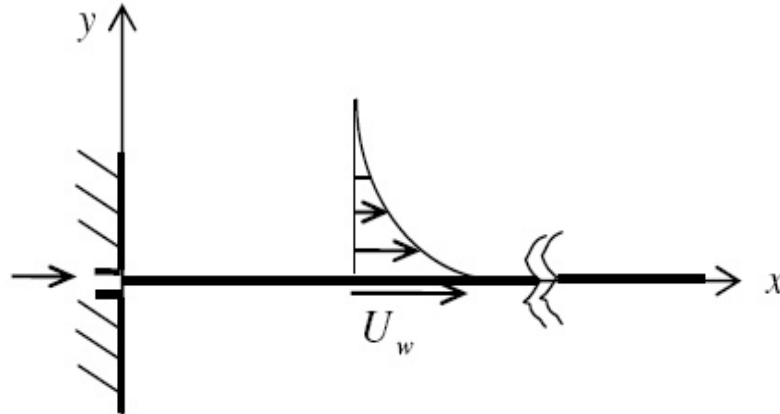


**Fig. 3.1** The physical model on a continuous moving surface

Crane [72] has studied the boundary layer flow of a Newtonian fluid caused by a linearly stretched surface. It is one of the rare problems in fluid dynamics that admits an exact closed form solution. Weidman and Magyari [208] investigated the solutions to the boundary layer equations for different types of stretching when the stretching velocity is linear, a quadratic or general polynomial, and for exponential and periodic wall stretching velocity.

It has been extended in various ways to include many important physical features, see, for example, Kumaran and Ramanaiyah [127], Banks [19], and Magyari and Keller [135]. Crane's original solution was provided for an impermeable plate. The flat surface with wall suction or injection has practical interest in mass transfer, drying, transpiration cooling, etc. The effect of transpiration across a permeable surface moving at constant speed was considered by Erickson et al. [82] and that for a linearly increasing surface was examined by Gupta and Gupta [96]. Further investigations for permeable

stretching sheets are given in Magyari and Keller [137]. Authors of many papers are interested in finding out analytical solutions and if it does not exist, then to suggest suitable approximate solutions which can be used by practising engineers.

We consider in Section 3.1 the boundary layer of Newtonian fluid over an impermeable stretching wall [43] and in Section 3.2 the boundary layer of a power-law non-Newtonian fluid along an impermeable sheet moving with a constant velocity [39].

### 3.1 NEWTONIAN FLUID FLOW

Analytic solutions to similarity boundary layer equations are given for boundary layer flows of Newtonian fluid over a stretching wall with power law stretching velocity. The Crane's solution is generalized as the solution to the problem is given by an exponential series. We give how the coefficients can be evaluated.

#### 3.1.1 GOVERNING EQUATIONS FOR BOUNDARY LAYERS

The problem considered here is the steady boundary layer flow due to a moving flat surface in an otherwise quiescent Newtonian fluid medium moving at a speed of  $U_w(x)$ . In the absence of body force and external pressure gradient, laminar boundary layer equations expressing conservation of mass and the momentum boundary layer equations for an incompressible fluid are written as (1.1) and

$$(3.1) \quad u \frac{\partial u}{\partial x} + v \frac{\partial u}{\partial y} = \mu_c \frac{\partial^2 u}{\partial y^2},$$

where  $\mu_c$  is the kinematic viscosity of the ambient a fluid which will be assumed constant [127]. We consider the boundary-layer flow induced by a continuous surface stretching with velocity  $U_w(x)$ . The surface is assumed in general to be permeable and a lateral suction/injection with a certain velocity distribution  $v_w(x)$  is applied. Accordingly, the boundary conditions are

$$(3.2) \quad u(x, 0) = U_w(x), \quad v(x, 0) = v_w(x), \quad \lim_{y \rightarrow \infty} u(x, y) = 0$$

The streamfunction  $\psi$  is formulated by (2.6) and equation (3.1) reduces to

$$(3.3) \quad \frac{\partial \psi}{\partial y} \frac{\partial^2 \psi}{\partial y \partial x} - \frac{\partial \psi}{\partial x} \frac{\partial^2 \psi}{\partial y^2} = \mu_c \frac{\partial^2 \psi}{\partial y^3}.$$

3. BOUNDARY LAYER FLOWS DUE TO A MOVING FLAT PLATE IN AN OTHERWISE QUIESCENT FLUID

---

Sakiadis studied the boundary layer over a continuously stretching surface with a constant speed. For similarity, only a certain variation of the surface velocity  $U_w(x)$  is allowed. Following the papers by Sakiadis [175] and Tsou et al. [205], the boundary condition on the surface was generalized such that the velocity was extended to be a function of distance from the slot, where the surface was stretched out. A power-law velocity distribution was the most common case. We take the velocity of the plate in the form

$$U_w(x) = Ax^\kappa, \quad v_w(x) = B x^{(\kappa-1)/2},$$

where  $A$ ,  $B$  and  $\kappa$  are constants,  $A > 0$ . The case  $B < 0$  corresponds to the suction and  $B > 0$  to the injection of the fluid. If the wall is impermeable then  $B = 0$ . Under transformation

$$\psi = \sqrt{\frac{2\mu_c}{A(\kappa+1)}} Ax^{\frac{\kappa+1}{2}} f(\eta), \quad \eta = \sqrt{\frac{A(\kappa+1)}{2\mu_c}} yx^{\frac{\kappa-1}{2}}$$

equation (3.3) can be written

$$(3.4) \quad f''' + ff'' - \frac{2\kappa}{\kappa+1} f'^2 = 0,$$

and the boundary conditions (3.2) become

$$(3.5) \quad f(0) = f_w, \quad f'(0) = 1, \quad \lim_{\eta \rightarrow \infty} f'(\eta) = 0,$$

where

$$f_w = -B \left[ \mu_c A \frac{\kappa+1}{2} \right]^{-\frac{1}{2}}.$$

Now, the velocity components are given by

$$\begin{aligned} u(x, y) &= Ax^\kappa f'(\eta), \\ v(x, y) &= - \left( \frac{2\mu_c A}{\kappa+1} \right)^{1/2} x^{(\kappa-1)/2} \left[ \frac{\kappa+1}{2} f(\eta) + \frac{\kappa-1}{2} \eta f'(\eta) \right]. \end{aligned}$$

We note that the same boundary value problem appears for the steady free convection flow over a vertical semi-infinite flat plate embedded in a fluid saturated porous medium of ambient temperature  $T_\infty$ , and the temperature of the plate is  $T_w = T_\infty + \bar{A} x^\kappa$ . There is a difference in the region of  $\kappa$  between the two physical problem. For flows in a porous medium, there is a physical meaning when  $-1/2 < \kappa < +\infty$  (see [113]), and for boundary layer flows over a stretching wall  $-\infty < \kappa < -1$ , and  $-1/2 < \kappa < +\infty$  [19].

Banks [19] has proved if the wall is impermeable then the boundary value problem (3.4), (3.5) does not admit similarity solution when  $-1 < \kappa \leq -1/2$ . Numerical solutions were given in papers [19] and [113]. For some special cases of  $\kappa$  problem (3.4), (3.5) is exactly solvable. These particular cases are  $\kappa = 1$  and  $\kappa = -1/3$ . For impermeable case with  $\kappa = 1$  we refer to the exact solution by Crane [72] and for the permeable case Gupta and Gupta [96]. For an impermeable case with  $\kappa = -1/3$  the exact solution in [19] and the exact analytic solution for the permeable case by Magyari and Keller [137].

By generalizing Crane's solution we give exponential series solution to the nonlinear boundary value problem (3.4), (3.5) (see [43]) for both permeable and impermeable cases. Numerical results are also presented.

### 3.1.2 EXACT SOLUTIONS

Exact solutions are known for some special values of  $\kappa$ . These are  $\kappa = 1$  and  $\kappa = -1/3$ .

i.)  $\kappa = 1$ :

The solution to the boundary-value problem (3.4), (3.5) for the velocity  $U_w(x) = Ax$ , ( $\kappa = 1$ ) of an impermeable surface,  $v_w(X) = 0$ , has been reported by Crane [72]. Thus, the stream function of Crane's problem has the form

$$\psi = \sqrt{\frac{\mu_c}{A}} Ax f(\eta), \quad \eta = \sqrt{\frac{A}{\mu_c}} y,$$

where  $f(\eta)$  is the solution to the ordinary differential equation

$$f''' + f f'' - f'^2 = 0,$$

subject to the boundary conditions

$$f(0) = 0, \quad f'(0) = 1, \quad \lim_{\eta \rightarrow \infty} f'(\eta) = 0.$$

Crane's well known solution for  $f(\eta)$  when is

$$(3.6) \quad f(\eta) = 1 - e^{-\eta},$$

and the velocity components are

$$\begin{aligned} u(x, y) &= A x e^{-\eta}, \\ v(x, y) &= -(\mu_c A)^{1/2} (1 - e^{-\eta}). \end{aligned}$$

For that solution one gets  $f''(0) = -1$ .

For permeable case the solution has been given by Gupta and Gupta [96]

$$(3.7) \quad f(\eta) = f_w - \frac{1}{f_0} [1 - e^{f_0\eta}],$$

with

$$f_0 = -\frac{1}{2} [f_w + \sqrt{f_w^2 + 4}].$$

In this way the velocity field is obtained as

$$\begin{aligned} u(x, y) &= A x e^{f_0\eta}, \\ v(x, y) &= -(\mu_c A)^{1/2} \left[ f_w - \frac{1}{f_0} (1 - e^{f_0\eta}) \right], \end{aligned}$$

and  $f''(0) = f_0$ .

ii.)  $\kappa = -1/3$ :

The exact solution for  $\kappa = -1/3$  and  $f_w = 0$  can be given

$$f(\eta) = \sqrt{2} \tanh(\eta/\sqrt{2}),$$

and for that solution one obtains  $f''(0) = 0$ .

### 3.1.3 THE EXPONENTIAL SERIES SOLUTION

The aim of this section is to show that Crane's solution can be generalized for any  $\kappa$  by exponential series solution to the boundary value problem (3.4), (3.5). We present a method how to determine the approximate local solution  $f(\eta)$ . We use the shooting method and replace the condition at infinity by one at  $\eta = 0$ . Therefore, (3.4), (3.5) is converted into an initial value problem of (3.4) with initial conditions

$$(3.8) \quad f(0) = f_w, \quad f'(0) = 1, \quad f''(0) = \gamma.$$

We consider the nonlinear differential equation (3.4) as a system of Briot-Bouquet differential equations [59]. Applying the results of paper [43], we can assume that

$$(3.9) \quad f(\eta) = \alpha \left( A_0 + \sum_{i=1}^{\infty} A_i a^i e^{-\alpha i \eta} \right),$$

where  $\alpha > 0$ ,  $A_0 = 1$ , and  $A_i$  ( $i = 1, 2, \dots$ ) are coefficients.

The conditions in (3.5) yield the following equations:

$$(3.10) \quad \alpha \left( A_0 + \sum_{i=1}^{\infty} A_i a^i \right) = f_w,$$

$$(3.11) \quad -\alpha^2 \sum_{i=1}^{\infty} i A_i a^i = 1.$$

It is evident that the third of the boundary conditions is automatically satisfied. Substituting (3.9) into (3.4) one gets

$$-\sum_{i=1}^{\infty} i^3 A_i Z^i + \left( A_0 + \sum_{i=1}^{\infty} A_i Z^i \right) \sum_{i=1}^{\infty} i^2 A_i Z^i - \frac{2\kappa}{\kappa+1} \left( \sum_{i=1}^{\infty} i A_i Z^i \right)^2 = 0$$

or

$$-\sum_{i=1}^{\infty} i^3 A_i Z^i + A_0 \sum_{i=1}^{\infty} i^2 A_i Z^i + \sum_{i=2}^{\infty} \sum_{k=1}^{i-1} k^2 A_k A_{i-k} Z^i - \frac{2\kappa}{\kappa+1} \sum_{i=1}^{\infty} \sum_{k=1}^{i-1} k(i-k) A_k A_{i-k} Z^i = 0.$$

Equating the coefficients of like powers of  $Z$ , we get recurrence relations for  $A_2, A_3, \dots$  and we obtain

$$\begin{aligned} A_2 &= -\frac{1}{4} A_1^2 \frac{\kappa-1}{\kappa+1}, \\ A_3 &= \frac{1}{72} A_1^3 \frac{(\kappa-1)(3\kappa-5)}{(\kappa+1)^2}, \\ A_4 &= -\frac{1}{864} A_1^4 \frac{(\kappa-1)(6\kappa^2-19\kappa+17)}{(\kappa+1)^3}, \\ A_5 &= \frac{1}{86400} A_1^5 \frac{(\kappa-1)(93\kappa^3-464\kappa^2+783\kappa-484)}{(\kappa+1)^4}, \\ A_6 &= -\frac{1}{2592000} A_1^6 \frac{(\kappa-1)(432\kappa^4-2889\kappa^3+7461\kappa^2-8759\kappa+4139)}{(\kappa+1)^5}, \\ A_7 &= \frac{1}{4572288000} A_1^7 \frac{(\kappa-1) P_5(\kappa)}{(\kappa+1)^6}, \\ P_5(\kappa) &= 115839\kappa^5 - 983892\kappa^4 + 3399550\kappa^3 - 6012140\kappa^2 \\ &\quad + 5447171\kappa - 2081728 \\ A_8 &= -\frac{1}{64012032000} A_1^8 \frac{(\kappa-1) P_6(\kappa)}{(\kappa+1)^7}, \\ P_6(\kappa) &= 44854\kappa^6 - 2521077\kappa^5 + 10974320\kappa^4 - 25899165\kappa^3 + 35072231\kappa^2 \\ &\quad - 25921218\kappa + 8309255 \\ A_9 &= \frac{1}{9217732608000} A_1^9 \frac{(\kappa-1) P_7(\kappa)}{(\kappa+1)^8}, \\ P_7(\kappa) &= 5288733\kappa^7 - 64112391\kappa^6 + 337072482\kappa^5 - 997781298\kappa^4 \\ &\quad + 1799062257\kappa^3 - 1980424339\kappa^2 + 1236353168\kappa - 341103412 \\ &\quad \vdots \end{aligned}$$

The coefficients  $A_2, A_3, A_4, \dots$  are expressed as functions of  $\kappa$ . We note that our computations indicate that all the coefficients obtained above can be written in the form

$$A_n = A_1^n \frac{\kappa - 1}{(\kappa + 1)^{n-1}} P_{n-2}(\kappa),$$

where  $P_{n-2}$  is a polynomial of  $\kappa$  of order  $n-2$ . When  $\kappa = 1$  is substituted then we get that each coefficient  $A_k, k > 1$  is equal to zero. With  $A_1 = 1$ , this case results the Crane's solution (3.6) or Gupta's solution (3.7) for impermeable or permeable case, respectively.

$\kappa$	$a$	$\alpha$	$f''(0)$
-5	-0.7410	0.8687	-1.4033
-4	-0.7207	0.8575	-1.4417
-3	-0.6831	0.8364	-1.5156
-2	-0.5915	0.7826	-1.7166
-1.5	-0.4678	0.7040	-2.0337
-1/3	-1.5919	0.7957	-5.2423
-1/6	-1.5089	1.1868	-1.1407
-1/8	-1.4521	1.1859	-0.7543
-1/10	-1.4207	1.1786	-0.6684
0	-1.3186	1.1419	-0.6433
1/3	-1.1358	1.0628	-0.8300
1/2	-1.0864	1.0403	-0.8896
3/4	-1.0351	1.0166	-0.9540
1	-1	1	-1

**Table 3.1. For impermeable case ( $f_w = 0$ )**

The shear stress at the surface is

$$(3.12) \quad \tau_w = \left[ \rho \mu A^3 \frac{\kappa + 1}{2} \right]^{\frac{1}{2}} x^{\frac{3\kappa-1}{2}} f''(0),$$

where  $f''(0)$  can be calculated as

$$f''(0) = \alpha^3 \sum_{i=1}^{\infty} i^2 A_i a^i.$$

From system (3.10), (3.11) with coefficients  $A_2, A_3, A_4, \dots$  and with the choice of  $A_1 = 1$  one can obtain the values of parameters  $a$  and  $\alpha$ . Table 3.1 and Table 3.2 represent the numerical results for some values of  $\kappa \in$

3. BOUNDARY LAYER FLOWS DUE TO A MOVING FLAT PLATE IN AN OTHERWISE  
QUIESCENT FLUID

---

$(-\infty, -1) \cup (-1/2, +\infty)$ ,  $f_w = 0$  and  $f_w = 1$  on the base of the first 10 terms in the series.

The radius of the convergence of the series can be found by applying the ratio test and the series converges absolutely for

$$\eta > -\frac{1}{\alpha} \left[ \ln \left( \lim_{n \rightarrow \infty} \left| \frac{A_n}{A_{n+1}} \right| \right) - \ln |a| \right].$$

We note that the sequence of terms  $A_n/A_{n+1}$  converges very slowly, and for the determination of the convergence interval an alternative method was given by Samuel and Hall [174].

$\kappa$	$a$	$\alpha$	$f''(0)$
-5	-0.3195	1.5663	-1.9547
-4	-0.3140	1.5615	-1.9883
-3	-0.3036	1.5523	-2.0538
-2	-0.2765	1.5279	-2.2376
-1.5	-0.2359	1.4889	-2.5620
-1/3	-0.5357	1.7320	-1.0014
-1/6	-0.4753	1.6890	-1.2179
-1/8	-0.4656	1.6819	-1.2553
-1/10	-0.4604	1.6781	-1.2757
0	-0.4433	1.6654	-1.3445
1/3	-0.4099	1.6400	-1.4878
1/2	-0.4000	1.6323	-1.5325
3/4	-0.3985	1.6240	-1.5820
1	-0.3820	1.6180	-1.6180

**Table 3.2.** For permeable case ( $f_w = 1$ )

### 3.2 NON-NEWTONIAN FLUID FLOW

The problems of the boundary layer over a continuous surface moving in an otherwise quiescent fluid environment have attracted considerable attention ([58], [85], [93], [130], [131], [137], [138]). In this section we use the power-law rheological model for the flow of a fluid over a sheet. In the absence of an exact solution in closed form, numerical solutions for the velocity distribution in the boundary layer for different power exponents will be presented, and the dependence of the skin friction parameter and the boundary layer thickness on the power exponent  $n$  are examined.

### 3.2.1 BOUNDARY LAYER EQUATIONS

Consider the two-dimensional steady flow of a non-Newtonian fluid of density  $\rho$  modeled by a power law fluid due to Ostwald-de Waele over a flat plate moving continuously with a constant velocity  $U_w$  in an otherwise quiescent fluid medium [39].

The boundary layer equations are

$$(3.13) \quad \frac{\partial u}{\partial x} + \frac{\partial v}{\partial y} = 0$$

and

$$(3.14) \quad u \frac{\partial u}{\partial x} + v \frac{\partial u}{\partial y} = \frac{K}{\rho} \frac{\partial}{\partial y} \left[ \left| \frac{\partial u}{\partial y} \right|^{n-1} \frac{\partial u}{\partial y} \right].$$

The boundary conditions of the flow can be expressed as

$$(3.15) \quad u(x, 0) = U_w, \quad v(x, 0) = 0, \quad \lim_{y \rightarrow \infty} u(x, y) = 0.$$

If a flat plate in surroundings at rest is moved with constant velocity  $U_w$ , the no-slip condition means that boundary layer exists close to the wall (see Fig. 3.1). The moving plate emerges from the wall. This fixes the origin of the coordinate system and has an analog to the leading edge of a flat plate at zero incidence in a flow. Both permit only then a steady solution in a spatially fixed coordinate system.

### 3.2.2 SIMILARITY SOLUTION

The stream function  $\psi$  is defined by (2.6) then

$$(3.16) \quad \frac{\partial \psi}{\partial y} \frac{\partial^2 \psi}{\partial y \partial x} - \frac{\partial \psi}{\partial x} \frac{\partial^2 \psi}{\partial y^2} = \mu_{cn} \frac{\partial}{\partial y} \left[ \left| \frac{\partial^2 \psi}{\partial y^2} \right|^{n-1} \frac{\partial^2 \psi}{\partial y^2} \right].$$

The boundary conditions can be expressed for  $\psi$  as

$$\frac{\partial \psi}{\partial y}(x, 0) = U_w, \quad \frac{\partial \psi}{\partial x}(x, 0) = 0, \quad \lim_{y \rightarrow \infty} \frac{\partial \psi}{\partial y}(x, 0) = 0.$$

In (3.16) applying the similarity variables

$$\psi(x, y) = \mu_{cn}^{\frac{1}{n+1}} U_w^{\frac{2n-1}{n+1}} x^{\frac{1}{n+1}} f(\eta) \quad \text{and} \quad \eta = \mu_{cn}^{-\frac{1}{n+1}} U_w^{\frac{2-n}{n+1}} y x^{-\frac{1}{n+1}},$$

one can get the nonlinear ordinary differential equation

$$(3.17) \quad \left(|f''|^{n-1} f''\right)' + \frac{1}{n+1} f f'' = 0$$

with boundary conditions

$$(3.18) \quad f(0) = 0, \quad f'(0) = 1, \quad \lim_{\eta \rightarrow \infty} f'(\eta) = 0.$$

**Remarks.** (i) Let us note that from (3.17) it follows  $f''(\eta) < 0$  in  $(0, +\infty)$  and

$$\lim_{\eta \rightarrow \infty} f''(\eta) = 0.$$

(ii) Equation (3.17) is the same as the Blasius equation for  $n = 1$ , but the boundary conditions differ from the usual conditions applied in case of Blasius problem (see Section 2.1).

Here, the non-dimensional velocity components are obtained by  $f$  as follows:

$$\begin{aligned} u(x, y) &= U_w f'(\eta), \\ v(x, y) &= v^*(x) [\eta f'(\eta) - f(\eta)], \end{aligned}$$

with

$$v^*(x) = \frac{U_w}{n+1} \text{Re}_x^{-\frac{1}{n+1}},$$

when for power-law non-Newtonian fluids the local Reynolds number  $\text{Re}_x$  is defined by

$$\text{Re}_x = \frac{\rho U_w^{2-n} x^n}{K}.$$

### 3.2.3 NUMERICAL RESULTS

Equation (3.17) subject to conditions (3.18) must be solved. The shooting method is applied by using the standard fourth order Runge-Kutta method for the determination of  $f'$  which provides the velocity component  $u$ . The calculations were done by using Maple 12 for three various parameters of  $n$  ( $n = 0.3; 0.7; 1$ ). The numerical integration is restricted to the finite dimensions ( $\eta_{\max} = 300$ ), where we ensure the condition  $\lim_{\eta \rightarrow \eta_{\max}} f'(\eta) = 0$ .

Velocity profiles  $f'(\eta) = u(x, y)/U_w$ , calculated from the boundary value problem (3.17), (3.18) are seen in Fig. 3.2. plotted for pseudoplastic fluids. Generally, the shear stress at the wall is of prime interest. From (1.11) and (3.2.2) we get

$$(3.19) \quad \tau_w(x) = \left[ \frac{\rho^n \mu U_w^{3n}}{x^n} \right]^{\frac{1}{n+1}} |f''(0)|^{n-1} f''(0).$$

3. BOUNDARY LAYER FLOWS DUE TO A MOVING FLAT PLATE IN AN OTHERWISE QUIESCENT FLUID

---

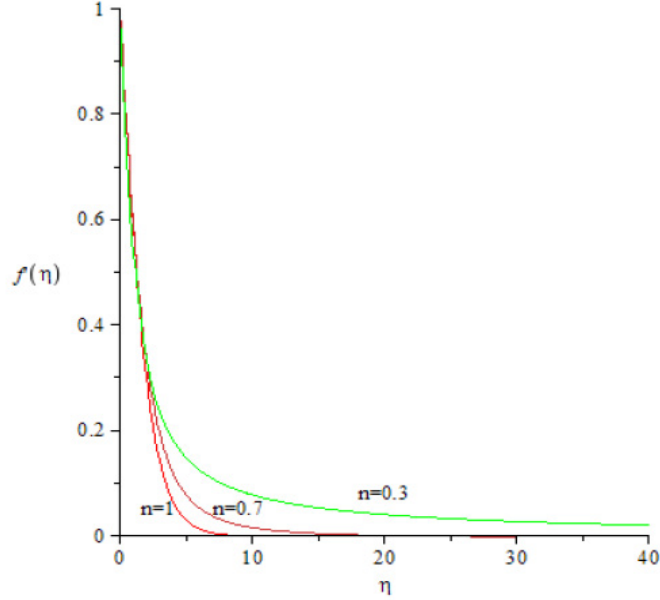


Fig. 3.2 Dimensionless velocity profiles for  $n=0.3, 0.7, 1$

The shear stress parameter  $-|f''(0)|^{n-1} f''(0)$  can be determined from the numerical solution (see Table 3.3).

$n$	$-f''(0)$	$- f''(0) ^{n-1} f''(0)$
0.3	0.5539	0.8376
0.7	0.4568	0.5778
1	0.4437	0.4437

Table 3.3.

On the base of Table 3.3. and Fig. 3.2 we note that the skin friction parameter  $[-f''(0)]^n$  decreases with an increase of  $n$  and it gives the following conclusions:

- (i) by a small  $n$  fluid exert a greater shear stress on the plate,
- (ii) the boundary thickness tends to increase with decreasing power law index  $n$ .

For Newtonian fluid and continuous surface boundary layer  $f''(0) = -0.4437$  while the corresponding numerical constant for the Blasius flow is 0.332 [205]. Thus, the friction coefficient for continuous moving surface exceeds that for the flat plate.

## 4 BOUNDARY LAYER FLOW ON A MOVING WALL

### 4.1 NEWTONIAN FLUID FLOW

The theoretical analysis for the boundary layer flow of a non-Newtonian fluid, represented by a power-law model, over a flat surface which has a constant velocity opposite in direction to that of the uniform mainstream or in the same direction as the uniform mainstream is examined. Boundary layer behavior on a moving surface is an important type of flow, which occurs in a number of engineering processes, e.g., the cooling of polymer films or sheets and metallic plates on conveyers.

Historically, in 1908, the boundary layer flow past a steady flat surface was the first example considered by Blasius. Weyl [212] established the existence of a unique solution and Callegari and Friedman [61] developed an analytical solution to the classical problem of a uniform stream past a semi-infinite flat plate. In 1968, Steinheuer [191] examined the boundary layer above a moving surface in the same or in the opposite direction of the main stream. In 1972, Klemp and Acrivos [123] studied the Blasius problem when the plate moves in the direction opposite to that of main stream. In both papers ([123], [191]) on the basis of numerical results, the authors showed that similarity solutions of such boundary layer problems exist up to a certain critical value of the velocity ratio  $U_w/U_\infty$ . Hussaini and Lakin [110] have proved this fact and Hussaini et al. [111] studied the analyticity of the solutions. It turned out that for a semi-infinite plate, the existence of solutions depends on the ratio of the plate surface velocity to the free stream velocity. It has been proved that a solution exists only if this parameter does not exceed a certain critical value, and numerical calculations were done to show that this solution is non-unique [152].

We recall that  $x \geq 0$  and  $y \geq 0$  denote the Cartesian coordinates along and normal to the plate with  $y = 0$  is the plate and the coordinate  $x$  is as taken positive in the direction of the mainstream. The plate origin is located at  $x = y = 0$ .

The governing differential equations for Newtonian fluids in a two-dimensional case are the following:

$$(4.1) \quad \frac{\partial u}{\partial x} + \frac{\partial v}{\partial y} = 0$$

and

$$(4.2) \quad u \frac{\partial u}{\partial x} + v \frac{\partial u}{\partial y} = \frac{\mu}{\rho} \frac{\partial^2 u}{\partial y^2},$$

where  $u$  and  $v$  represent the components of the fluid velocity in the direction of increasing  $x$  and  $y$ .

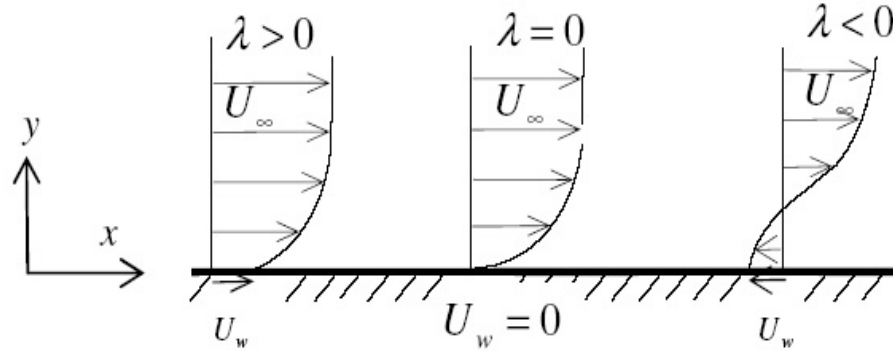


Fig. 4.1 Velocity profiles in the boundary layer for velocity ratio  $\lambda$  ( $\lambda > 0$ ,  $\lambda = 0$ ,  $\lambda < 0$ )

## 4.2 NON-NEWTONIAN FLUID FLOW

Since the non-linear fluid rheology is encountered in numerous industrial applications, the study of non-Newtonian fluid motion is an important part of the fluid mechanics. The power-law model provides an adequate representation of many non-Newtonian fluids over the most important range of shear stress. In 1960, the theoretical analysis of a non-Newtonian power-law problem was first performed in [4] and [179]. In the first paper, the authors derived the equations governing the similarity flow of a non-Newtonian fluid, and obtained numerical similarity solutions to the boundary-layer equations. Recently, for non-Newtonian power-law fluid the variation of the velocity profiles and of the skin friction coefficient have been determined numerically for different values of velocity ratio parameter and power-law index and the effects of these parameter have been investigated by Ishak and Bachok [114].

### 4.2.1 BOUNDARY LAYER EQUATION

Consider an incompressible uniform parallel flow of the non-Newtonian fluid, with a constant velocity  $U_\infty$  along an impermeable semi-infinite flat plate whose surface is moving with a constant velocity  $U_w$  in the opposite direction to the main stream.

The governing differential equations in a two-dimensional case are the

following:

$$(4.3) \quad \frac{\partial u}{\partial x} + \frac{\partial v}{\partial y} = 0$$

and

$$(4.4) \quad u \frac{\partial u}{\partial x} + v \frac{\partial u}{\partial y} = \frac{K}{\rho} \frac{\partial}{\partial y} \left[ \left| \frac{\partial u}{\partial y} \right|^{n-1} \frac{\partial u}{\partial y} \right].$$

The appropriate boundary conditions are:

$$(4.5) \quad u(x, 0) = -U_w, \quad v(x, 0) = 0, \quad \lim_{y \rightarrow \infty} u(x, y) = U_\infty.$$

In terms of the stream function  $\psi$  defined in (2.6) equation (4.3) is satisfied automatically and equation (4.4) can be written as

$$(4.6) \quad \frac{\partial \psi}{\partial y} \frac{\partial^2 \psi}{\partial y \partial x} - \frac{\partial \psi}{\partial x} \frac{\partial^2 \psi}{\partial y^2} = \mu_{cn} \frac{\partial}{\partial y} \left[ \left| \frac{\partial^2 \psi}{\partial y^2} \right|^{n-1} \frac{\partial^2 \psi}{\partial y^2} \right].$$

The boundary conditions are

$$(4.7) \quad \frac{\partial \psi}{\partial y}(x, 0) = -U_w, \quad \frac{\partial \psi}{\partial x}(x, 0) = 0, \quad \lim_{y \rightarrow \infty} \frac{\partial \psi}{\partial y}(x, 0) = U_\infty.$$

Let us define the stream function  $\psi$  and similarity variable  $\eta$  as

$$(4.8) \quad \psi(x, y) = [\mu_{cn} U_\infty^{2n-1} x]^{\frac{1}{n+1}} f(\eta), \quad \eta = \mu_{cn}^{-\frac{1}{n+1}} U_\infty^{\frac{2-n}{n+1}} y x^{-\frac{1}{n+1}}.$$

The boundary value problem (4.6), (4.7) is transformed by means of dimensionless variables into the following nonlinear ordinary differential equation:

$$(4.9) \quad \left( |f''|^{n-1} f'' \right)' + \frac{1}{n+1} f f'' = 0,$$

with the boundary conditions

$$(4.10) \quad f(0) = 0, \quad f'(0) = -\lambda, \quad \lim_{\eta \rightarrow \infty} f'(\eta) = 1,$$

where the velocity ratio parameter is  $\lambda = U_w/U_\infty$ .

Remark, when  $\lambda = 0$ , and  $n = 1$ , equation (4.9) with (4.10) is the Blasius problem (over stationary plate). When  $\lambda > 0$  the fluid and the plate move in the opposite directions, while they move in the same directions if  $\lambda < 0$  (see Fig. 4.1).

Equation (4.9) can be readily integrated to yield

$$(4.11) \quad f''(\eta) = f''(0) \exp \left[ -\frac{1}{n(n+1)} \int_0^\eta \frac{f(z)}{|f''(z)|^{n-1}} dz \right],$$

that is the shear stress  $f''(\eta)$  has the same sign as the skin friction at the wall  $f''(0)$ .

Now, consider the initial value problem

$$(4.12) \quad \left( |f''|^{n-1} f'' \right)' + \frac{1}{n+1} f f'' = 0,$$

$$(4.13) \quad f(0) = 0, \quad f'(0) = -\lambda, \quad f''(0) = \gamma,$$

the solution is obtained if only  $f''(0)$  were known such that the corresponding solution satisfies (4.10). The real number  $f''(0)$  provides the non-dimensional drag coefficient ([4], [177])

$$(4.14) \quad C_{D,\tau} = (n+1)^{\frac{1}{n+1}} \text{Re}^{\frac{-n}{n+1}} |f''(0)|^{n-1} f''(0),$$

where the Reynolds number is  $\text{Re} = U_\infty^{2-n} L^n / \mu_{cn}$ .

The main physical quantity of interest is the value of  $f''(0) = \gamma$ . It is important to investigate how the values of  $f''(0)$  vary with the velocity ratio parameter  $\lambda$ . We employ the Runge-Kutta method with shooting technique to solve (4.9) subject to the boundary conditions (4.10). The numerical calculations show that there is a critical value  $\lambda_c$  for any fixed  $n$  such that solution exists only if  $\lambda \leq \lambda_c$ . The variation of  $f''(0)$  with  $\lambda$  for different values of  $n$  is examined. The influences of  $\lambda$  and  $n$  on the parameter  $f''(0)^n$  are represented in Fig. 4.2. The numerical results indicate that there is a critical value  $\lambda_c$  for any fixed  $n$  such that solution exists only if  $\lambda \leq \lambda_c$ . The value of  $\lambda_c$  depends on  $n$ . This phenomena is represented in Table 4.3 and on Fig. 4.3.

$n$	$\lambda$											
	-1	-0.8	-0.6	-0.4	-0.2	0	0.15	0.25	0.3			
	one solution						lower	upper	lower	upper	lower	upper
0.5	$2.8 \cdot 10^{-6}$	0.071	0.161	0.244	0.306	0.331	0.007	0.311	0.033	0.262	0.067	0.213
1	1.249	0.105	0.195	0.265	0.313	0.332	0.006	0.317	0.032	0.284	0.060	0.252
1.5	$3.1 \cdot 10^{-4}$	0.146	0.239	0.305	0.348	0.365	0.001	0.353	0.024	0.324	0.059	0.298

Table 4.1. The values of  $f''(0)$

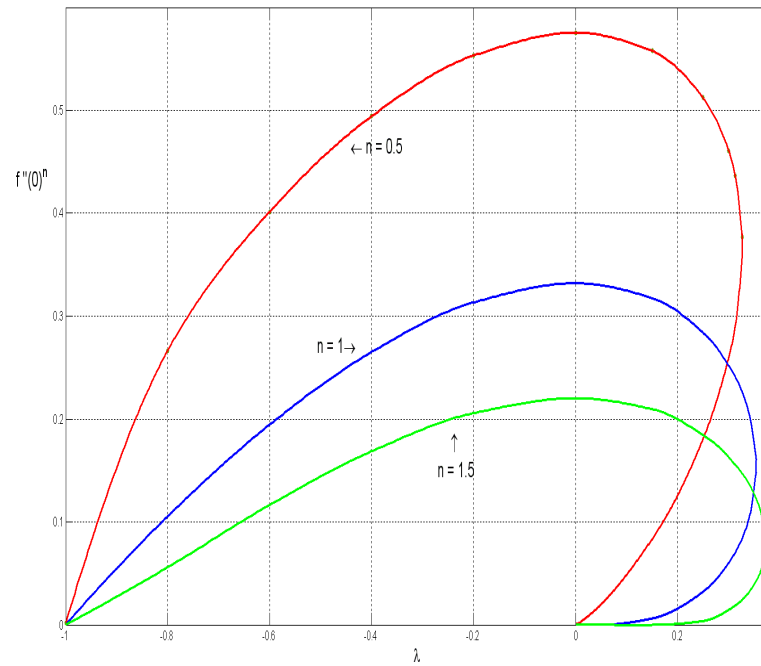


Fig. 4.2 The variation of  $f''(0)^n$  with  $\lambda$  for different values of  $n$

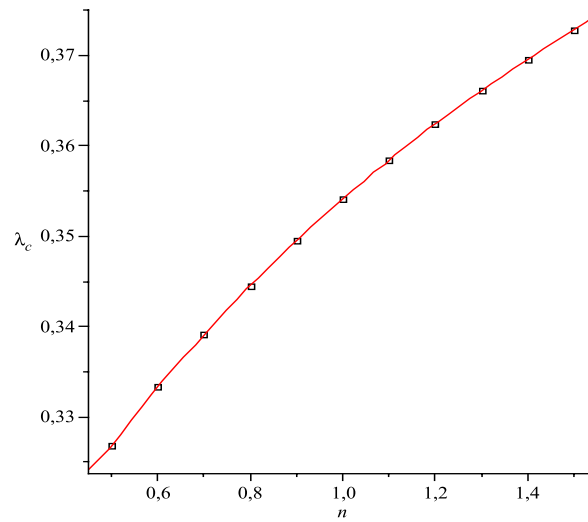


Fig. 4.3 Variation of  $\lambda_c(n)$  with  $n$

The nonlinear ordinary differential equation (4.9) with the boundary conditions in (4.10) was solved for some values of the power-law index  $n$  and velocity ratio parameter  $\lambda$  by an iterative transformation method using MATLAB in [53]. The fourth order Runge-Kutta method was implemented and  $\eta_{max}$  was determined when the local error was less than  $10^{-6}$ . The results of the numerical calculations are represented for  $f''(0)$ , and  $\eta_{max}$  by taking different values for  $\lambda$  and  $n$  in Table 4.1-4.2.

$n$	$\lambda$											
	-1	-0.8	-0.6	-0.4	-0.2	0	0.15	0.25	0.3			
	one solution						lower	upper	lower	upper	lower	upper
0.5	9001	56.3	37.4	30.3	27.1	26.1	180.44	26.90	82.98	29.28	57.83	32.53
1	300.0	31.8	25.9	23.3	22.1	21.7	81.94	21.99	47.21	22.82	38.32	23.74
1.5	4.6	6.9	6.4	6.1	5.96	5.92	11.9	4.52	8.21	5.31	7.85	5.99

Table 4.2. The values of  $\eta_{max}$

If  $\lambda > 0$ , then there is one solution (see e.g., Fig. 4.4). Figs. 4.5-4.7 exhibit the upper and lower solutions for velocities  $u(x, y)/U_\infty$  as a function of  $\eta$  to show the effect of a positive parameter  $\lambda$  for different power-law exponent  $n$ . We see that  $f'$  monotonically increases from  $-\lambda$  to 1.

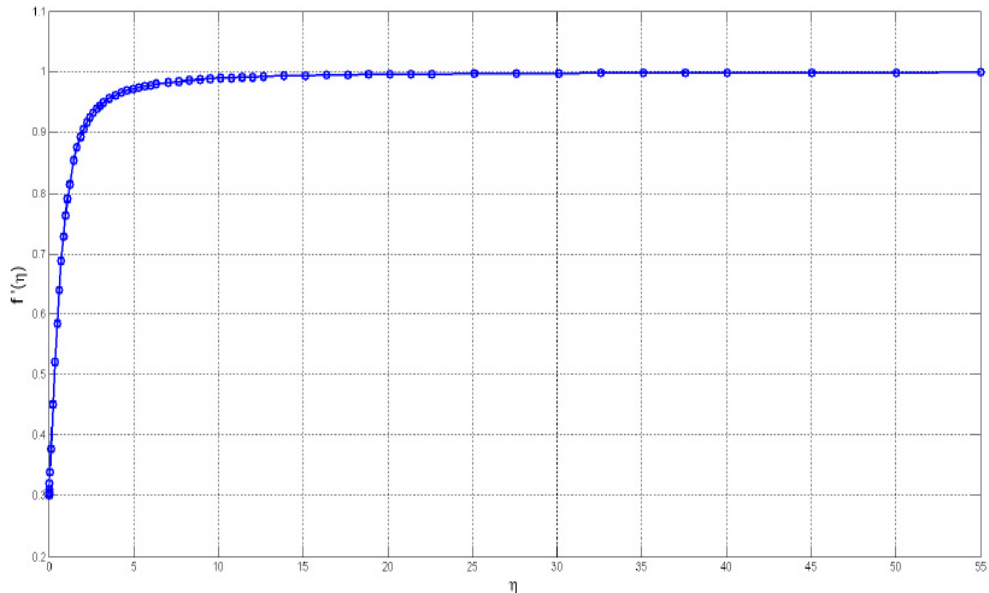


Fig. 4.4 Velocity distribution for  $\lambda = -0.3$  and  $n = 0.1$

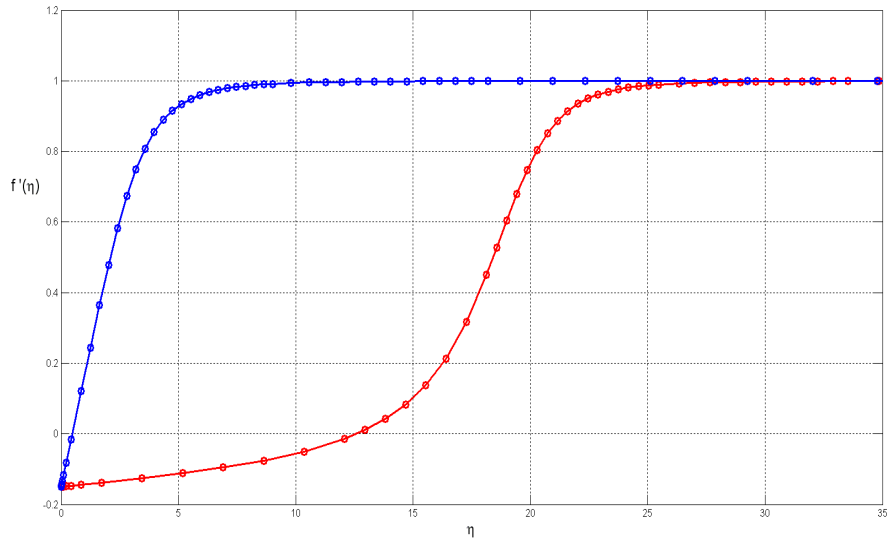


Fig. 4.5 Velocity distribution for  $\lambda = 0.15$  and  $n = 0.5$

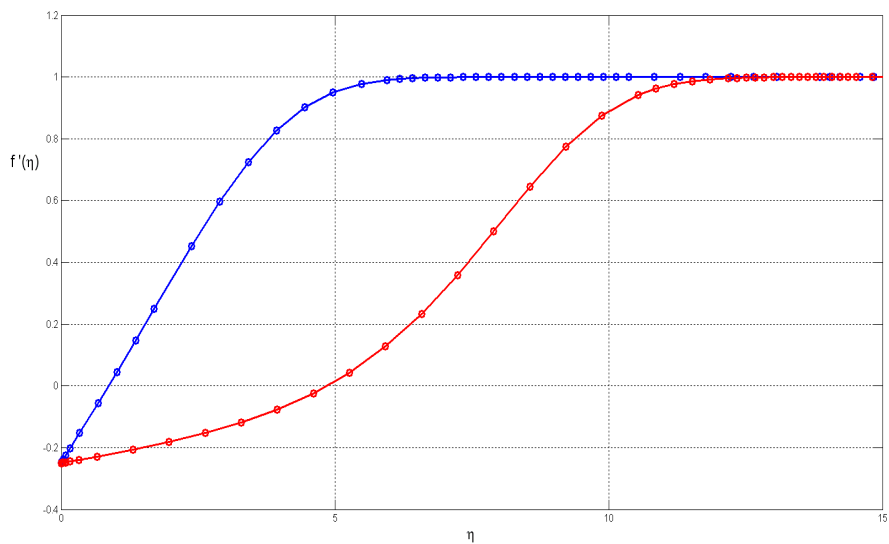
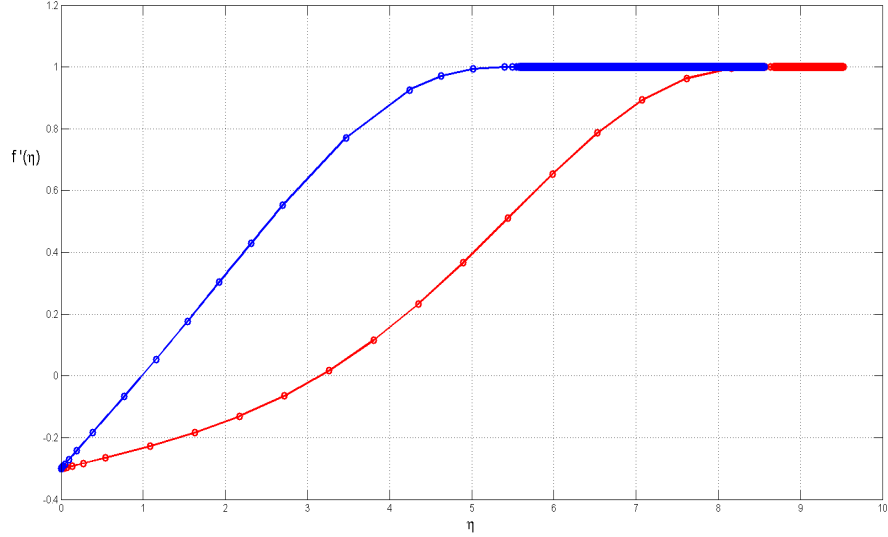


Fig. 4.6 Velocity distribution for  $\lambda = 0.25$  and  $n = 1$



**Fig. 4.7** Velocity distribution for  $\lambda = 0.3$  and  $n = 1.5$

$n$	0.7	0.8	0.9	1.0	1.1	1.2	1.3	1.4	1.5
$\lambda_c$	0.3391	0.3445	0.3495	0.3541	0.3584	0.3624	0.3661	0.3696	0.3728

**Table 4.3.** The values of  $\lambda_c$

For pseudoplastic, Newtonian and dilatant media, Figs. 4.8-4.10 introduce the effect of the power exponent  $n$  and  $\lambda$  on the profiles for  $f''(\eta)$  which is included in the shear stress. The boundary layer thickness increases as the value of  $\lambda > 0$  increases, and  $f''(\eta)$  reaches a maximum in the interior of the flow field. Klemp and Acrivos [123] remarked that at this similarity solution, the downstream influence has not been neglected on the flow. The reason is the lack of the characteristic length in the case of the semi-infinite surface. If the solution exists, it must be self-similar in order to remain independent of whatever length scale is chosen. Therefore, both upstream and downstream effects on the solution at any point in the flow must be such that the shape of the similarity solution.

Our aim is to give upper estimation on  $\lambda_c$ . As in [73], we employ the following Crocco-like transformation  $w = f'$  and  $G(w) = f''$ . By this approach we arrive at the following problem

$$(4.15) \quad G (G' |G|^{n-1})' + \frac{w}{n+1} = 0, \quad w \in (-\lambda, 1),$$

$$(4.16) \quad G(1) = 0, \quad G'(-\lambda) = 0.$$

4. BOUNDARY LAYER FLOWS ON A MOVING SURFACE

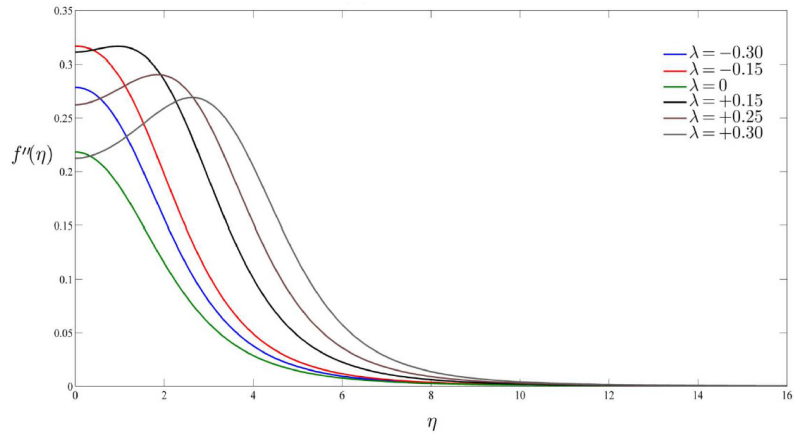


Fig. 4.8 The graph of  $f''(\eta)$  for  $n = 0.5$  applying different  $\lambda$

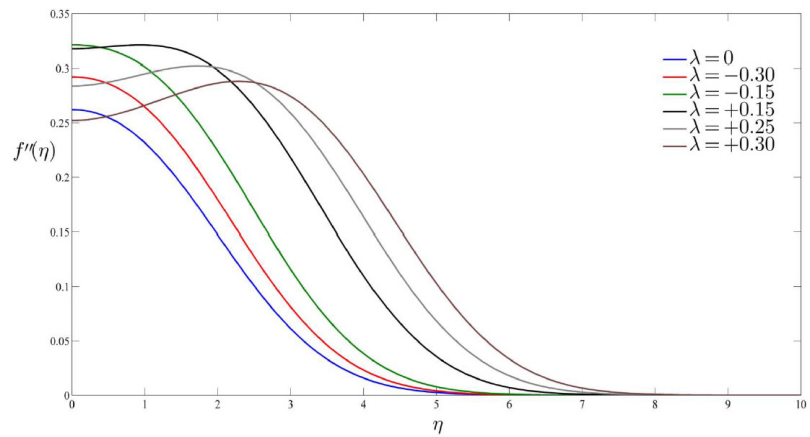


Fig. 4.9 The graph of  $f''(\eta)$  for  $n = 1$  applying different  $\lambda$

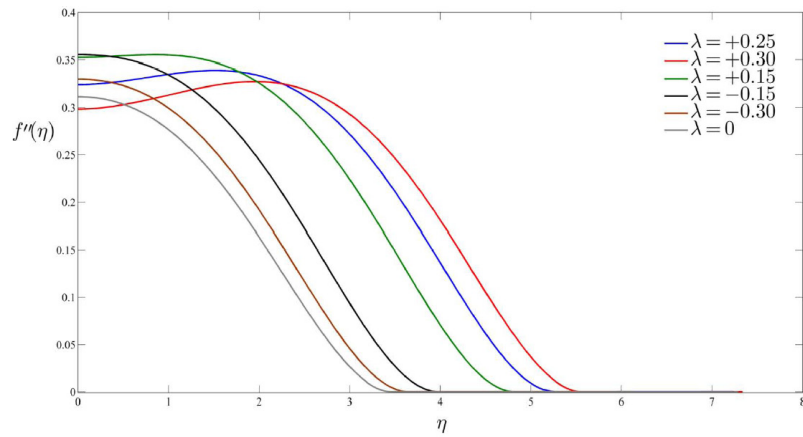


Fig. 4.10 The graph of  $f''(\eta)$  for  $n = 1.5$  applying different  $\lambda$

Equation (4.15) can be also written in the form

$$(4.17) \quad G |G|^{n-1} G'' + (n-1) |G|^{n-1} G'^2 + \frac{w}{n(n+1)} = 0.$$

We find that if  $G$  is a solution to (4.17) then  $-G$  is also its solution. So, the sign of  $G(w)$  is determined by  $G(0)$ . Without loss of generality we can assume that  $G(0) > 0$ .

Using the transformation  $x = w + \lambda$ , [ $G(w) = g(x)$ ] to map the interval  $-\lambda < w < 1$  to  $0 < x < 1 + \lambda$ , equations (4.15) or (4.17) and boundary conditions (4.16) can be formulated as

$$(4.18) \quad g(x) |g(x)|^{n-1} g''(x) + (n-1) |g(x)|^{n-1} g'^2 + \frac{x-\lambda}{n(n+1)} = 0$$

or

$$(4.19) \quad (g(x)^{n-1} g'(x))' = \frac{\lambda-x}{n(n+1)g(x)},$$

with

$$(4.20) \quad g'(0) = 0, \quad g(1+\lambda) = 0.$$

For the Newtonian case ( $n = 1$ ) with  $\lambda = 0$ , problem (4.9), (4.10) is reduced to the well-known Blasius problem.

When  $n = 1$ ,  $\lambda \leq 0$ , the existence, uniqueness and analyticity of solution to (4.9), (4.10) were shown by Callegari and Friedman [61] and Callegari and Nachman [62] using the Crocco variable formulation. If  $\lambda > 0$ , Hussaini and Lakin proved that there is a critical value  $\lambda_c$  such that solution exists only if  $\lambda \leq \lambda_c$  (see [110]). The numerical value of  $\lambda_c$  was found to be 0.3541... . The analyticity of solutions to (4.18), (4.19) has been presented by Hussaini et. al. [111] and also upper bound on the critical value of the wall velocity parameter  $\lambda_c$  has been derived which was found to be 0.46824... . The non-uniqueness and analyticity of solution for  $\lambda \leq \lambda_c$  has been proved in [111]. Allan investigated the effect of the parameter  $\lambda$  on the boundary layer thickness in [8].

For non-Newtonian fluids ( $n \neq 1$ ) with  $\lambda = 0$ , in the paper by Nachman and Callegari [155], the existence, uniqueness, and some analytical results for problem (4.9),(4.10) were established when  $0 < n < 1$ . The existence and uniqueness result for  $n > 1$  was considered in [25] via Crocco variable transformation. In [38] it was shown that for the non-Newtonian case there also exists analytic solution to the problem (4.9), with  $f(0) = 0$ ,  $f'(0) = 0$ ,

$\lim_{\eta \rightarrow \infty} f'(\eta) = 1$ ; moreover, the coefficients in the power series solution  $f(\eta) = \eta^2 \sum_{k=0}^{\infty} a_k \eta^{3k}$  and the convergence radius have been determined.

When  $n \neq 1$ ,  $\lambda \neq 0$ , the boundary layer equation (4.9) with (4.10) has been solved numerically through employing Runge-Kutta method by Ishak and Bachok [114] and the effects of power-law index  $n$  and velocity ratio parameter  $\lambda$  was analyzed for some values of  $n$  and  $\lambda$ . Moreover, the behavior of the skin friction parameter ( $f''(0)$ ) was examined. It was found that similarly to the Newtonian case dual solutions exist for some  $\lambda < \lambda_c$ , and  $\lambda_c$  varies with power-law index  $n$ . From the numerical results it was established that the drag force is reduced for dilatant fluids ( $n > 1$ ) compared to the case  $0 < n < 1$ .

If  $\lambda > \lambda_c$ , the flow separates. The boundary layer structure collapses and the boundary layer approximations are no longer applicable.

In [44] we provided upper bound for the critical velocity parameter for non-Newtonian fluids as in [111] it was for Newtonian fluids.

#### 4.2.2 PROPERTIES OF THE SOLUTION $g$

In this section we summarize some properties of solution  $g$  to (4.18), (4.20) (for the proof we refer to [44]):

1. If  $g(0) = \alpha > 0$  then  $g$  and  $g'$  are positive and  $g^n(x)$  is convex in  $(0, \lambda)$ .
2. There exists exactly one value  $x_0$  in  $(\lambda, 1 + \lambda)$  such that  $g^n(x)$  has its maximum value at  $x_0$ .
3. The initial value  $\alpha$  of  $g$  and the maximal value  $\beta$  of  $g$  satisfy the inequality  $0 < g(x_0) = \beta < 2\alpha$ .
4. For the solution  $g$  of (4.18), (4.20) the following equality holds:

$$(4.21) \quad \frac{n}{n+1} (\beta^{n+1} - \alpha^{n+1}) - \int_0^{x_0} (x_0 - \xi) g'(\xi) ([g(\xi)]^n)' d\xi = \frac{1}{6(n+1)} (3\lambda x_0^2 - x_0^3).$$

5. For  $x_0$ , the lower bound  $x_0 \geq 2\lambda$  is valid.
6. For  $g(0) = \alpha$  and  $g(x_0) = \beta$  the estimation

$$\beta^{n+1} - \alpha^{n+1} \geq \frac{2\lambda^3}{3(n+1)}$$

holds.

**7.** For any positive  $n$ , except  $n = 1/2$  and  $n = 1/3$ , the positive solution to (4.18) and (4.20) satisfies the estimation

$$\frac{\lambda^3}{3(2^n - 1)(n + 1)} \leq \alpha^{n+1} \leq \frac{n^2}{(n + 1)(2n - 1)(3n - 1)},$$

where  $g(0) = \alpha > 0$  is the skin friction coefficient.

#### 4.2.3 UPPER BOUND ON $\lambda_c$

When  $n = 1$ , it is known that there exists a solution to (4.9), (4.10) only if  $\lambda \leq \lambda_c$ . In [111] the critical value  $\lambda_c$  was determined numerically  $\lambda_c = 0.3541 \dots$  [110], and upper bounds are provided for  $\lambda_c$  analytically. For non-Newtonian fluids the numerical calculations (see [114]) indicate that generally  $\lambda_c$  depends on the power-law index  $n$ , i.e.,  $\lambda_c = \lambda_c(n)$ . Here we derive upper bounds for  $\lambda_c$  depending on  $n$ .

By an integration from 0 to  $1 + \lambda$ , from equality from (4.21), one can get (see [44])

$$(4.22) \quad -\frac{n}{n+1}\alpha^{n+1} - I(1+\lambda) = \frac{1}{6(n+1)}(3\lambda(1+\lambda)^2 - (1+\lambda)^3),$$

where

$$(4.23) \quad I(\nu) = \int_0^\nu (1 + \lambda - \xi) g'(\xi) (|g(\xi)|^{n-1} g(\xi))' d\xi.$$

Therefore,

$$(4.24) \quad \frac{((1 + \lambda)^3 - 3\lambda(1 + \lambda)^2)}{6} = n\alpha^{n+1} + (n + 1)I(1 + \lambda).$$

Next, we provide three upper bounds for  $\lambda$  depending on the applied estimation of the right side of (4.24).

**Case (i.)** Simply take that the right side of (4.24) is positive then  $1 - 2\lambda \geq 0$ , that means

$$(4.25) \quad \lambda \leq \frac{1}{2} \text{ for any } n.$$

**Case (ii.)** Here we use the inequality  $I(1 + \lambda) > 0$ , then

$$(4.26) \quad \left(2 + \frac{2n}{(2^n - 1)(n + 1)}\right) \lambda^3 + 3\lambda^2 - 1 \leq 0.$$

We note that (4.26) corresponds to the one obtained for  $n = 1$  in [111]. Numerical solutions to (4.26) for different values of  $n$  are demonstrated in Table 4.4 for different values of  $n$  and compared to the numerical results by Ishak and Bachok [114].

$n$	$\lambda_c$ [114]	$\lambda_c(ii)$
0.6	0.3333	0.46578
0.8	0.3445	0.47104
1	0.3541	0.47533
1.2	0.3641	0.47889
1.4	0.3636	0.48187
1.6		0.48438
1.8		0.48650
2		0.48832
3		0.49421
4		0.49708

**Table 4.4.** Upper bounds for  $\lambda$

**Case(iii.)** Now, we use the relation that  $I(1 + \lambda) > I(\lambda)$ , then one gets the following inequality for  $\lambda$

$$(4.27) \quad \left[ 2BC + \frac{1}{n(n+1)2^{2+\frac{1}{n}}} \right] \lambda^6 + \left[ \frac{1}{5n(n+1)2^{\frac{1}{n}-2}} + 3B \right] \lambda^5 + [2AC - B] \lambda^3 + 3A\lambda^2 - A \leq 0,$$

where  $A = \frac{n^2}{(2n-1)(3n-1)}$ ,  $B = \frac{(2^n-1)^{\frac{1}{n}}}{3(n+1)}$ ,  $C = 1 + \frac{n}{(n+1)(2^n-1)}$  are constants depending on  $n$ .

The numerical results obtained from (4.27) are demonstrated in Table 4.5 for  $0.6 \leq n \leq 4$  and compared to the numerical results obtained in [114]. The calculated numerical values give slightly better approximations for  $\lambda_c$  as in the case (ii). Remark, that even for  $n = 1$  the upper bound for  $\lambda_c$  is worse than in [111] due to the applied inequality:

$$(4.28) \quad (a + b)^q \leq 2^{q-1} (a^q + b^q) \quad \text{for } a, b > 0 \quad \text{and} \quad q \geq 1,$$

applied for the case (iii) with  $q = 1 + 1/n$ .

$n$	$\lambda_c$ [114]	$\lambda_c(iii)$
0.6	0.3333	0.46522
0.8	0.3445	0.46944
1	0.3541	0.47317
1.2	0.3641	0.47648
1.4	0.3636	0.47939
1.6		0.48194
1.8		0.48417
2		0.48613
3		0.49262
4		0.49593

**Table 4.5.** Upper bounds for  $\lambda$ 

#### 4.2.4 THE ANALYTIC SOLUTION

We can show the existence of analytic solution  $g(x)$  to (4.18) with initial conditions  $g(x_0) = \beta$ ,  $g'(x_0) = 0$ .

In [44] it was provided that solution  $g(x)$  has a convergent power series expansion near zero of the form

$$(4.29) \quad g(x) = \sum_{k=0}^{\infty} a_k (x - x_0)^{2k} = \beta - \frac{x_0 - \lambda}{2n(n+1)} \frac{1}{\beta^n} (x - x_0)^2 + \sum_{k=2}^{\infty} a_k (x - x_0)^{2k}$$

in  $[x_0, 1 + \lambda]$ . For the determination of the coefficients  $a_k$  ( $k \geq 2$ ) we refer the paper [51]. We remark to that in the interval  $[0, x_0]$  the power series expansion of the solution to (4.18) can be obtained similarly with the modifications  $\beta$  to  $\alpha$  and  $x_0$  to 0.

### 4.3 COMPARISON OF SIMILARITY SOLUTIONS WITH NUMERICAL SOLUTIONS

Now, the flow induced by a flat plate, with finite length, moving reversely to a parallel ambient stream of a power-law non-Newtonian fluid is considered. This problem has been investigated in Section 4.2.

A horizontal plate, with finite length  $L$ , moves with constant velocity  $U_w$  from right to left against a horizontal free stream which moves with constant velocity from the left to the right. The moving plate forces the fluid in front of it to move to the left.

As it was noted, the boundary layer theory is valid only for some special conditions. Instead of the boundary layer equations (1.1), (1.6), the system

of full equations (1.1), (1.4), (1.5) is considered, where  $p$  is the pressure and  $\mu_{app}$  is the apparent viscosity calculated by the relationship (1.12):

$$\mu = K \left\{ 2 \left[ \left( \frac{\partial u}{\partial x} \right)^2 + \left( \frac{\partial v}{\partial y} \right)^2 \right] + \left( \frac{\partial u}{\partial y} + \frac{\partial v}{\partial x} \right)^2 \right\}^{(n-1)/2}.$$

The flow is governed by the Reynolds number which is given by

$$(4.30) \quad \text{Re} = \frac{\rho U_{\infty}^{2-n} L^n}{K}.$$

This means that the results for this problem are quite different from those of Steinheuer [191], and Klemp and Acrivos [123] for a Newtonian fluid and what we presented for power-law non-Newtonian flows by the similarity method. Our investigation is based on the numerical solution of the complete system of equations using the commercial code ANSYS FLUENT Version 14.0. The two-dimensional, steady, laminar solver is used in the momentum equations. In our computations we apply the coupled scheme for coupling of the pressure and the velocity with the non-Newtonian power-law model (1.12). A double precision accuracy was used and a convergence criterion of  $10^{-8}$  was applied for the velocity components. The CFD (Computational Fluid Dynamics) has been used extensively in the literature, both for Newtonian (see e.g., [54], [167]) and non-Newtonian fluids ([188], [189], [216]). The boundary parallel to the plate were placed far away from the plate (at distance  $20L$ , where  $L$  is the plate length. Larger computational field is not necessary as in our examples we calculate for large Reynolds numbers. According to the ANSYS FLUENT code, the applied boundary conditions are the following:

- "velocity inlet" where the horizontal velocity is constant and the vertical velocity is zero,
- "pressure outlet" where the static pressure is placed equal to ambient pressure and all other flow quantities are extrapolated from the interior domain,
- boundaries parallel to the plate, are defined as "symmetry" where the velocity gradients in the vertical direction are forced to be zero,
- the plate is defined as "moving wall".

<i>Fluid</i>	Newtonian	dilatant [49]	pseudoplastic [118]
$n$ [-]	1	1.475	0.8
$K$ [ $Pa s^n$ ]	0.001003	0.000313	0.319
$\rho$ [ $kg/m^3$ ]	998	1340	1070

**Table 4.6.**

The numerical calculations were carried out for  $L = 0.06$  [m],  $U_\infty = 0.2$  [m/s] and three types of fluids: water ( $n = 1$ ), dilatant fluid ( $n = 1.475$ ) and pseudoplastic fluid ( $n = 0.8$ ). The material properties are summarized in Table 4.6.

We compare the theoretical or similar velocity solution  $u/U_\infty$  with the numerical solutions obtained by ANSYS FLUENT when the similarity variable  $\eta$  is applied. For a Newtonian fluid in Fig. 4.11 it is clearly seen that with increasing distance  $x/L$  from the leading edge, the numerically calculated dimensionless velocity profiles  $u(x, y)/U_\infty$  always approach the similarity solution  $f'(\eta)$  associated with (4.9), (4.10) obtained by the iterative transformation method and denoted by 'ITM'.

For the outflow ( $x/L = 1$ ) the numerical and similar solutions are exhibited in Figs. 4.12-14. The solutions  $u(x, y)/U_\infty$  to (1.1), (1.4), (1.5) with (1.12) on the one hand and the similarity solution (4.9), (4.10) on the other hand, for different values of  $n$  and  $\lambda$  at Figs. 4.15-4.19 become undistinguishable. Figs. 4.20-4.22 exhibit the wall shear stress for different values of  $n$  and  $\lambda$ .

The shear stress obtained from the similarity solution is a function of  $x$ , and it has an asymptote at zero, while the numerical solution of the momentum equations provides a finite value for the shear stress at zero. However, except a close neighborhood of the leading edge, the numerical values calculated with ANSYS are very close to those of the similarity solution.

For numerical simulations the discretization error was determined by Richardson's extrapolation. The error in absolute value for the velocity component  $u$  is not greater than  $10^{-4}$ . For the shear stress the absolute value of the error is remarkable on the interval  $[0, 0.01]$ , otherwise the error is very small.

Comparing the theoretical (similar) velocity solution  $u/U_\infty$  with the numerical solutions obtained by ANSYS FLUENT, satisfactory agreement has been found. Therefore, the similarity solutions verify the numerical simulations calculated by ANSYS FLUENT.

We summarize the advantages of the similarity method and the numerical simulation obtained with ANSYS.

The finite volume solution calculated with ANSYS has the following advantages: there is no assumption on the pressure and on the velocity components and on their derivatives; the momentum equation is a vector equation, it describes the phenomenon more accurately as it doesn't contain the assumptions which was made for the similarity solutions; at the leading edge ( $x = 0$ ), the similarity solution is not applicable as the similarity variable  $\eta$  is not defined there.

The similarity solution has the advantages over the finite volume solution:

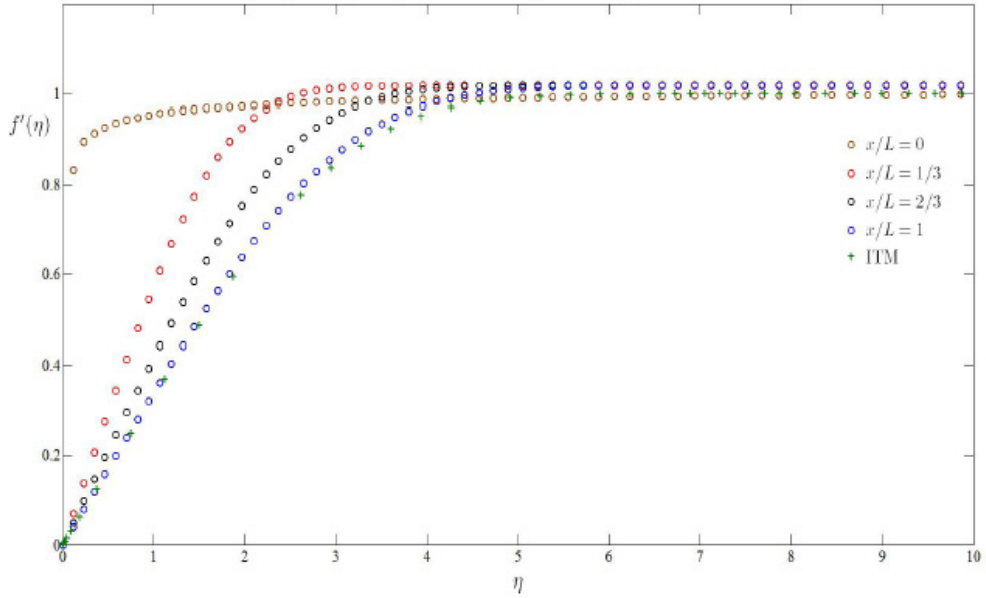


Fig. 4.11 Numeric and similar velocity profiles of a Newtonian fluid at different distances from the leading edge

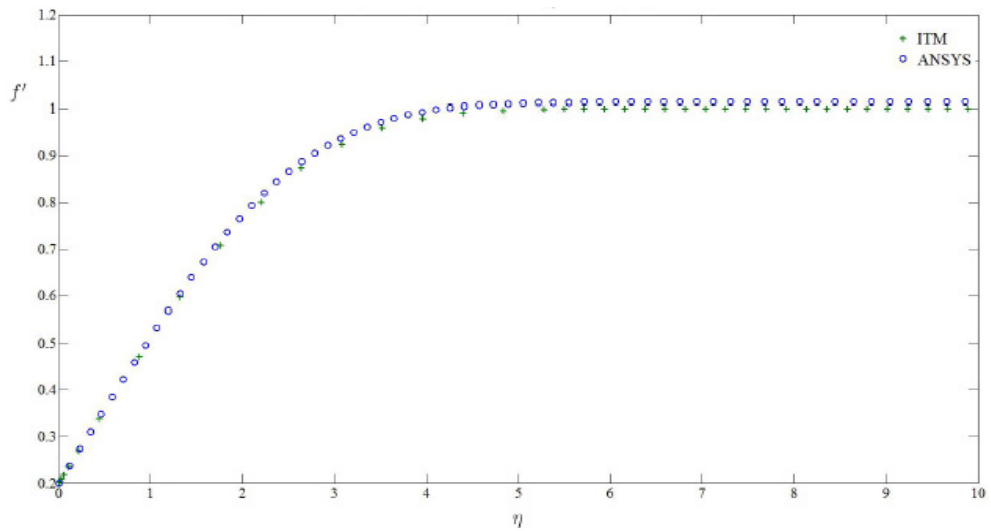


Fig. 4.12 Comparison of numeric and similar velocity profiles of a Newtonian fluid for  $\lambda = -0.2$

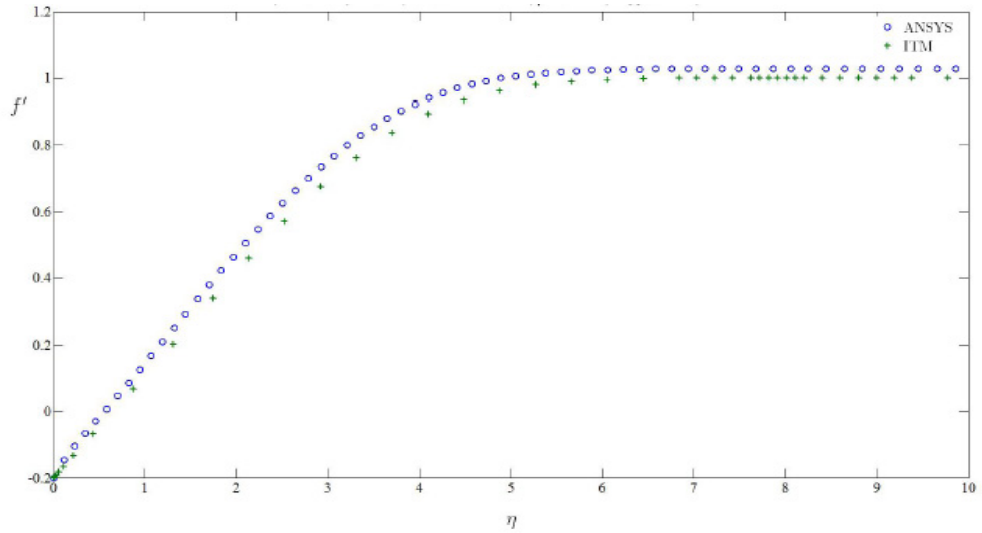


Fig. 4.13 Comparison of numeric and similar velocity profiles of a Newtonian fluid for  $\lambda = 0.2$

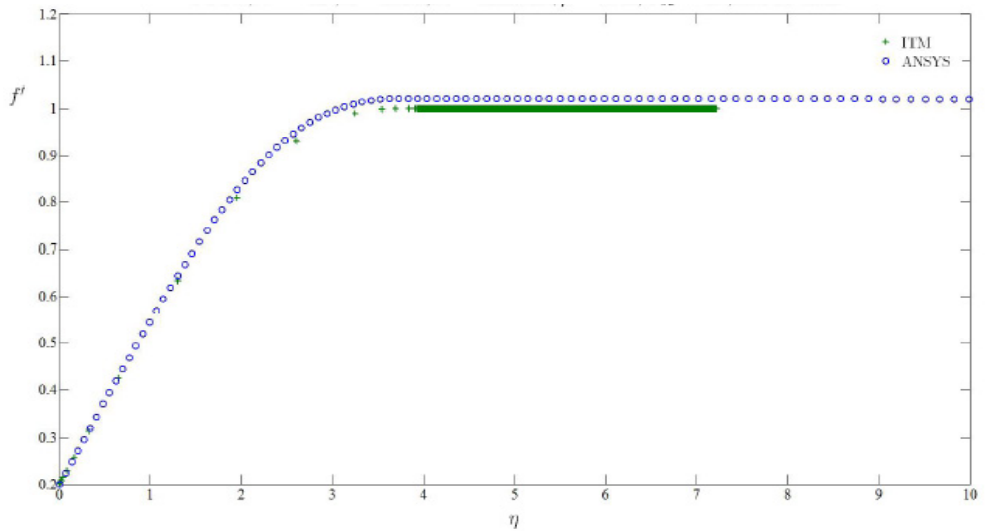


Fig. 4.14 Comparison of numeric and similar velocity profiles of a dilatant non-Newtonian fluid for  $\lambda = -0.2, n = 1.475$

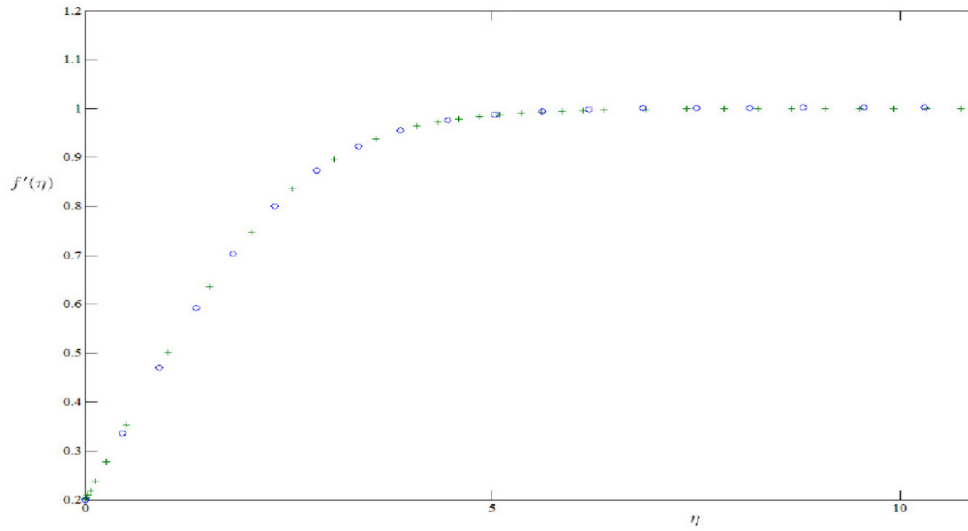


Fig. 4.15 Comparison of numeric and similar velocity profiles of a pseudoplastic non-Newtonian fluid for  $\lambda = -0.2$ ,  $n = 0.8$

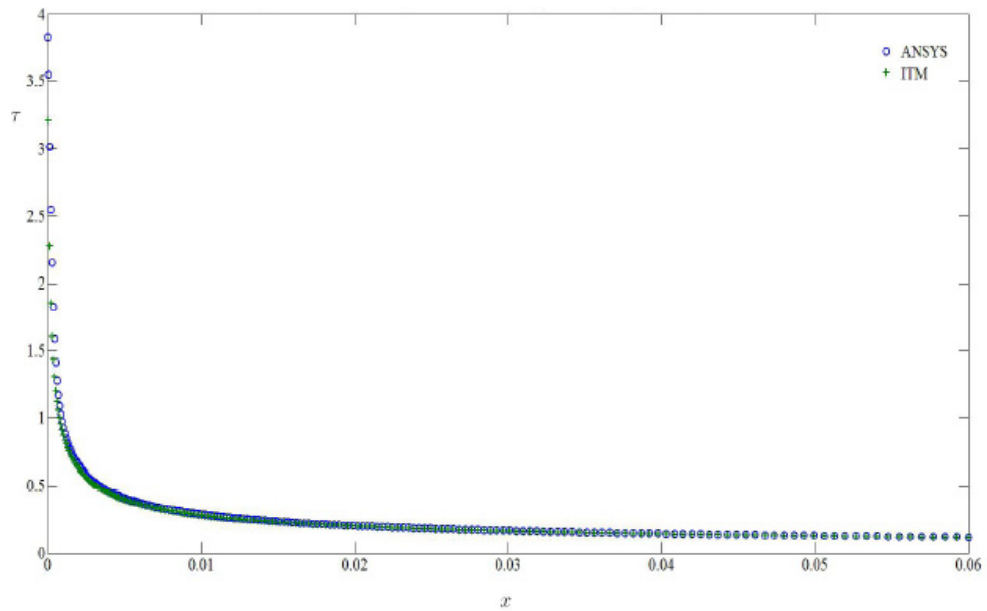
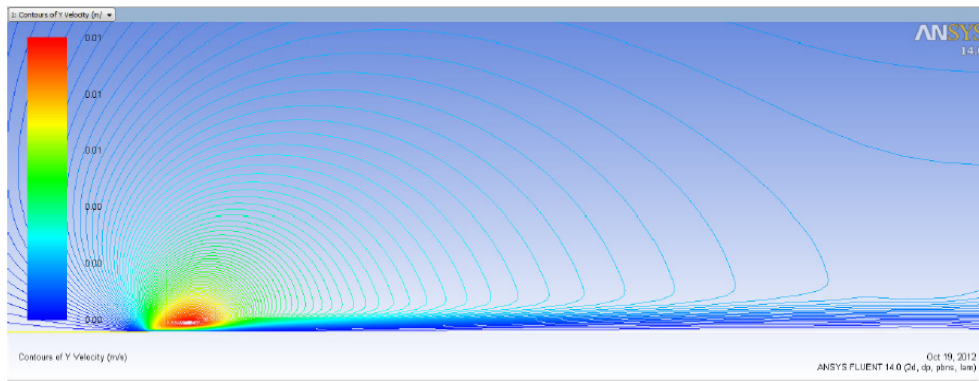


Fig. 4.16 The wall shear stress  $\tau_w$  for  $\lambda = -0.2$  and  $n = 1$

## 4. BOUNDARY LAYER FLOWS ON A MOVING SURFACE

the length of the surface is not included in the equation; in case of industrial applications, it is often important to model very long sheets; such calculations can be very time-consuming; the numerical solution of the initial value problems, or even the boundary value problems are less time-consuming than of the momentum equation; stable methods are available for the solution of the initial value problems of ordinary differential equations, the solution to the similarity problem does not require mesh, so it does not affect the result.



**Fig. 4.17** Velocity component  $v$  for  $n = 1$

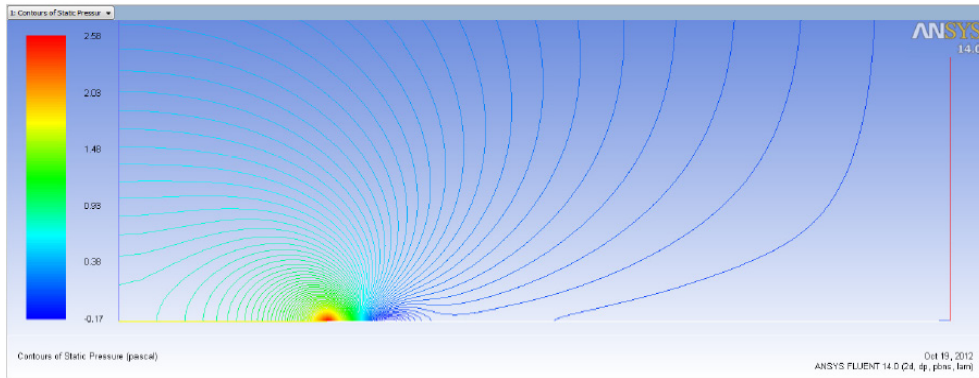


**Fig. 4.18** Static pressure for  $n = 1$

Figures 4.17-4.18 exhibit the velocity component  $u$  and the pressure for Newtonian fluid. As a consequence of our calculations, we find that for both the pressure and the velocity distributions Prandtl's boundary layer assumptions are valid.

## 5 SIMILARITY SOLUTIONS TO HYDRODYNAMIC AND THERMAL BOUNDARY LAYER

### 5.1 MARANGONI EFFECT

The film flows are ubiquitous in manufacturing, in engineering, in physics and in life sciences. In many practical film models, surface tension plays a significant role, e.g. in surface coatings, biofluid and agrochemical applications. When a free liquid surface is present, the surface tension variation resulting from the concentration or temperature gradient along the surface can induce motion in the fluid called solutal capillary, or thermocapillary motion, respectively.

The study of liquid movement resulting from thermocapillarity (or so called Marangoni) convection is very important for a liquid system either in microgravity or in normal gravity [17]. Under normal gravity, liquid movement is mainly driven by buoyancy force because of the temperature-dependent density, while the liquid is exposed to a temperature gradient field. As the size of the liquid system decreases especially having the size decrease in the direction of gravity, the buoyancy effect begins to diminish and the Marangoni effect will then dominate the system as the main driving force for liquid interface movement. In the absence of gravity, Marangoni convection always plays a main role in the determination of the fluid movement because of varying liquid surface tension in a temperature gradient. It has significance in the processing of materials, especially in small scale and low gravity hydrodynamics [156].

Marangoni convection appears in many industrial processes and space technologies, e.g., in the flip-chip industry, in tribology, in surface coatings, in crystal growth melts, where the flow produces undesirable effects (see [14], [66], [67], [140]) and it occurs around vapor bubbles during nucleation [67]. In several papers authors investigate Marangoni driven boundary layer flow in nanofluids. These fluids can tremendously enhance the heat transfer characteristics of the base fluid and have many industrial applications in lubrication theory, in heat exchangers and coolants. Nanofluids are studied when different types of nanoparticles ([16], [60], [75]). Marangoni flow has also significance in welding, semiconductor processing and other fields of space science. Its mathematical model is studied in [16], [68] and [107].

In the lubrication theory, a thin film flow consists of a spread of fluid bounded by free surface. Due to the Marangoni effect, even small surface tension can lead to significant changes. On lubricated surfaces, the problem of lubricant migration is examined in highly stressed lubricated machine el-

ements (e.g. in bearings). The frictional heat makes the moving machine elements warmer than its surroundings. In bearing systems, which are open at one side, the conditions for the appearance of the Marangoni effect are given. The bearing runs dry, when the temperature gradient is high enough and the force induced by the Marangoni effect overcomes the capillary forces, which pull the lubricant into the bearing contact. The Marangoni phenomena causes the temperature driven migration on tribological surfaces, the oil film flows away from the hot to the cooler regions, and it leads to the lack of lubricant. Klien et al. [125] have shown experimental results on the influence of the temperature gradient and of the lubricant properties on the migration speed. Dewetting is often undesirable: dry spots on tribological surfaces can lead to spontaneous failures [125], dewetting of tear film in the eye is a serious health problem, dewetting in printing often appears with nonuniform coating patterns. However, dewetting is desirable some cases, e.g., waxy coatings on plant leaves or balling up water on freshly polished cars [160].

The Marangoni effect has been investigated for various substances in geometries with flat surfaces by similarity analysis (see [14], [16], [65], [98], [164], [222]), [223]. Arufane and Hirata [14] presented a similarity analysis for just the velocity profile for Marangoni flow when the surface tension variation is linearly related to the surface position. Christopher and Wang [66] studied Prandtl number effects for Marangoni convection over flat surface and presented approximate analytical solutions for the temperature profile. They showed that the calculated temperature distribution in vapor bubble attached to a surface and in the liquid surrounding the bubble was primarily due to the heat transfer through the vapor rather than in liquid region and the temperature variation along the surface was not linear but could be described by a power-law function [65]. Using the similarity transformation, the governing system of non-linear partial differential equations are transformed into a pair of similarity non-linear ordinary differential equations, one for the stream function and one for the temperature. The velocity and temperature distributions can be given by numerically by using the Runge-Kutta method ([16], [64], [65], [67]), analytical approximate solutions can be determined for these problems by using Adomian decomposition method and Padé technique ([120], [221], [222], [223]) or by power series method [38].

In this section, we investigate a similarity analysis for Marangoni convection inducing flow over a flat surface due to an imposed temperature gradient. The analysis assumes that the temperature variation is a power law function of the location and the surface tension is assumed to depend on the temperature linearly.

We first present the derivation of the equations and show how the boundary layer approximation leads to the two point boundary value problem and

the similarity solutions. The new model, written in terms of stream function and temperature, consists of two strongly coupled ordinary differential equations. Its analytical approximate solutions are represented in terms of exponential series. The influence of various physical parameters on the flow and heat transfer characteristics are discussed.

### 5.1.1 BOUNDARY LAYER EQUATIONS

Consider the steady laminar boundary layer flow of a viscous Newtonian fluid over a flat surface in the presence of surface tension due to temperature gradient at the wall. Assuming that the surface is impermeable, the surface tension varies linearly with temperature and the interface temperature is a power-law function of the distance along the surface. The governing equations for two-dimensional Navier-Stokes and energy equations describing thermocapillary flows in a liquid layer of infinite extent is considered. The layer is bounded by a horizontal rigid plate from one side and opened from the other one. The rigid boundary is considered as thermally insulated. The physical properties of the liquid are assumed to be constant except the surface tension. For Newtonian fluid the balance laws of mass, momentum and energy can be written in the form [156]:

$$(5.1) \quad \frac{\partial u}{\partial x} + \frac{\partial v}{\partial y} = 0,$$

$$(5.2) \quad u \frac{\partial u}{\partial x} + v \frac{\partial u}{\partial y} = \mu_c \frac{\partial^2 u}{\partial y^2},$$

$$(5.3) \quad u \frac{\partial T}{\partial x} + v \frac{\partial T}{\partial y} = \alpha_t \frac{\partial^2 T}{\partial y^2},$$

where  $\alpha_t$  denotes the thermal diffusivity,  $\mu_c = \mu/\rho$ .

Marangoni effect is incorporated as a boundary condition relating the temperature field to the velocity. The boundary conditions at the surface (at  $y = 0$ ) are

$$(5.4) \quad \mu \left. \frac{\partial u}{\partial y} \right|_{y=0} = -\sigma_T \left. \frac{\partial T}{\partial x} \right|_{y=0},$$

$$(5.5) \quad v(x, 0) = 0,$$

$$(5.6) \quad T(x, 0) = T(0, 0) + \bar{A}x^{m+1}$$

and as  $y \rightarrow \infty$

$$(5.7) \quad u(x, \infty) = 0,$$

$$(5.8) \quad \left. \frac{\partial T}{\partial y} \right|_{y=\infty} = 0,$$

where  $\sigma_T = d\bar{\sigma}/dT$ ,  $\bar{A}$  denotes the temperature gradient coefficient,  $m$  is a parameter relating to the power law exponent. Napolitano and Golia [157] have shown that similarity solution of Marangoni boundary layer exists when the interface temperature gradient varies as a power of  $x$ . When  $T(x, 0)$  is proportional to  $x$ , it was examined by Slavtchev and Miladovina [190]. When  $T(x, 0)$  is proportional to  $x^2$ , it was examined by Al-Mudhaf and Chamka [7] and Magyari and Chamka [140], and when  $T(x, 0)$  is proportional to  $x^{m+1}$ , the solution was investigated by Christopher and Wang [66], [67], Arifin et al. [16] and Zheng et al. [223]. The case  $m = 0$  refers to a linear profile,  $m = 1$  to the quadratic one. The minimum value of  $m$  is  $-1$  which corresponds to no temperature variation on the surface and no Marangoni induced flow.

Introducing the stream function  $\psi$  by (2.6) equation (5.2) is reduced to

$$(5.9) \quad \frac{\partial\psi}{\partial y} \frac{\partial^2\psi}{\partial y\partial x} - \frac{\partial\psi}{\partial x} \frac{\partial^2\psi}{\partial y^2} = \mu_c \frac{\partial^3\psi}{\partial y^3}.$$

Applying similarity functions

$$\psi = C_1 x^a f(\eta), \quad \Theta = \frac{T - T(0, 0)}{\bar{A} x^{m+1}}$$

and similarity variable  $\eta = C_2 x^b y$  with  $C_1 = \sqrt[3]{(m+1)\mu\sigma_T\bar{A}/\rho^2}$ ,  $C_2 = \sqrt[3]{(m+1)\rho\sigma_T\bar{A}/\mu^2}$ ,  $a = (m+2)/3$  and  $b = (m-1)/3$  one can obtain from the partial differential equation (5.9) one single ordinary differential equation of the third order

$$(5.10) \quad f''' - \frac{2m+1}{3} f'^2 + \frac{m+2}{3} f f'' = 0$$

and boundary conditions (5.4)-(5.8) become

$$(5.11) \quad f(0) = 0, \quad f''(0) = -1, \quad f'(\infty) = 0.$$

For equation (5.3) by the similarity temperature function  $\Theta$  with the corresponding boundary conditions we get

$$(5.12) \quad (m+1)f'\Theta - \frac{m+2}{3}f\Theta' = \frac{1}{\text{Pr}}\Theta'',$$

$$(5.13) \quad \Theta(0) = 1, \quad \Theta'(\infty) = 0,$$

where  $\text{Pr} = \mu/(\rho\alpha_t)$  is the Prandtl number. For the dimensionless stream function  $f(\eta)$  and the temperature field  $\Theta(\eta)$ , the system (5.10), (5.12) is derived and the primes denote the differentiation with respect to  $\eta$ .

Now, the velocity components can be expressed by similarity function  $f$  as follows

$$u(x, y) = \frac{\partial \psi}{\partial y} = \kappa^2 \sqrt[3]{\frac{\rho}{\mu}} x^{\frac{2m+1}{3}} f'(\eta),$$

$$v(x, y) = -\frac{\partial \psi}{\partial x} = -\frac{\kappa}{3} x^{\frac{m-1}{3}} \left[ (m+2) \sqrt[3]{\frac{\mu}{\rho}} f(\eta) + (m-1) \kappa \sqrt[3]{\frac{\rho}{\mu}} x^{\frac{m-1}{3}} y f'(\eta) \right],$$

where  $\kappa = \sqrt[3]{(m+1) \sigma_T \bar{A} / \rho}$ ,  $\sigma_T = \text{constant}$ .

It should be noted that  $u$  and  $v$  are proportional to  $x^{\frac{2m+1}{3}}$  and  $x^{\frac{m-1}{3}}$ , respectively. It means, that for  $m = -1/2$  the velocity component  $u$  is a constant on the upper surface of the boundary layer. If  $m = 1$  then  $\eta = \sqrt[3]{2\rho\sigma_T\bar{A}/\mu^2}y$ . In the case of  $m > 1$ ,  $v$  is proportional to  $x^{\frac{m-1}{3}}$  and is strictly monotone increasing to infinity as  $x$  tends to infinity, which is not accepted in physics. Therefore, we restrict our investigations to the interval  $-1 < m \leq 1$ .

We note that the special case  $m = 1$  do admits explicit solution. In [72] and [136] the solution to (5.10), (5.11) is given by :

$$(5.14) \quad f(\eta) = 1 - e^{-\eta}$$

and easy computation shows that

$$(5.15) \quad \Theta(\eta) = \Phi(\text{Pr}) - \Psi(\text{Pr}) e^{-\eta} + \Omega(\text{Pr}) e^{-2\eta},$$

with  $\Phi(\text{Pr}) = \frac{1}{\frac{\text{Pr}-1}{\text{Pr}} + \frac{\text{Pr}}{\text{Pr}-2} - 2} \frac{\text{Pr}-1}{\text{Pr}}$ ,  $\Psi(\text{Pr}) = \frac{2}{\frac{\text{Pr}-1}{\text{Pr}} + \frac{\text{Pr}}{\text{Pr}-2} - 2}$ ,  $\Omega(\text{Pr}) = \frac{1}{\frac{\text{Pr}-1}{\text{Pr}} + \frac{\text{Pr}}{\text{Pr}-2} - 2} \frac{\text{Pr}}{\text{Pr}-2}$  is the solution to (5.12), (5.13).

Due to the inherent complexity of such flows, to give exact analytical solutions of Marangoni flows are almost impossible. Exact analytical solutions were given by Magyari and Chamka for thermosolutal Marangoni convection when the wall temperature and concentration variations are quadratic functions of the location [140].

Our goal is to present approximate exponential series solution to the nonlinear boundary value problem (5.10), (5.11), moreover to (5.12), (5.13) for any  $m$  when  $-1 < m \leq 1$ . Several values of the power law exponent and Prandtl number are considered. Numerical results are exhibited. The influences of the effects of these parameters are illustrated [48].

### 5.1.2 EXPONENTIAL SERIES SOLUTION

First, our aim is to generalize solution (5.14) for any  $m$  and to determine the approximate local solution of  $f(\eta)$  to (5.10), (5.11). We replace the

condition at infinity by one at  $\eta = 0$ . Therefore, and is converted into an initial value problem of (5.10) with initial conditions

$$(5.16) \quad f(0) = 0, \quad f'(0) = \zeta, \quad f''(0) = -1.$$

In view of the third of the boundary conditions (5.11), let us take the solution of the initial value problem (5.10), (5.16) in the form

$$(5.17) \quad f(\eta) = \alpha \left( A_0 + \sum_{i=1}^{\infty} A_i d^i e^{-\alpha \eta^i} \right),$$

where  $\alpha > 0$ ,  $A_0 = 3/(m+2)$ ,  $A_i$  ( $i = 1, 2, \dots$ ) are coefficients and  $\alpha > 0$  and  $d$  are constants. Conditions in (5.11) yield the following equations:

$$(5.18) \quad \alpha \left( A_0 + \sum_{i=1}^{\infty} A_i d^i \right) = 0,$$

$$(5.19) \quad \alpha^3 \sum_{i=1}^{\infty} i^2 A_i d^i = -1.$$

It may be remarked that the classic Briot-Bouquet theorem [59] guarantees the existence of formal solutions (5.17) to the boundary value problem (5.10), (5.16); the value of  $A_0$  and also the convergence of formal solutions.

Let us introduce the new variable  $Z$  such as  $Z = de^{-\alpha \eta}$ .

It is evident that the third boundary condition in (5.11) is automatically satisfied. From differential equation (5.10) with (5.17) we get

$$(5.20) \quad - \sum_{i=1}^{\infty} i^3 A_i Z^i + \frac{m+2}{3} \left( A_0 + \sum_{i=1}^{\infty} A_i Z^i \right) \sum_{i=1}^{\infty} i^2 A_i Z^i - \frac{2m+1}{3} \left( \sum_{i=1}^{\infty} i A_i Z^i \right)^2 = 0.$$

Equating the coefficients of like powers of  $Z$  one can obtain the expressions



From system (5.18), (5.19) with the choice of  $A_1 = 1$  the parameter values of  $d$  and  $\alpha$  can be numerically determined. By these parameters the complete series solution (5.17) is reached.

Table 5.1 shows the calculated values of  $d$ ,  $\alpha$  and  $f'(0)$  and Fig. 5.1 the variation of  $f(0)$  with  $m$ .

The series forms for  $f(\eta)$  and  $f'(\eta)$  are given below for some special values of the exponent  $m$  ( $m = -0.5$ ;  $m = 0$ ;  $m = 1$ ) :

$$\begin{aligned}
 m &= -0.5 : \\
 f(\eta) &= 2.1277 - 2.8062(e^{-1.0639\eta}) + 0.92528(e^{-1.0639\eta})^2 \\
 &\quad - 0.33898(e^{-1.0639\eta})^3 + 0.12667(e^{-1.0639\eta})^4 \\
 &\quad - 0.047564(e^{-1.0639\eta})^5 + 0.017882(e^{-1.0639\eta})^6 \\
 &\quad - 0.00672(e^{-1.0639\eta})^7 + 0.00253(e^{-1.0639\eta})^8 \\
 &\quad - 0.00095(e^{-1.0639\eta})^9 + 0.00036(e^{-1.0639\eta})^{10} \\
 f'(\eta) &= 2.9855(e^{-1.0639\eta}) - 1.9687(e^{-1.0639\eta})^2 \\
 &\quad + 1.0819(e^{-1.0639\eta}) - 0.5391(e^{-1.0639\eta})^4 \\
 &\quad + 0.2530(e^{-1.0639\eta})^5 - 0.1141(e^{-1.0639\eta})^6 \\
 &\quad + 0.0501(e^{-1.0639\eta})^7 - 0.0215(e^{-1.0639\eta})^8 \\
 &\quad + 0.00910(e^{-1.0639\eta})^9 - 0.0038(e^{-1.0639\eta})^{10}
 \end{aligned}$$

$$\begin{aligned}
 m &= 0 : \\
 f(\eta) &= 1.4819 - 1.6832(e^{-0.9879\eta}) + 0.23898(e^{-0.9879\eta})^2 \\
 &\quad - 0.04524(e^{-0.9879\eta})^3 + 0.00909(e^{-0.9879\eta})^4 \\
 &\quad - 0.00185(e^{-0.9879\eta})^5 + 0.00038(e^{-0.9879\eta})^6 \\
 &\quad - 0.00007(e^{-0.9879\eta})^7 + 0.000015(e^{-0.9879\eta})^8 \\
 &\quad - 0.000003(e^{-0.9879\eta})^9 + 0.0000006(e^{-0.9879\eta})^{10} \\
 f'(\eta) &= 1.6629(e^{-0.9879\eta}) - 0.47219(e^{-0.9879\eta})^2 \\
 &\quad + 0.13408(e^{-0.9879\eta})^3 - 0.0359(e^{-0.9879\eta})^4 \\
 &\quad + 0.00916(e^{-0.9879\eta})^5 - 0.00224(e^{-0.9879\eta})^6 \\
 &\quad + 0.00053(e^{-0.9879\eta})^7 - 0.00012(e^{-0.9879\eta})^8 \\
 &\quad + 0.000028(e^{-0.9879\eta})^9 - 0.000006(e^{-0.9879\eta})^{10}
 \end{aligned}$$

$$\begin{aligned}
 m &= 1 : \\
 f(\eta) &= 1 - e^{-\eta} \\
 f'(\eta) &= e^{-\eta}
 \end{aligned}$$

It can be seen that for the case  $m = 1$  the obtained solution coincides with the exact solution (5.14). The effect of the exponent  $m$  on the velocity profiles  $f'(\eta)$  is illustrated in Fig. 5.2. The values of  $f'(0) = \zeta$  decrease as  $m$  is changing from negative values to positive ones.

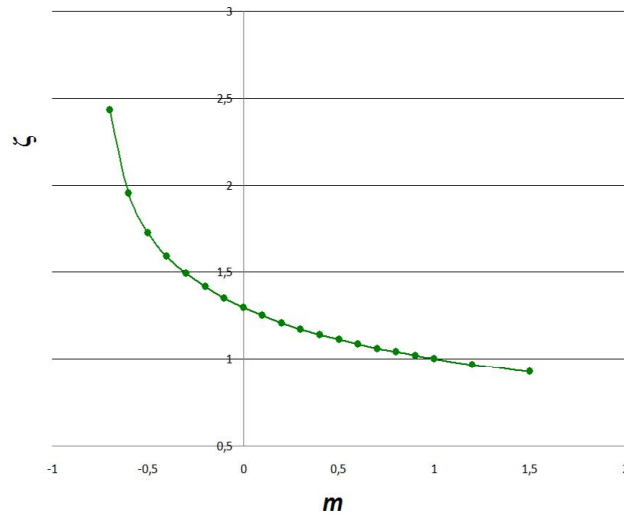


**Fig. 5.1** Variation of  $\zeta$  with  $m$

Applying the series solution to  $f$  the second order linear differential equation (5.12) for  $\Theta$  can be solved similarly, which presents the temperature distribution. Here we define  $\Theta(\eta)$  as the series

$$\Theta(\eta) = B_0 + \sum_{i=1}^{\infty} B_i d^i e^{-\alpha \eta^i},$$

with coefficients  $B_i$  ( $i = 0, 1, 2, \dots$ ) and hence the individual coefficients will be determined from differential equation (5.12) with (5.17) as follows

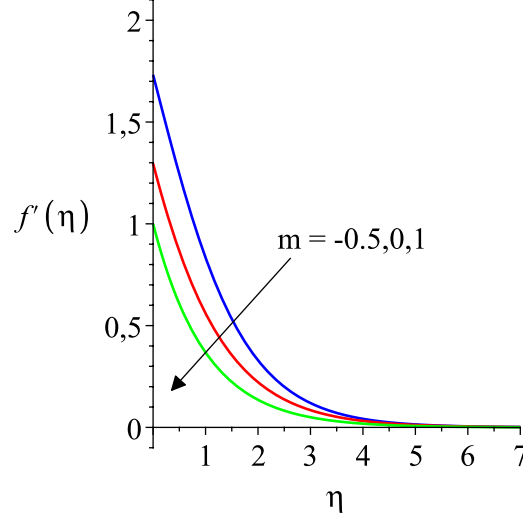


Fig. 5.2 Variation of  $f'$  with  $\eta$

$$\begin{aligned}
 B_1 &= A_1 B_0 \frac{Pr}{Pr-1} (m+1) \\
 B_2 &= \frac{1}{12} \frac{A_1^2 B_0 Pr}{(Pr-1)(Pr-2)} (3m^2 Pr + m^2 + 6mPr + 3Pr - 1) \\
 (5.22) \quad B_3 &= -\frac{1}{216} \frac{A_1^3 B_0 Pr}{(Pr-1)(Pr-2)(Pr-3)} F(Pr, m) \\
 F(Pr, m) &= ((m^3 - m)(3Pr^2 - 19Pr - 2) + (m^2 - 1)(4Pr^2 - 20Pr + 4)) \\
 &\vdots
 \end{aligned}$$

Remark that these coefficients as expressions of  $B_0$  can be calculated only for non integer values of the low Prandtl numbers. In (5.13) the second boundary condition is automatically satisfied, and from the first condition coefficient  $B_0$  is to be determined, i.e., from the equation

$$B_0 + B_1 d + B_2 d^2 + B_3 d^3 + \dots = 1$$

together with (5.22) (see Table 5.2).

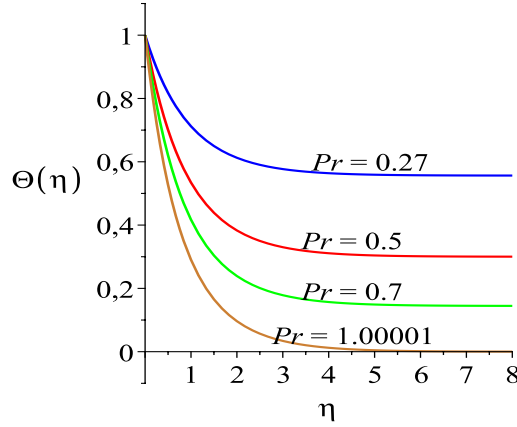


Fig. 5.3 Variation of  $\Theta$  with  $Pr$  ( $0.27 \leq Pr \leq 1.00001$ ) for  $m = 1$

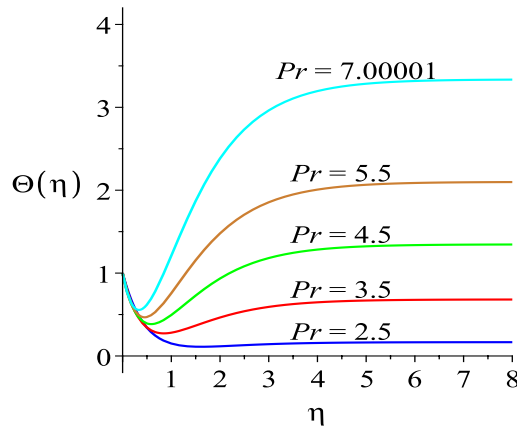


Fig. 5.4 Variation of  $\Theta$  with  $Pr$  ( $2.5 \leq Pr \leq 7.00001$ ) for  $m = 1$

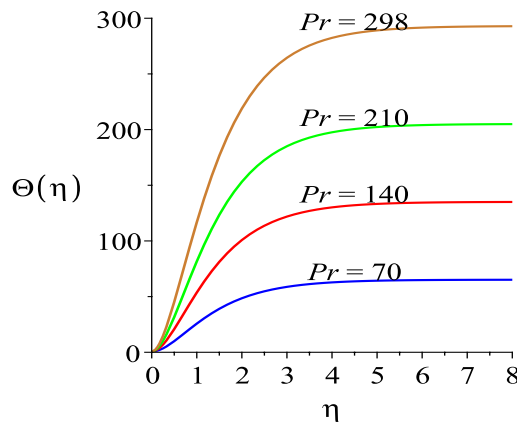


Fig. 5.5 Variation of  $\Theta$  with  $Pr$  ( $70 \leq Pr \leq 298$ ) for  $m = 1$

$Pr \setminus m$	-0.5	0	1
0.27	0.699360103	0.617716289	0.556343613
0.7	0.261867340	0.187464188	0.144444444
2.5	-6.868890324	0.732352234	0.166666667
5.5	-0.010101191	-0.020338815	2.100000049
70	-129.5918440	90.92275412	391/6
298	-521.5866457	-253.8172206	7326/25

**Table 5.2.** The values of  $B_0$

For  $\Theta(\eta)$  with Prandtl number  $Pr = 298$  and three values of  $m$  ( $m = -0.5; 0; 1$ ) the first ten terms are given below

$$\begin{aligned}
 m &= -0.5 : \\
 \Theta(\eta) &= -521.59 + 690.22(e^{-1.0639\eta}) - 228.35(e^{-1.0639\eta})^2 \\
 &\quad + 83.601(e^{-1.0639\eta})^3 - 31.324(e^{-1.0639\eta})^4 \\
 &\quad + 11.728(e^{-1.0639\eta})^5 - 4.4378(e^{-1.0639\eta})^6 \\
 &\quad + 1.6497(e^{-1.0639\eta})^7 - 0.6357(e^{-1.0639\eta})^8 \\
 &\quad + 0.2268(e^{-1.0639\eta})^9 - 0.0955(e^{-1.0639\eta})^{10}
 \end{aligned}$$

$$\begin{aligned}
 m &= 0 : \\
 \Theta(\eta) &= -253.81 + 433.90(e^{-0.9879\eta}) - 185.85(e^{-0.9879\eta})^2 \\
 &\quad + 23.32(e^{-0.9879\eta})^3 - 11.64(e^{-0.9879\eta})^4 \\
 &\quad - 0.6457(e^{-0.9879\eta})^5 - 1.77477(e^{-0.9879\eta})^6 \\
 &\quad - 0.87084(e^{-0.9879\eta})^7 - 0.69922(e^{-0.9879\eta})^8 \\
 &\quad - 0.51095(e^{-0.9879\eta})^9 - 0.40457(e^{-0.9879\eta})^{10}
 \end{aligned}$$

$$\begin{aligned}
 m &= 1 : \\
 \Theta(\eta) &= \frac{7326}{25} - \frac{44104}{75}(e^{-\eta}) + \frac{22201}{75}(e^{-\eta})^2
 \end{aligned}$$

It may be noted that the Prandtl number  $Pr = 298$  corresponds to the power transformer oil. We point out that for the case  $m = 1$  the solution  $\Theta(\eta)$  coincides with the exact solution (5.15).

The effects of the power law exponent  $m$  and the Prandtl number are exhibited in Figs. 5.3-5.12.  $Pr = 0.27$  corresponds to the mercury and  $Pr = 0.7$  to the air. Figs. 5.3-5.5 illustrate the influence of the Prandtl

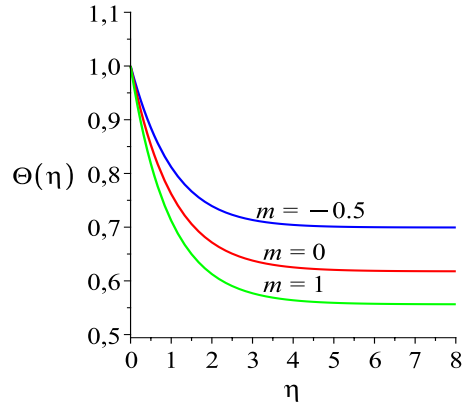


Fig. 5.6 Variation of  $\Theta$  for  $Pr = 0.27$

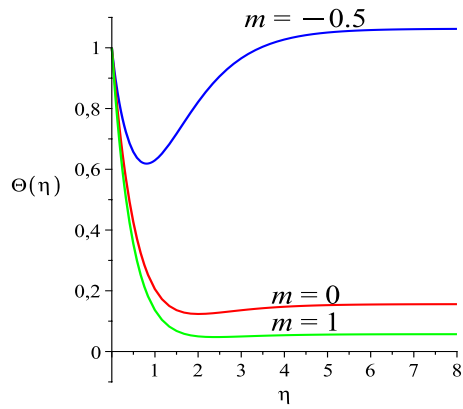


Fig. 5.7 Variation of  $\Theta$  for  $Pr = 2.2$

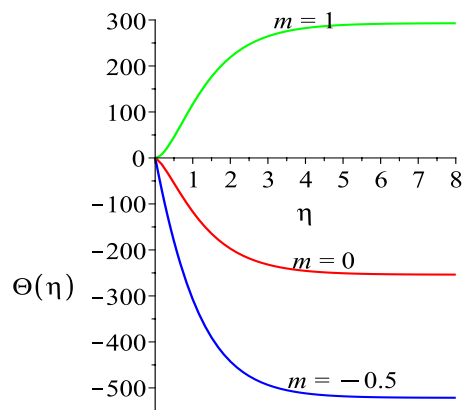


Fig. 5.8 Variation of  $\Theta$  for  $Pr = 298$

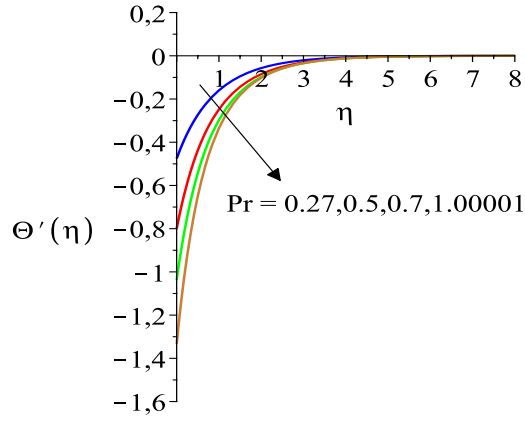


Fig. 5.9 The effect of the Prandtl number on  $\Theta'$  for  $m = 1$  ( $0.27 \leq Pr \leq 1.00001$ )

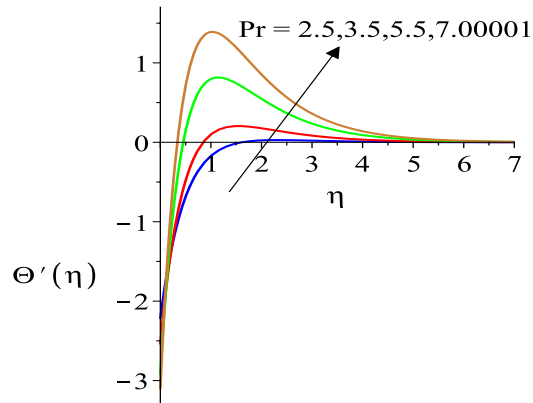


Fig. 5.10 The effect of the Prandtl number on  $\Theta'$  for  $m = 1$  ( $2.5 \leq Pr \leq 7.00001$ )

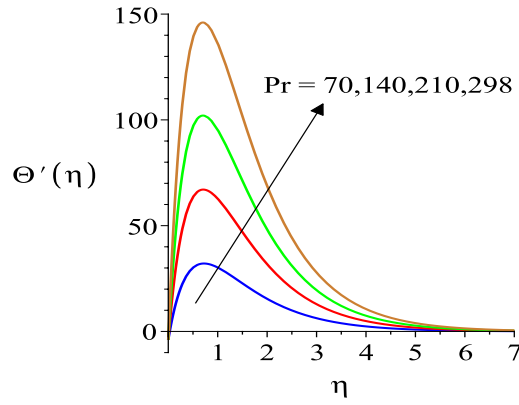


Fig. 5.11 The effect of the Prandtl number on  $\Theta'$  for  $m = 1$  ( $70 \leq \text{Pr} \leq 298$ )

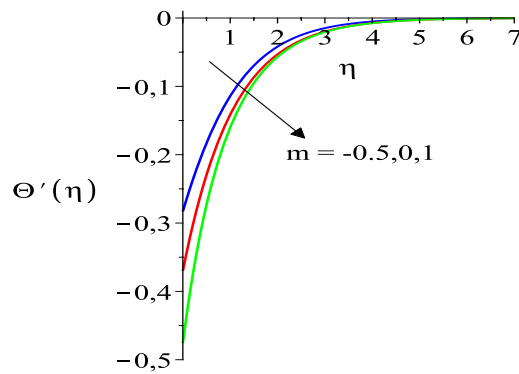


Fig. 5.12 The effect of  $m$  on  $\Theta'$  for  $\text{Pr} = 0.27$  ( $m = -0.5; 0; 1$ )

number on the temperature  $\Theta$  for  $m = 1$ . It can be observed in Fig. 5.3 that for low Prandtl numbers  $0.27 \leq \text{Pr} \leq 1.00001$  the maximum value of  $\Theta$  decreases as  $\text{Pr}$  increases while for high Prandtl numbers  $2.5 \leq \text{Pr} \leq 7.00001$  and  $70 \leq \text{Pr} \leq 298$  the maximum value of  $\Theta$  increases as  $\text{Pr}$  increases. In all three cases the boundary layer thickness increases as  $\text{Pr}$  increases. Figs. 5.6-5.8 depict the effect power exponent  $m$  for fixed values of  $\text{Pr}$ . It can be observed in Figs. 5.6-5.7 that the boundary layer thickness increases as  $m$  increases and the maximum value of  $\Theta$  decreases as  $m$  increases for  $\text{Pr} = 0.27; 2.2$ , while for high Prandtl number ( $\text{Pr} = 298$ ) the reverse effect of  $m$  on the maximum of  $\Theta$  can be seen. Figs. 5.9-5.11 illustrate the effect of  $\text{Pr}$  on  $\Theta'$  for  $m = 1$  and Fig. 5.12 represents the effect of  $m$  for  $\Theta'$  with  $\text{Pr} = 0.27$ .

To sum up, we can observe the effects of the power exponent and the Prandtl number in the figures and it is seen that the values of  $f'$  decrease as power exponent  $m$  increases. Moreover, the boundary layer thickness increases as  $m$  or  $\text{Pr}$  increases. From the temperature profiles, it is observed that for low Prandtl number the temperature  $\Theta$  decreases as  $\text{Pr}$  increases and for high Prandtl numbers the influence of  $\text{Pr}$  is opposite.

## 5.2 CONVECTIVE BOUNDARY CONDITION

Boundary layer flows with internal heat generation past a horizontal plate continues to receive considerable attention because of its practical applications in a broad spectrum of engineering systems like cooling of nuclear reactors, thermal insulation, combustion chamber and geothermal reservoirs.

Many principal past studies concerning natural convection flows over a semi-infinite vertical plate immersed in an ambient fluid have been found in the literature ([18], [27]). In many cases, these problems may admit similarity solutions.

The idea of using a convective boundary condition was recently introduced by Aziz [18], while Magyari [141] revisited this work, and obtained an exact solution for the temperature boundary layer in a compact integral form. Bataller [23] investigated the same problem by considering radiation effects on Blasius and Sakiadis flows ([5], [30], [69], [102], [103], [128]). The effects of suction and injection have been studied by the similarity analysis by Ishak [115] and a couple of recent papers have been devoted to the subject of boundary layer flow with convective boundary conditions (see e.g., [11], [45], [97], [100], [101], [144], [162], [169], [193], [194], [217], [218]). The similarity solutions to the convective heat transfer problems for Newtonian fluids have been studied by Aziz [18] and Magyari [141] for impermeable plate and by Ishak [115] for permeable plate. Motivated by the above mentioned investigations,

we consider the heat transfer characteristics of a viscous and incompressible power-law non-Newtonian fluid over a permeable moving sheet in a uniform shear flow with a convective surface boundary condition ([45], [50]).

### 5.2.1 BASIC EQUATIONS

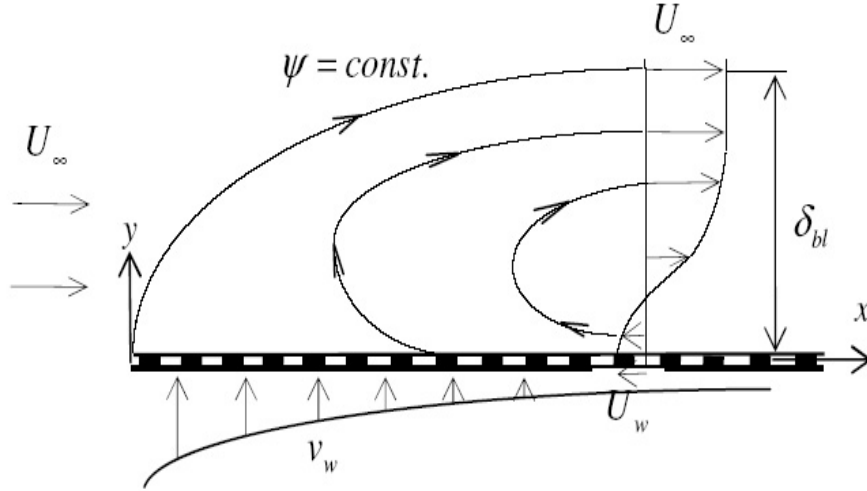


Fig. 5.13 Representation of the boundary layer velocity

We consider a uniform laminar flow of an incompressible viscous fluid with constant velocity  $U_\infty$  at high Reynolds number, past a parallel porous semi-infinite plate moving with a constant velocity  $U_w$  in the direction opposite to the main stream (see Fig. 5.13). The fluid temperature is  $T_\infty$  over the top surface of the flat plate. It is assumed that the bottom surface of the plate is heated by convection from a hot fluid of temperature  $T_f$ .

Within the framework of the above-noted assumptions, the governing equations of motion and heat transfer for non-Newtonian power-law flow neglecting pressure gradient and body forces can be described by the equations (1.1), (1.6) and (1.7) [225]:

$$(5.23) \quad \frac{\partial u}{\partial x} + \frac{\partial v}{\partial y} = 0,$$

$$(5.24) \quad u \frac{\partial u}{\partial x} + v \frac{\partial u}{\partial y} = \frac{K}{\rho} \frac{\partial}{\partial y} \left[ \left| \frac{\partial u}{\partial y} \right|^{n-1} \frac{\partial u}{\partial y} \right],$$

$$(5.25) \quad u \frac{\partial T}{\partial x} + v \frac{\partial T}{\partial y} = \frac{\partial}{\partial y} \left( \alpha_t \frac{\partial T}{\partial y} \right).$$

The applicable boundary conditions for the present model are :

i.) on the plate surface  $y = 0$  (no slip, permeable surface and convective surface heat flux)

$$(5.26) \quad u(x, 0) = -U_w,$$

$$(5.27) \quad v(x, 0) = v_w(x),$$

$$(5.28) \quad -k \frac{\partial T}{\partial y} = h_f(T_f - T_w),$$

where  $h_f$  is the heat transfer coefficient, and  $k$  denotes the thermal conductivity;  $v_w(x)$  is the mass transfer velocity at the surface, and  $v_w(x) > 0$  for injection (blowing),  $v_w(x) < 0$  for suction and  $v_w(x) = 0$  for impermeable surface. As indicated in [199], a similarity solution is possible only if the injection/suction velocity  $v_w$  has an  $x$  variation of the form  $x^{\frac{-n}{n+1}}$ .

ii.) matching with the free stream as  $y \rightarrow \infty$

$$(5.29) \quad u(x, \infty) = U_\infty,$$

$$(5.30) \quad T(x, \infty) = T_\infty.$$

For the uniform temperature  $T_w$  over the top surface of the plate we have the relations:  $T_f > T_w > T_\infty$ .

Introducing the stream function, the equation of continuity (1.1) is satisfied identically. On the other hand, we have

$$(5.31) \quad \frac{\partial \psi}{\partial y} \frac{\partial^2 \psi}{\partial y \partial x} - \frac{\partial \psi}{\partial x} \frac{\partial^2 \psi}{\partial y^2} = \mu_{cn} \frac{\partial}{\partial y} \left[ \left| \frac{\partial^2 \psi}{\partial y^2} \right|^{n-1} \frac{\partial^2 \psi}{\partial y^2} \right],$$

and conditions (5.26), (5.27), (5.29) can be written as

$$(5.32) \quad \psi_y(x, 0) = 0, \quad \psi_x(x, 0) = v_w(x), \quad \psi_y(x, \infty) = U_\infty.$$

Equation (5.31) with the transformed boundary conditions has the form (see Section 2.2 and [45]):

$$(5.33) \quad \left( |f''|^{n-1} f'' \right)' + \frac{1}{n+1} f f'' = 0,$$

$$(5.34) \quad f(0) = f_w, \quad f'(0) = -\lambda, \quad f'(\infty) = \lim_{\eta \rightarrow \infty} f'(\eta) = 1,$$

where

$$f_w = -(n+1) v_w(x) \left( \frac{x^n}{\mu_{cn} U_\infty^{2n-1}} \right)^{\frac{1}{n+1}}$$

determines the transpiration rate at the surface. Then  $f_w > 0$  corresponds to suction,  $f_w < 0$  to injection and  $f_w = 0$  to impermeable surface. The dimensionless velocity components have the form

$$\begin{aligned} u(x, y) &= U_\infty f'(\eta), \\ v(x, y) &= \frac{U_\infty}{n+1} \text{Re}_x^{-\frac{1}{n+1}} (\eta f'(\eta) - f(\eta)), \\ \eta &= \text{Re}_x^{\frac{1}{n+1}} \frac{y}{x}, \quad \text{Re}_x = \rho \frac{U_\infty^{2-n} x^n}{K}. \end{aligned}$$

The thermal diffusivity can be defined as

$$(5.35) \quad \alpha_t = \omega \left| \frac{\partial u}{\partial y} \right|^{n-1}$$

for  $u \neq 0$  ( $\omega$  positive constant) and  $\alpha_t = 0$  for  $u = 0$  (see paper by Zheng et al. [225]). Hence, from equation (5.25) we have

$$(5.36) \quad u \frac{\partial w}{\partial x} + v \frac{\partial w}{\partial y} = \omega \frac{\partial}{\partial y} \left( \left| \frac{\partial u}{\partial y} \right|^{n-1} \frac{\partial w}{\partial y} \right).$$

Defining the non-dimensional temperature by

$$\Theta(\eta) = w(x, y),$$

i.e.,

$$T = T_\infty + \Theta(\eta)(T_f - T_\infty),$$

we get

$$(5.37) \quad \left( |f''(\eta)|^{n-1} \Theta'(\eta) \right)' + \frac{\text{Pr}}{n+1} f(\eta) \Theta'(\eta) = 0,$$

where  $\text{Pr} = K/\rho\omega$  is the Prandtl number. The transformed boundary conditions for the energy equation (5.37) is

$$\Theta'(0) = - \left( \frac{\mu_{cn}}{U_\infty^{2-n}} x \right)^{\frac{1}{n+1}} \frac{h_f(x)}{k} (1 - \Theta(0))$$

and substituting

$$(5.38) \quad \bar{a} = \frac{c}{k} \left( \frac{\mu_{cn}}{U_\infty^{2-n}} \right)^{\frac{1}{n+1}},$$

one can obtain

$$(5.39) \quad \Theta'(0) = -\bar{a}(1 - \Theta(0))$$

under the assumption that the heat transfer coefficient

$$h_f = cx^{-1/(n+1)}.$$

We note that for Newtonian case it was shown in [18], [23], [115] and [210] that similarity solutions exist if  $h_f$  is proportional to  $x^{-1/2}$ . For a uniform surface temperature  $\Theta(0) = 1$  holds and from (5.39)  $\Theta'(0) = 0$ . This adiabatic case has been analyzed by Magyari for Newtonian fluid [141].

Boundary condition (5.30) can be formulated as

$$(5.40) \quad \Theta(\infty) = \lim_{\eta \rightarrow \infty} \Theta(\eta) = 0.$$

There is no exact solution to (5.33), (5.34) and (5.37), (5.39), (5.40), therefore we solve the boundary value problems associated with the similarity problems numerically to examine the behavior of the solutions.

### 5.2.2 NUMERICAL RESULTS

The symbolic algebra software Maple 12 was used to solve the nonlinear ordinary differential equation (5.33) subject to the boundary conditions in (5.34) by applying the Runge-Kutta-Fehlberg fourth-fifth method. On the flow and thermal fields the influence of the governing parameters, the Prandtl number, the power-law index  $n$ , the convective parameter  $\bar{a}$  and the constant value  $f_w$  characterizing the transpiration rate at the surface is discussed.

Fig. 5.15 shows the Maple generated numerical solution to the velocity profiles for different values of  $n$ . The velocity gradient at the surface, which represents the skin friction coefficient, increases with increasing  $n$  (see [38]) and also with increasing  $f_w$  (see Fig. 5.14 and [115]). Suction thins the boundary layer and increases the wall slope. Hence, the wall shear stress is higher for suction compared to injection. Blowing thickens the boundary layer and make the profile S-shaped.

For fixed Prandtl numbers 0.72 and 50, for selected values of the power index  $n$ , for a range of parameters  $\bar{a}$ , for  $f_w = -1; 0; 2$  the numerical data for  $-\Theta'(0)$  and  $\Theta(0)$  were calculated [45]. Fig. 5.16 shows the temperature profiles for different Prandtl numbers and Fig. 5.17 for different values of  $n$ . Fig. 5.16 represents that the heat transfer rate at the surface is higher as Pr is increasing. Moreover, the heat transfer rate at the surface is higher for dilatant fluids ( $n > 1$ ) than for pseudoplastics ( $n < 1$ ).

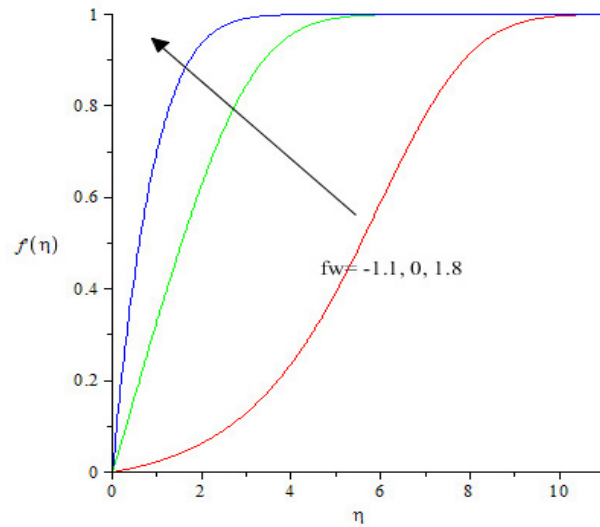


Fig. 5.14 The profiles of  $f'(\eta)$  for different values of  $f_w$

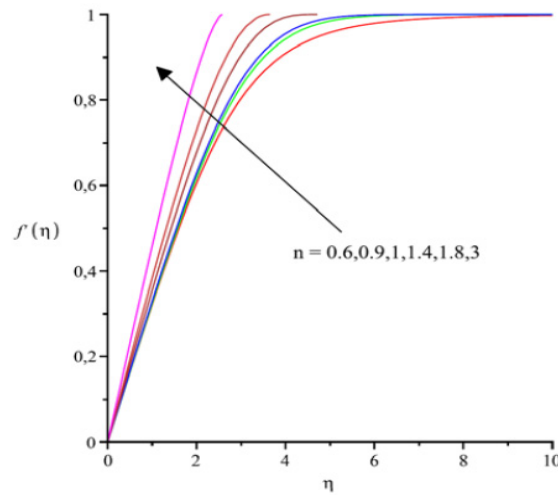


Fig. 5.15 The profiles of  $f'(\eta) = u(x, y)/U_\infty$  for different values of  $n$

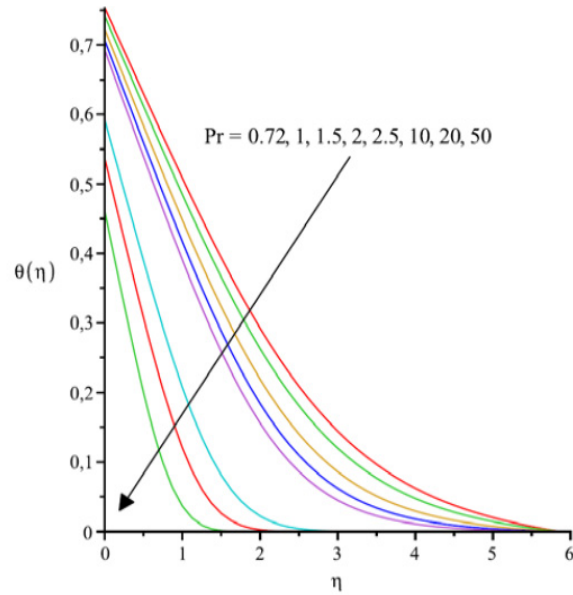


Fig. 5.16 Temperature profiles for different values of  $Pr$  when  $n = 0.5$ ,  $f_w = 0$  and  $\bar{a}=1$

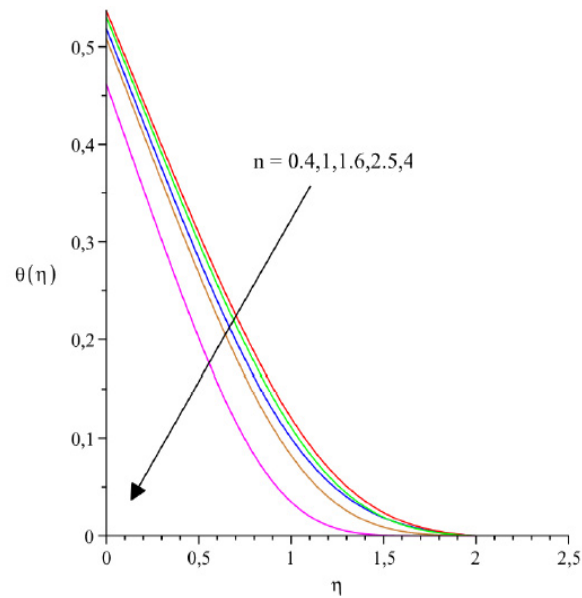
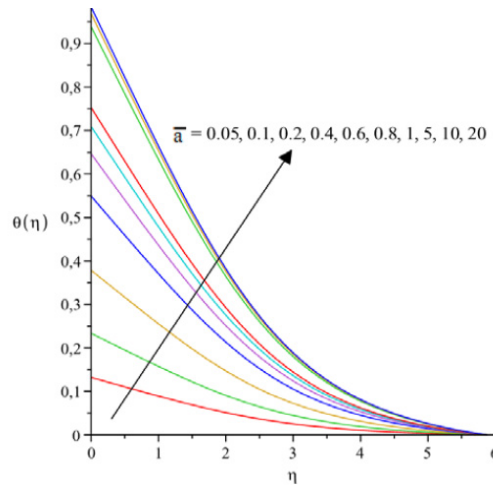


Fig. 5.17 Temperature profiles for different values of  $n$  when  $Pr = 10$ ,  $f_w = 0$  and  $\bar{a}=1$

In case of Newtonian fluid ( $n = 1$ ), the numerical values show a good agreement with those reported by Aziz [18] and Ishak [115].

Fig. 5.19 exhibits that the heat transfer rate at the surface is higher for suction and smaller for injection. This is due to the fact that the surface shear stress increases for suction. Fig. 5.18 shows the numerical solutions for different values of  $\bar{a}$  when  $Pr = 0.72$  for a pseudoplastic fluid with  $n = 0.5$ . We see that the surface temperature increases as  $\bar{a}$  increases.



**Fig. 5.18** Temperature profiles for different values of  $\bar{a}$  when  $Pr = 0.72$ ,  $f_w = 0$  and  $n = 0.5$

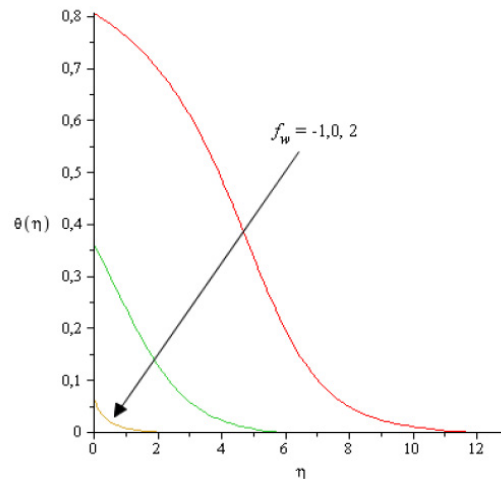


**Fig. 5.19** Temperature profiles for different values of  $f_w$  when  $n = 0.5$ ,  $Pr = 1$  and  $\bar{a} = 0.2$

## 6 CONCLUSIONS

Due to the practical necessity, it is important to study the influence of the non-Newtonian behavior on the lubrication velocity and temperature fields. Within the thin boundary layer, the wall shear stress and the friction drag of the surface can also be estimated.

This dissertation is concerned to derive useful information in the boundary layer by calculating the velocity and the temperature distributions, and predict the drag coefficients for non-Newtonian power-law fluids.

The main results of the dissertation are listed below:

**1.** *Applying a similarity transformation, the boundary layer governing equations (2.17) and (2.18) for the two-dimensional steady flow of an incompressible, non-Newtonian power-law fluid flow along a stationary, horizontal plate situated in a fluid stream moving with constant velocity  $U_\infty$  have been reduced to an ordinary differential equation called generalized Blasius equation (2.25). For non-Newtonian fluid flows using a modified version of Töpfer's method, instead of the boundary value problem (2.25)–(2.26) an initial value problem (2.31)–(2.33) has been solved to determine the non-dimensional velocity gradient  $f''(\eta)$ . The influence of the power exponent  $n$  on the velocity components has been examined. From the velocity profiles  $f'(\eta) = u(x, y)/U_\infty$  and  $v(x, y)/v^*(x) = \eta f'(\eta) - f(\eta)$ , we have concluded that the boundary layer thickness decreases as  $n$  increases (Figs. 2.2–2.3). The non-dimensional velocity gradient  $f''(\eta)$  is decreasing from a positive  $f''(0) = \gamma$  at the wall to zero outside the viscous boundary layer (Fig. 2.4). It was observed that the rate of decrease is greater with increasing the value  $n$  (Fig. 2.4). I found that the effect of power  $n$  on  $f''(0)$  is significant (Fig. 2.5); it is decreasing up to  $n \approx 0.7$  and after it is monotonically increasing [38], [51], [47].*

**2.** *It was shown that there exists a series solution of the form  $f(\eta) = \eta^2 \sum_{k=0}^{\infty} a_k \eta^{3k}$  to the generalized Blasius problem (2.25), (2.26), where the first three coefficients are given by*

$$a_0 = \frac{\gamma}{2}, \quad a_1 = -\frac{\gamma^{3-n}}{5!n(n+1)}, \quad a_2 = \frac{\gamma^{5-2n}(21-10n)}{8!n^2(n+1)^2},$$

*and for the further coefficients the recursive formula (2.43) was given. The radius of convergence of the power series can be calculated by (2.45). The numerical simulations exhibit that the radius of convergence is significantly increasing with increasing power exponent  $n$  [38].*

**3.** *From the continuity equation (2.17) and momentum equation (2.18) for a non-Newtonian power-law fluid flow with fluid velocity  $U_\infty = \tilde{B}y^\sigma$ , a*

boundary value problem has been derived applying the similarity transformation method. The basic equations are subjected to the boundary conditions in (2.46) and are transformed to (2.56), (2.57). If  $n \neq 2$ , the velocity components are expressed with similarity variables in (2.60) and (2.61). The similarity solutions are determined in power series form and the recursive formula (2.67) has been obtained for the determination of the coefficients. Numerical calculations were obtained for some values of  $n$  (0.5; 1; 1.5) and for different values of  $\sigma$  ( $-1/2$ ;  $-1/3$ ; 0) (see Figs.2.7-2.12). On the base of simulations, it was observed that with increasing the power exponent  $n$ , the boundary layer thickness and the parameter  $[f''(0)]^n$  involved in the wall shear stress are decreasing both for  $\sigma = 0$  and  $\sigma = -1/2$ . For the non-Newtonian power-law fluids when  $n \neq 2$ , my results [42], [46] generalize Cossali's results obtained for the Newtonian case [70].

4. For permeable and non-permeable surface moving with velocity  $U_w(x) = Ax^\kappa$  in an otherwise quiescent fluid medium, the Crane's solution [72], and Gupta and Gupta's solutions [96] are generalized into the exponential series form  $f(\eta) = \alpha (A_0 + \sum_{i=1}^{\infty} A_i a^i e^{-\alpha i \eta})$ , where  $\alpha > 0$ , and  $A_0 = 1$ ,  $A_i$  ( $i = 1, 2, \dots$ ) denote the coefficients. A method was presented for the determination of the coefficients when the surface is impermeable or permeable. The values of  $f''(0)$  involved in the wall shear stress

$$(6.1) \quad \tau_w = \left[ \rho \mu A^3 \frac{\kappa + 1}{2} \right]^{\frac{1}{2}} x^{\frac{3\kappa-1}{2}} f''(0),$$

have been calculated for each case (see Tables 3.1-2). [43]

5. The fluid flow properties over an impermeable flat plate moving with a constant velocity  $U_w$  in an otherwise quiescent fluid medium are examined. The boundary layer equations (2.17), (2.18) are considered with the boundary conditions given in (3.15). The similarity solutions satisfy the equation (2.25) with boundary conditions

$$f(0) = 0, \quad f'(0) = 1, \quad \lim_{\eta \rightarrow \infty} f'(\eta) = 0.$$

The simulations were carried out for pseudoplastic media. It was observed that the skin friction parameter in absolute value, the value of  $[-f''(0)]^n$  and the boundary layer thickness decrease as the power exponent  $n$  increases [39].

6. According to our simulations of the flow characteristics in a uniform mainstream  $U_\infty$  over a surface moving with velocity  $U_w$  in the direction opposite to that of main stream, it was observed that similarity solution exists

only if the velocity ratio  $\lambda = U_w/U_\infty < \lambda_c$ . An iterative method was determined for the solution of the boundary value problem (2.25), (4.10) to evaluate the skin friction parameter  $f''(0)$  for different values of  $n$  and  $\lambda$ . It was shown that the upper bound  $\lambda_c$  increases as  $n$  increases (see Fig.4.3). On the base of numerical simulations, we represented how  $[f''(0)]^n$  changes with  $\lambda$  for different power exponents  $n$  (see Fig.4.2) [53]. For some values of  $\lambda$ , it was observed that  $f''$  is strictly monotonically decreasing for negative values of  $\lambda$  while for positive  $\lambda$  it takes its maximum in the boundary layer. Upper bounds were given for  $\lambda_c$  [44], thus generalizing the results of Hussaini, Lakin and Nachman [111].

7. The similarity solutions are compared with numerical simulations obtained by using the commercial code ANSYS FLUENT when a flat surface is moving parallel to an ambient stream of a power-law fluid media. Instead of the boundary layer equations (1.1), (1.6), the system of full equations (1.1), (1.4), (1.5) is considered, where the apparent viscosity is calculated by the relationship (1.12). In our computations, the coupled scheme for the pressure and the velocity is applied. Comparing the theoretical (similar) velocity solution  $u/U_\infty$  with the numerical solutions obtained by ANSYS FLUENT, satisfactory agreement has been found. Therefore, the similarity solutions verify the numerical simulations calculated by ANSYS FLUENT. Moreover, the numerical pressure and velocity distributions prove the validity of Prandtl's boundary layer assumptions.

8. Assuming that the solid surface is impermeable, the surface tension varies linearly with the temperature and the interface temperature is a power-law function of the distance along the surface, the Marangoni effect has been investigated for Newtonian fluid flow. The power in the temperature gradient was denoted by  $m$  with minimum value -1, which corresponds to no temperature variation on the surface and no Marangoni induced flow. The similarity solution has been determined in exponential series form. For  $m = 1$ , our solution is the same as Crane's solution [72]. Applying solutions of  $f$ , the temperature profiles were generated in series form and the influence of  $m$  and the Prandtl number  $Pr$  was investigated. It was observed that  $f'$  decreases with increasing  $m$ . The thermal boundary layer thickness increases with increasing  $m$ , or  $Pr$ . From the temperature profiles, it is observed that for low Prandtl number the temperature decreases as  $Pr$  increases and for high Prandtl numbers the influence of  $Pr$  is opposite [48].

9. The boundary layer flow with internal heat generation past a horizontal surface has been investigated. The heat transfer characteristics of a

6. CONCLUSIONS

---

*viscous and incompressible power-law non-Newtonian fluid over a permeable moving sheet in a uniform shear flow with a convective surface boundary condition were examined using the similarity method ([45], [50]). Both the hydrodynamic and thermal boundary layer thickness increase as  $\lambda$  increases, or  $Pr$  decreases, or  $n$  decreases. Our calculations indicate that the velocity gradient at the surface, which is involved in the wall shear stress and in the drag coefficient, increases with increasing  $n$  and also with increasing  $f_w$  which characterizes the transpiration rate at the surface. Suction thins the thermal boundary layer and increases the wall slope. Blowing thickens the boundary layer and make the profile S-shaped. The heat transfer rate at the surface is higher for suction and smaller for injection. Moreover, the heat transfer rate at the surface is higher for dilatant fluids than for pseudoplastics. For a Newtonian fluid, our numerical results are in good agreement with those reported by Aziz [18] and Ishak [115].*

## 7 ACKNOWLEDGEMENT

My kindest thanks belongs to my co-authors Ondrej Dosly (Masary University, Plzen, Czech Republic), Pavel Drábek (University of West Bohemia, Brno, Czech Republic), Siavash Sohrab (Northwestern University, Evanston IL, USA), Miklós Rontó (University of Miskolc), Kálmán Marossy (University of Miskolc), Erika Rozgonyi (University of Miskolc), Imre Gombkötő (University of Miskolc), János Kovács (Institute of Materials and Environmental Chemistry, Chemical Research Center, Hungarian Academy of Sciences), Krisztián Hriczó and Zoltán Csáti (University of Miskolc), for their essential contribution to our joint papers, and their helpful advice in my field of research. I wish to express my deepest gratitude to Árpád Elbert and Miklós Farkas, for his inspiring attitude, never-ending optimism and continuous encouragement.

I would also like to thank Ibolya Hapák for the careful revision of the language of this work.

I owe my most sincere thanks to my family for their patience, and continuous support that they have always shown to me.

This research was (partially) carried out in the framework of the Center of Excellence of Mechatronics and Logistics at the University of Miskolc.

## BIBLIOGRAPHY

- [1] Abbasbandy S.: A numerical solution of Blasius equation by Adomian's decomposition method and comparison with homotopy perturbation method, *Chaos Solitons Fractals*, **31** (2007), 257-260.
- [2] Abedian, B., Kachanov, M.: On the effective viscosity of suspensions, *International Journal of Engineering Science*, **48** (2010), 962-965.
- [3] J.A.D. Ackroyd, A series method for the solution of laminar boundary layers on moving surfaces, *J. Appl. Math. Phys. (ZAMP)*, **29** (1978), 729-741.
- [4] Acrivos A., Shah M.J., Peterson E.E.: Momentum and heat transfer in laminar boundary flow of non-Newtonian fluids past external surfaces, *AIChE J.*, **6** (1960), 312-317.
- [5] Ahmad F., Al-Barakati W.H.: An approximate analytic solution of the Blasius problem, *Comm. Nonlinear Sci. Num. Simul.*, **14** (2009), 1021-1024.
- [6] Ahmad F.: Degeneracy in the Blasius problem, *Electron J. Differ Equations*, **92** (2007), 1-8.
- [7] Al-Mudhaf A., Chamka A.J.: Similarity solutions for MHD thermosolutal Marangoni convection over a flat surface in the presence of heat generation or absorption effects, *Heat & Mass Transfer*, **42** (2005), 112-121.
- [8] Allan F.M.: Similarity solutions of a boundary layer problem over moving surfaces, *Appl. Math. Lett.*, **10** (1997), 81-85.
- [9] Altan, T., Oh S., Gegel H.: *Metal Forming Fundamentals and Applications*, American Society of Metals, Metals Park 1979.
- [10] Ames W.F.: *Nonlinear Ordinary Differential Equations in Transport Processes*, Academic Press 1968.
- [11] Aman F., Ishak A., Pop I.: Heat transfer at a stretching/shrinking surface beneath an external uniform shear flow with a convective boundary condition, *Sains Malaysiana*, **40** (2011), 1369-1374.
- [12] Anderson J.D.: Ludwig Prandtl's boundary layer, *Physics Today*, 2005 December, 42-48.
- [13] Andersson H.I., Irgens F.: *Film flow of power law fluid*, In: N.P. Cheremisinoff (ed.) *Encyclopedia of Fluid Mechanics, Polymer Flow Engineering*, Vol.9 pp. 617-648, Texas Gulf Publishing, 1990.
- [14] Arafune K., Hirata A.: Interactive solutal and thermal Marangoni convection in a rectangular open boat, *Numerical Heat Transfer Part A*, **34** (1998), 421-429.

## BIBLIOGRAPHY

- 
- [15] Ariel P.D., Hayat T., Asghar S.: Homotopy perturbation method and axisymmetric flow over a stretching sheet, *Internat. J. Nonlinear Sciences and Numerical Simulation*, **7** (2006), 399-406.
- [16] Arifin N.M., Nazar R., Pop I.: Marangoni-driven boundary layer flow in nanofluids, In Latest Trends on Theoretical and Applied Mechanics, Fluid Mechanics and Heat & Mass Transfer, Corfu Island, Greece, July 22-24. 2010, WSEAS Press, 32-35.
- [17] Dell'Avenana P., Monti R., Gaeta F. S.: Marangoni flow and coalescence phenomena in microgravity. *Adv. Space Res.*, **16** (1995), (7)95-(7)98.
- [18] Aziz A.: A similarity solution for laminar thermal boundary layer over a flat plate with a convective surface boundary condition, *Comm. Nonlinear Sci. Numer. Simulation*, **14** (2009), 1064-1068.
- [19] Banks W.H.H.: Similarity solutions of the boundary-layer equations for a stretching wall, *J. Mec. Theor. Appl.*, **2** (1983), 375-392.
- [20] Barenblatt G.I.: Scaling laws for fully developed turbulent shear flows. Part 1. Basic hypotheses and analysis, *J. Fluid Mech.*, **248** (1993), 513-520.
- [21] Barenblatt G.I., Protokishin V.M.: Scaling laws for fully developed turbulent shear flows. Part 2. Processing of experimental data, *J. Fluid Mech.* **248** (1993), 521-529.
- [22] Barnes H.A.: A brief history of the yield stress, *Appl. Rheol.*, **9** (1999), 262-266.
- [23] Bataller R.C.: Radiation effects for the Blasius and Sakiadis flows with a convective surface boundary condition, *Appl. Math. Comput.*, **206** (2008), 832-840.
- [24] Bates T.W., Williamson B., Spearot J.A., Murphy C.K.: A correlation between engine oil rheology and oil film thickness in engine journal bearings, Technical Report 860376 Society of Automotive Engineers 1986.
- [25] Benlahsen M., Guedda M., Kersner R.: The generalized Blasius equation revisited, *Mathematical and Computer Modelling*, **47** (2008), 1063-1076.
- [26] Bird R.B., Stewart W.E., Lightfoot E.N.: *Transport Phenomena*, John Wiley, 1960.
- [27] Bird R.B., Armstrong R.C., Hassager O.: *Dynamics of Polymeric Liquids, Fluid Dynamics*, John Wiley, New York 1987.
- [28] Bird R.B., Öttinger H.C.: Transport properties of polymeric liquids, *Ann. Revs. Phys. Chem.*, **54** (1992), 371-406.

## BIBLIOGRAPHY

- 
- [29] Bird R.B., Graham M.D.: *General Equations of Newtonian Fluid Dynamics*, Chapter 3 of *The Handbook of Fluid Dynamics*, (ed.: Richard W. Johnson) CRC Press, Boca Raton 1998.
- [30] Blasius H.: Grenzsichten in Flüssigkeiten mit kleiner Reibung, *Z. Math. Phys.*, **56** (1908), 1-37.
- [31] Bognár G.: On the solution of some nonlinear boundary value problem, In: Lakshmikantham V.(ed.): *World Congress of Nonlinear Analysts, Proceedings of the First World Congress of Nonlinear Analysts '92*, Tampa,USA, Walter de Gruyter, Berlin-New York 2449-2458.(ISBN:3-11-013215-X)
- [32] Bognár G.: The application of isoperimetric inequalities for nonlinear eigenvalue problems, *WSEAS Transactions on Systems*, **1** (2002), 119-124.
- [33] Bognár G., Dábek P.: The  $p$ -Laplacian equation with superlinear and supercritical growth, multiplicity of radial solutions, *Nonlinear Analysis Series A, Theory & Methods*, **60** (2005), 719-728.
- [34] Bognár G., Rontó M., Rajabov N.: On initial value problems related  $p$ -Laplacian and pseudo-Laplacian, *Acta Math. Hungar.*, **108** (2005), 1-12.
- [35] Bognár G.: Local analytic solutions to some nonhomogeneous problems with  $p$ -Laplacian, *E. J. Qualitative Theory of Diff. Equ.*, **4**. (2008), 1-8.
- [36] Bognár G.: Numerical and analytic investigation of some nonlinear problems in fluid mechanics, in N. Mastorakis (ed.): *Computers and Simulation in Modern Science*, WSEAS Press (2008) ISBN: 978-960-474-032-1, 172-180.
- [37] Bognár G.: Estimation on the first eigenvalue for some nonlinear Dirichlet eigenvalue problems, *Nonlinear Analysis: Theory, Methods & Applications*, **71** (2009), e2442-2448.
- [38] Bognár G.: Similarity solutions of boundary layer flow for non-Newtonian fluids, *Int. J. Nonlinear Scie. Numerical Simulations*, **10** (2009), 1555-1566.
- [39] Bognár G.: Boundary layer problem on conveyor belt, VI Conferencia Científica Internacional de Ingeniería Mecánica, COMEC 2010 Cuba, 1-5. ISBN:978-959-250-602-2
- [40] Bognár G., S. H. Sohrab: Periodic flows associated with solutions of Hill equation, Chapter 13. In: N. Mastorakis (ed.): *Computers and Simulation in Modern Science Vol.IV*. WSEAS Press 2010. ISBN: 978-960-474-276-7, 145-155.
- [41] Bognár G., Marossy K., Rozgonyi E.: Calculation of the temperature distribution for polymer melt, In: *Latest Trends on Engineering Mechanics, Structures, Engineering Geology* WSEAS Press 2010, 348-353. ISBN: 978-960-474-203-5

BIBLIOGRAPHY

---

- [42] Bognár G.: Power series solutions of boundary layer problem for non-Newtonian fluid flow driven by power law shear, In: S. Lagakos et al. Recent Advances in Applied Mathematics, Harvard Univ. Cambridge, USA, Jan. 27-29, 2010. American Conference on Applied Mathematics, Mathematics and Computers in Science and Engineering A Series of Ref Books and Textbooks, WSEAS Press ISBN: 978-969-474-150-2, 244-250.
- [43] Bognár G.: Analytic solutions to the boundary layer problem over a stretching wall, *Computers and Mathematics with Applications*, **61** (2011), 2256-2261.
- [44] Bognár G.: On similarity solutions to boundary layer problems with upstream moving wall in non-Newtonian power-law fluids, *IMA J. Applied Mathematics*, **77** No.4 (2012), 546-562.
- [45] Bognár G., Hriczó K.: Similarity Solution to a thermal boundary layer model of a non-Newtonian fluid with a convective surface boundary condition, *Acta Polytechnica Hungarica*, **8** (2011), 131-140.
- [46] Bognár G.: Analytic solutions to a boundary layer problem for non-Newtonian fluid flow driven by power law velocity profile, *WSEAS Transactions on Fluid Mechanics*, **6** (2011), 22-31.
- [47] Bognár G.: On similarity solutions for non-Newtonian boundary layer flows, *Electronic Journal of Qualitative Theory of Differential Equations*, **2012** No.2 (2012), 1-8.
- [48] Bognár G., Hriczó K.: Series solutions for Marangoni convection on a vertical surface, *Mathematical Problems in Engineering*, Volume 2012, Article ID 314989, 18 pages, doi:10.1155/2012/3149899
- [49] Bognár G., Gombkötő I., Hriczó K.: Power-law non-Newtonian fluid flow on an inclined plane, *International Journal of Mathematical Models and Methods in Applied Sciences*, **6** (2012), 72-80.
- [50] Bognár G., K. Hriczó: Laminar thermal boundary layer model for power-law fluids over a permeable surface with convective boundary condition, In: Recent Advances in Fluid Mechanics, Heat & Mass Transfer, 198-203. ISBN: 978-1-61804-065-7
- [51] Bognár G.: The boundary layer problems of power-law fluids, *Math. Bohemica*, **137** (2012), 139-148.
- [52] Bognár G., Kovács J.: Non-isothermal steady flow of power-law fluids between parallel plates, *International Journal of Mathematical Models and Methods in Applied Sciences*, **6** (2012), 122-129.

## BIBLIOGRAPHY

- 
- [53] Bognár G., Csáti Z.: Iterative transformation method for the generalized Blasius equation, XXVI microCAD International Scientific Conference, Miskolc, 29-30 March 2012, E10 ISBN: 978-963-661-773-8
- [54] Boiron O., Deplano V., Pelissier R.: Experimental and numerical studies on the starting effect on the secondary flow in a bend, *Journal of Fluid Mechanics* **574** (2007), 109-129.
- [55] Boyd J.P.: The Blasius function in the complex plane, *J. Experimental Math.*, **8** (1999), 381-394.
- [56] Boyd J.P.: The Blasius function: Computations before computers, the value of tricks, undergraduate projects, and open research problems, *SIAM Review*, **50** (2008), 791-804.
- [57] Brewster M.E., Chapman S.J., Fitt A.D., Please C.P.: Asymptotics of slow flow of very small exponent power-law shear-thinning fluids in a wedge, *European J. Appl. Math.*, **6** (1995), 559-571.
- [58] Brighi B., Hoernel J-D.: Asymptotic behavior of the unbounded solutions of some boundary layer equations, arxiv:math/0512345v1 (2005)
- [59] Briot Ch., Bouquet J.K.: Étude des fonctions d'une variable imaginaire, *Journal de l'École Polytechnique, Cahier*, **36** (1856), 85-131.
- [60] Buongiorno J.: Convective transport in nanofluids, *ASME J. Heat Transfer*, **128** (2006), 240-250.
- [61] Callegari A.J., Friedman M.B.: An analytical solution of a nonlinear, singular boundary value problem in the theory of viscous flows, *J. Math. Anal. Appl.*, **21** (1968), 510-529.
- [62] Callegari A.J., Nachman A.: Some singular nonlinear differential equations arising in boundary layer theory, *J. Math. Anal. Appl.*, **64** (1978), 96-105.
- [63] Chapman S.J., Fitt A.D., Please C.P.: Extrusion of power-law shear-thinning fluids with small exponent, *International Journal of Non-Linear Mechanics*, **32** (1997), 187-199.
- [64] Chen C.H.: Marangoni effects on forced convection of power-law liquids in a thin film over a stretching surface, *Physics Letters A*, **370** (2007), 51-57.
- [65] Christopher D.M., Wang B-X.: Marangoni convection around a bubble in microgravity, heat transfer, In: Proceedings of the 11th International Heat Transfer Conference, 3, Taylor and Francis, Levittown, PA, 1998, 489-494.
- [66] Christopher D.M., Wang B-X.: Prandtl number effects for Marangoni convection over a flat surface, *Int. J. Thermal Sci.*, **40** (2001), 564-570.

BIBLIOGRAPHY

---

- [67] Christopher D.M., Wang B-X.: Similarity simulation for Marangoni convection around a vapor bubble during nucleation and growth, *International Journal of Heat and Mass Transfer*, **44** (2001), 799-810.
- [68] Congedo P. M., Collura S.: Modeling and analysis of natural convection heat transfer in nanofluids, In: Proc. ASME Summer Heat Transfer Conf. 2009, **3** (2009), 569-579.
- [69] Cortell R.: Numerical solutions of the classical Blasius flat-plate problem, *Appl. Math. Comput.*, **170** (2005), 706-710.
- [70] Cossali G.E.: Power series solutions of momentum and energy boundary layer equations for a power law shear driven flow over a semi-infinite flat plate, *International Journal of Heat and Mass Transfer*, **49** (2006), 3977-3983.
- [71] Cowley S.J.: Laminar boundary-layer theory: A 20th century paradox?, In Aref H., Philips J.W.: *Mechanics for a New Millennium*, Kluwer Academic Publishers 2001, 389-412. DOI: 10.1007/0-306-46956-1-25
- [72] Crane L.J., Flow past a stretching sheet, *ZAMP*, **21** (1970), 645-647.
- [73] Crocco L.: Lo strato laminare nei gas, *Mon. Sci. Aer.*, Roma 1946.
- [74] Darby R.: *Chemical Engineering Fluid Mechanics*, Marcel Dekker Inc., New York 2001.
- [75] Das S.K., Choi S.U.S., Yu W., Pradeep T.: *Nanofluids: Science and Technology*, John Wiley, New Jersey, 2007.
- [76] Deen W M.: *Analysis of Transport Phenomena*, Oxford University Press, New York 1998.
- [77] Došlý O., Reháč P.: *Half-linear Differential Equations*, North-Holland Mathematics Studies **202**, Elsevier, Amsterdam, 2005.
- [78] Drábek P., Milota J.: *Methods of Nonlinear Analysis, Applications to Differential Equations*, Birkhäuser, Basel-Boston-Berlin, 2007.
- [79] Drummond C., Israelachvili J.: Dynamic phase transitions in confined lubricant fluids under shear, *Phys. Rev. E*, **63** (2001), 041506-1/11.
- [80] Einstein A.: A new determination of molecular dimensions, *Annals of Physics*, **19(4)** (1906), 289-306.
- [81] Einstein A.: A new determination of molecular dimensions, *Annals of Physics*, **19(34)** (1911), 591-592.
- [82] Erickson, L.E., Fan, L.T., Fox, V.G.: Heat and mass transfer on a moving continuous flat plate with suction or injection. *Ind. Eng. Chem.*, **5** (1966), 19-25.

## BIBLIOGRAPHY

- 
- [83] Falkner V.M., Skan S.W.: Some approximate solutions of the boundary layer equations, *Phil. Mag.*, **12** (1931), 865-896. ARC-Report 1314.
- [84] Fang T., Guo F., Lee C.F.: A note on the extended Blasius problem, *Appl. Math. Lett.*, **19** (2006), 613-617.
- [85] Fang T., Liang W., Lee C. F.: A new solution branch for the Blasius equation - A shrinking sheet problem, *Computers and Mathematics with Applications*, **56** (2008), 3088-3095.
- [86] Fazio R.: A similarity approach to the numerical solution of free boundary problems, *SIAM Rev.*, **40** (1998), 616-635.
- [87] Fisher, E.G.: *Extrusion of Plastics*, John Wiley, New York 1976.
- [88] Gaifullin A.M., Zubtsov A.B.: Flow past a plate with a moving surface, *Fluid Dynamics*, **44** (2009), 540-544.
- [89] Ghosh S.: *Micromechanical Analysis and Multi-Scale Modeling Using the Voronoi Cell Finite Element Method*, CRC Press/Taylor & Francis, 2011.
- [90] Ghosh S., Dimiduk D.: *Computational Methods for Microstructure-Property Relations*, Springer New York, 2011.
- [91] Goulo H.W.: Coefficient Identities for Powers of Taylor and Dirichlet Series, *American Mathematical Monthly*, LXXXI (1974), 3-14.
- [92] Granick S, Hu H W, Carson, A.: Nanorheology of confined polymer melts. 2. Nonlinear shear response at strongly adsorbing surfaces”, *Langmuir*, **10** (1994), 3867-3873.
- [93] Guedda M.: Nonuniqueness of solutions to differential equations for a boundary-layer approximations in porous media, *C. R. Mecanique*, **300** (2002), 279-283.
- [94] Guedda M.: A note on boundary-layer similarity flows driven by a power-law shear over a plane surface, *Fluid Dyn. Res.*, **39** (2007), DOI: 10.1016/j.fluidyn.2006.11.005
- [95] Guedda M.: Boundary-layer equations for a power-law shear driven flow over a plane surface of non-Newtonian fluids, *Acta Mechanica*, **202** (2009), DOI 10.1007/s00707-008-0106-7
- [96] Gupta P.S., Gupta A.S.: Heat and mass transfer on a stretching sheet with suction or blowing, *Can. J. Chem. Eng.*, **55** (1977) 744-746.
- [97] Hamad M.A.A., Uddin M.J.: Investigation of combined heat and mass transfer by Lie group analysis with variable diffusivity taking into account hydrodynamic slip and thermal convective boundary condition, *International Journal of Heat and Mass Transfer*, (2011), doi:10.1016/j.ijheatmasstransfer.2011.08.043

## BIBLIOGRAPHY

- 
- [98] Hamid R. A., Arifin N. M., Nazar R., Ali F.M., Pop I.: Dual solutions on thermosolutal Marangoni forced convection boundary layer with suction and injection, *Mathematical Problems in Engineering*, (2011), doi:10.1155/2011/875754.
- [99] Hansen A.G.: *Similarity Analysis of Boundary Value Problems in Engineering*, Academic Press, New York 1965.
- [100] Hayat T., Iqbal Z., Mustafa M.: Boundary layer flow of an Oldroyd-B fluid with convective boundary conditions, *Heat Transfer-Asian Research*, **40** (2011), 744-755.
- [101] Hayat T., Asad S., Qasim M.: Boundary layer flow of a Jeffrey fluid with convective boundary conditions, *International Journal for Numerical Methods in Fluids*, (2011), DOI: 10.1002/flid.2642
- [102] He J.H.: Approximate analytical solution of Blasius equation. *Comm. Non-linear Sci. Num. Simul.*, **3** (1998), 260-263.
- [103] He J.H.: A simple perturbation approach to Blasius equation, *Appl. Math. Comput.*, **140** (2003), 217-222.
- [104] Henrici P.: *Applied and computational complex analysis, Power series-integration-conformal mappings-location of zeros*, John Wiley, New York-London-Sydney-Toronto 1974.
- [105] Hille E.: *Ordinary Differential Equations in the Complex Domain*, John Wiley, New York 1976.
- [106] Hirano F., Sakai T.: Effect of temperature gradient on spreading behavior of mineral oils and related tribological phenomena, In: T. Sakurai: Proceedings of the JSLE-ASLE International Lubrication Conference, Tokyo Japan, June 9-11, 1975. Elsevier, Amsterdam-Oxford-New York, 631-638.
- [107] Ho C.J., Chen M.W., Li Z.W.: Numerical simulation of natural convection of nanofluid in a square enclosure: Effects due to uncertainties of viscosity and thermal conductivity, *Int. J. Heat Mass Transfer*, **51** (2008), 4506-4516.
- [108] Hori Y.: *Hydrodynamic Lubrication*, Springer-Verlag, Tokyo, 2006.
- [109] Howarth L.: On the solution of the laminar boundary layer equations, *Proc. R. Soc. Lond. A*, **164** (1938), 547-579.
- [110] Hussaini M.Y., Lakin W.D.: Existence and nonuniqueness of similarity solutions of a boundary-layer problem, *Quart. J. Mech. Appl. Math.*, **39** (1986), 177-191.

BIBLIOGRAPHY

---

- [111] Hussaini M.Y., Lakin W.D., Nachman, A.: On similarity solutions of a boundary layer problem with an upstream moving wall, *SIAM J. Appl. Math.*, **47** (1987), 699-709.
- [112] Ince E.L.: *Ordinary Differential Equations*, Dover Publ., New York 1956.
- [113] Ingham D.B., Brown S.N.: Flow past a suddenly heated vertical plate in a porous medium, *Proc. R. Soc. Lond. A*, **403** (1986), 51-80.
- [114] Ishak A., Bachok N.: Power-law fluid flow on a moving wall, *European J. Scie. Res.*, **34** (2009), 55-60.
- [115] Ishak A.: Similarity solution for flow and heat transfer over a permeable surface with convective boundary condition, *Appl. Math. Comput.*, **217** (2010), 837-842.
- [116] Jabbarzadeh A., Tanner R.I.: Molecular dynamics simulation and its application to nano-rheology, *Rheology Reviews*, 2006, 165 - 216.
- [117] Jaluria Y.: Fluid flow phenomena in materials processing - The 2000 Freeman Scholar Lecture, *Journal of Fluids Engineering*, **123** (2001), 173-210.
- [118] Jiao D., Sharma M.M.: Investigation of dynamic mud cake formation: the concept of minimum overbalance pressure, SPE 26323, Proceedings of the SPE 68th Annual Technical Conference & Exhibition, Houston, TX, October 3-6, 1993.
- [119] Von Kármán T.: Über laminare and turbulente Reibung, *ZAMM*, **1** (1921), 244-247.
- [120] Kechil S.A., Hashim I.: Series solutions of boundary-layer flows in porous media with lateral mass flux, *Heat Mass Transfer*, **44** (2008), 1179-1186.
- [121] Kim H.W., Jeng D.R., DeWitt K.J.: Momentum and heat transfer in power law fluid flow over two dimensional or axisymmetrical bodies, *Internat. J. Heat Mass Transfer*, **26** (1983), 245-259.
- [122] Kistler S.F., Schweizer P.M.: *Liquid Film Coating*, London, Chapman & Hall, 1997.
- [123] Klemp, J.B., Acrivos, A.A.: A method for integrating the boundary-layer equations through a region of reverse flow, *J. Fluid Mech.*, **53** (1972), 177-199.
- [124] Klemp, J.B., Acrivos, A.A.: A moving-wall boundary layer with reverse flow, *J. Fluid Mech.*, **76** (1976), 363-381.

BIBLIOGRAPHY

---

- [125] Klien S., Surberg C.H., Stehr W.: Temperature driven lubricant migration on tribological surfaces, Proc. ECOTRIB 2007 12-15.6.07, Ljubjana, Slovenia, 637-647.
- [126] Kou, S.: *Transport Phenomena and Materials Processing*, John Wiley, New York 1996.
- [127] Kumaran V., Ramanaiah G.: A note on the flow over a stretching sheet, *Acta Mech.*, **116** (1996), 229-233.
- [128] Liao S.J.: An explicit, totally analytic, solution for Blasius viscous flow problems, *Int. J. Non-Linear Mech.*, **34** (1999), 758-778.
- [129] Liao S.J.: A challenging nonlinear problem for numerical techniques, *J. Comput. Appl. Math.*, **181** (2005), 467-472.
- [130] Liao S.J.: A new branch of solutions of boundary-layer flows over a permeable stretching plate, *International Journal of Non-Linear Mechanics*, **42** (2007), 819-830.
- [131] Liao S.J., Pop I.: Explicit analytic solution for similarity boundary layer equations, *International Journal of Heat and Mass Transfer*, **47** (2004), 75-85.
- [132] Ludviksson Y., Lightfoot E.N.: The dynamics of thin films in the presence of surface tension gradients, *AIChE J.*, **17** (1966), 1166-1173.
- [133] Luengo G., Israelachvili J., Granick, S.: Generalized effects in confined fluids: New friction map for boundary lubrication, *Wear*, **200** (1996), 328-335.
- [134] Luengo G., Schmitt F., Hill R., Israelachvili J.: Thin Film Rheology and Tribology of Confined Polymer Melts: Contrasts with Bulk Properties, *Macromolecules*, **30** (1997), 2482-2494.
- [135] Magyari, E., Keller, B.: Heat and mass transfer in the boundary layers on an exponentially stretching continuous surface, *J. Phys. D; Appl. Phys.*, **32** (1999), 577-585.
- [136] Magyari E., Keller B.: Exact analytic solutions for free convection boundary layers on a heated vertical plate with lateral mass flux embedded in a saturated porous medium, *Heat Mass Transfer*, **36** (2000), 109-116.
- [137] Magyari E., Keller B.: Exact solutions for self-similar boundary layer flows induced by permeable stretching walls, *Eur. J. Mech. B Fluids*, **19** (2000), 109-122.
- [138] Magyari E., Keller B., Pop I.: The 'missing' self-similar free convection boundary layer flow over a vertical permeable surface in a porous medium, *Transp. Porous Media*, **46** (2002), 91-102.

## BIBLIOGRAPHY

- 
- [139] Magyari E., Keller B., Pop I.: Boundary-layer similarity flows driven by a power-law shear over a permeable plane surface, *Acta Mechanica*, **163** (2003), DOI 10.1007/s00707-003-0001-1
- [140] Magyari E., Chamkha A. J.: Exact analytical solutions for thermosolutal Marangoni convection in the presence of heat and mass generation or consumption, *Heat Mass Transfer*, **43** (2007), 965-974.
- [141] Magyari E.: The moving plate thermometer, *Int. J. Therm. Sci.*, **47** (2008), 1436-1441.
- [142] Magyari E.: Falkner-Skan flows past moving boundaries: an exactly solvable case, *Acta Mechanica*, **203** (2009), 13-21.
- [143] Magyari E.: Comment on “A similarity solution for laminar thermal boundary layer over a flat plate with a convective surface boundary condition” by A. Aziz, , *Comm. Nonlinear Sci. Numer. Simul.* 2009; 14:1064-8, *Comm. Nonlinear Sci. Numer. Simulat.*, **16** (2011), 599-601.
- [144] Makinde O.D.: Boundary layer flow of a nanofluid past a stretching sheet with a convective boundary condition, *International Journal of Thermal Sciences*, **50** (2011), 1326-1332.
- [145] Mang T., Dresel W.: *Lubricants and Lubrications*, Wiley-VCH, Weinheim, 2001.
- [146] Matar O.K., Troian S.M.: Dynamics and stability of surfactant coated thin spreading films, In: J.M. Drake, J. Klafter, R. Kopelman: *Mat. Res. Soc. Symp. Proc. Vol. 464*, 1997, 237-242. DOI: <http://dx.doi.org/10.1557/PROC-464-237>
- [147] Maxwell J. C.: On the dynamical theory of gases, *Philosophical Transactions of the Royal Society of London*, **157** (1867), 49.
- [148] Maxwell J. C.: *A treatise on electricity and magnetism*, (3rd ed.) Oxford: Clarendon Press, 1873.
- [149] McKelvey J.M.: *Polymer Processing*, John Wiley, New York, 1962.
- [150] Mehmood A., Ali A.: An application of He’s homotopy perturbation method in fluid mechanics, *Internat. J. Nonlinear Sciences and Numerical Simulation*, **10** (2009), 239-246.
- [151] Meksyn D.: *New Methods in Laminar Boundary-Layer Theory*, Pergamon London, New York, 1961.
- [152] Merkin J.H.: On dual solutions occurring in mixed convection in a porous medium, *J. Engineering Math.* **20** (1985), 171-179.

## BIBLIOGRAPHY

- 
- [153] Midlemann S.: *The Flow of High Polymers*, Interscience, New York 1968.
- [154] Na T. Y.: The non-newtonian squeeze film, *ASME J. Basic Eng.*, **88** (1966), 687-688.
- [155] Nachman A., Callegari A.J.: A nonlinear singular boundary value problem in the theory of pseudoplastic fluids, *SIAM J. Appl. Math.*, **38** (1980), 275-281.
- [156] Napolitano L.G.: Marangoni boundary layers. In: Proc. 3rd European Symposium on Material Science in Space, Grenoble, ESA SP-142.
- [157] Napolitano L.G., Golia C.: Coupled Marangoni boundary layers, *Acta Astronautica*, **8** (1981), 417-434.
- [158] Navier J-C.M.: Mémoire sur les lois du mouvement des fluides, *Mém. de l'Acad. d. Sci.* , **6** (1827), 389-416.
- [159] Nessil A., Larbi S., Belhaneche H., Malki M.: Journal bearings lubrication aspect analysis using non-Newtonian fluids, *Advances in Tribology*, **2013** (2013), Article ID 212568, 9 pages <http://dx.doi.org/10.1155/2013/212568>
- [160] O'Brien S.B.G, Schwartz L.W.: Theory and modeling of thin film flows, *Encyclopedia of Surface and Colloid Science*, Marcell Dekker, 2002, 5283-5297.
- [161] Ochoa M.V.: Analysis of drilling fluid rheology and tool joint effect to reduce errors in hydraulics calculations, Thesis, Texas A & M University, 2006.
- [162] Olanrewaju P.O., Gbadeyan J.A., Hayat T., Hendi A.A.: Effects of internal heat generation, thermal radiation and buoyancy force on a boundary layer over a vertical plate with a convective surface boundary condition, *South African Journal of Science*, **107** (2011), Art. #476, 6 pages. doi:10.4102/sajs.v107i9/10.476
- [163] Ostrowski A.: Sur le rayon de convergence de la série de Blasius, *C.R. Acad. Sci. Paris*, **227** (1948), 580-582.
- [164] Paullet J.E.: An uncountable number of solutions for BVP governing Marangoni convection, *Math. Comput. Modelling*, **52** (2010), 1708-1715.
- [165] Pohlhausen E.: Der Wärmeaustausch zwischen festen Körpern und Flüssigkeiten mit kleiner Reibung und kleiner Wärmeleitung, *ZAMM*, **1** (1921), 115-121.
- [166] Peker H. A., Karaoğlu O., Oturanc G.: The differential transformation method and Pade approximant for a form of Blasius equation, *Mathematical and Computational Applications*, **16** (2011), 507-513.

BIBLIOGRAPHY

---

- [167] Potherat A., Sommeria J., Moreau R.: Numerical simulations of an effective two-dimensional model for flows with a transverse magnetic field, *Journal of Fluid Mechanics*, **534** (2005), 115-143.
- [168] Prandtl L.: Über Flüssigkeitsbewegung bei sehr kleiner Reibung. Verh. III. Intern. Math. Kongr., Heidelberg, 1904, S. 484-491, Teubner, Leipzig, 1905.
- [169] Rahman M.M.: Locally similar solutions for hydromagnetic and thermal slip flow boundary layers over a flat plate with variable fluid properties and convective surface boundary condition, *Meccanica*, **46** (2011), 1127-1143, DOI: 10.1007/s11012-010-9372-2
- [170] Rayleigh J. W.: On the influence of obstacles arranged in rectangular order upon properties of a medium, *Philosophical Magazine*, **32** (1892), 481-491.
- [171] Rogers D.F.: *Laminar Flow Analysis*, Cambridge University Press 1992.
- [172] Ruschak K.J.: Coating flows, *Annu. Rev. Fluid Mech.*, **17** (1985), 65-89.
- [173] Safar Z. S.: Journal bearing operating with non-newtonian lubricant films, *Wear*, **53** (1979), 95-100.
- [174] Samuel T.D.M.A., Hall I. M.: On the series solution to the laminar boundary layer with stationary origin on continuous moving porous surface, *Math. Proc. Camb. Phil. Soc.*, **73** (1973), 223-229.
- [175] Sakiadis B.C.: Boundary layer behavior on continuous solid surfaces: I. Boundary layer equations for two-dimensional and axisymmetric flow, *AIChE J.*, **7** (1961), 26-28.
- [176] Sakiadis B.C.: Boundary layer behavior on continuous solid surfaces. II: The boundary layer on a continuous flat surface, *AIChE J.*, **7** (1961), 221-225.
- [177] Schlichting H., Gersten K.: *Boundary Layer Theory*, 8th revised and enlarged ed., Springer-Verlag, Berlin, Heidelberg 2000.
- [178] Schowalter W.R.: *Mechanics of Non-Newtonian fluids*, Pergamon Press, Oxford 1978.
- [179] Schowalter W.R.: The application of boundary layer theory to power-law pseudoplastic fluids: Similar solutions, *AIChE J.*, **6** (1960), 24-28.
- [180] Sedov L.I.: *Similarity and Dimensional Methods in Mechanics*, CRC Press, Boca Raton 1993.
- [181] Shukla J. B.: Theory for the squeeze film for power law lubricants, *ASME Paper* 64-Lub-4, 1964.

## BIBLIOGRAPHY

- 
- [182] Shukla J. B.: Load capacity and time relation for squeeze films in conical bearings, *Wear*, **7** (1964), 368-371.
- [183] Shukla J. B., Prakash J.: The rheostatic thrust bearing using power law fluids as lubricants, *Jpn. J. Appl. Phys.*, **8** (1969), 1557-1562.
- [184] Shukla J. B., Isa M.: Characteristics of non-newtonian power law lubricants in step bearings and hydrostatic step seals, *Wear*, **30** (1) (1974), 51-71.
- [185] Sinha P., Singh C.: Lubrication of a cylinder on a plane with non-newtonian fluid considering cavitation, *J. Lubr. Technol.*, **104** (1982), 168-172.
- [186] Sinha P., Singh C., Prasad K. R.: Effects of viscosity variation due to lubricant additives in journal bearings, *Wear*, **66** (1981), 175-188.
- [187] Sinha P., Shukla J. B., Prasad K. R., Singh C.: Nonnewtonian power law fluid lubrication of lightly loaded cylinders with normal and rolling motion, *Wear*, **89** (1983), 313-322.
- [188] Sivakumar P., Bharti R.P., R.P. Chhabra, R.P.: Effect of power-law index on critical parameters for power-law flow across an unconfined circular cylinder, *Chemical Engineering Science*, **61** (2006), 6035-6046.
- [189] Sivakumar P., Bharti R.P., Chhabra R.P.: Steady flow of power-law fluids across an unconfined elliptical cylinder, *Chemical Engineering Science*, **62** (2007), 1682-1702.
- [190] Slavtchev S., Miladinova S.: Thermocapillary flow in a liquid layer at minimum in surface tension, *Acta Mechanica*, **127** (1998), 209-224.
- [191] Steinheuer J.: Die Lösungen der Blasiuschen Grenzschichtdifferentialgleichung, *Abhandlg. der Braunschweigischen Wiss. Ges.*, **20** (1968), 96-125.
- [192] Stokes G.G.: On the theories of the internal friction of fluids on the motion, and of the equilibrium and motion of elastic solids, *Trans. Cambr. Phil. Soc.*, **8** (1849), 287-319.
- [193] Subhashini S.V., Samuel N.: Double-diffusive convection from a permeable vertical surface under convective boundary condition, *International Communications in Heat and Mass Transfer*, **38** (2011), 1183-1188.
- [194] Subhashini S.V., Samuel N.: Effects of buoyancy assisting and opposing flows on mixed convection boundary layer flow over a permeable vertical surface, *International Communications in Heat and Mass Transfer*, **38** (2011), 499-503.
- [195] Tadmor Z., Gogos C.: *Principles of Polymer Processing*, Wiley, New York 1979.

## BIBLIOGRAPHY

- 
- [196] Tadmor Z., Klein I.: *Engineering Principles of Plasticating Extrusion*, Polymer Science and Engineering Series. Van Norstrand Reinhold, New York 1970.
- [197] Tajvidi T., Razzaghi M., Dehghan M.: Modified rational Legendre approach to laminar viscous flow over a semi-infinite flat plate, *Chaos Solitons Fractals*, **35** (2008), 59-66.
- [198] Tanner R. I.: Non-newtonian lubrication theory and its application to the short journal bearing, *Aust. J. Appl. Sci.*, **14** (1963), 29-36.
- [199] Thompson E.R., Snyder W.T.: Drag reduction of a non-Newtonian fluid by fluid injection at the wall, *J. Hydronautics*, **2**(1968), 177-180.
- [200] Thompson P.A. Robbins M.O.: Shear flow near solids: Epitaxial order and flow boundary conditions, *Phys. Rev. A*, **41** (1990), 6830-6837.
- [201] Toor H.L.: The energy equation for viscous flow, *Industrial and Engineering Chemistry*, **48** (1956), 922-926.
- [202] Toor H.L.: Heat transfer in forced convection with internal heat generation, *AIChE J.*, **4** (1958), 319-323.
- [203] Töpfer K.: Bemerkung zu dem Aufsatz von H. Blasius: Grenzschichten in Flüssigkeiten mit kleiner Reibung. *Z. Math. Phys.*, **60** (1912), 397-398.
- [204] Tower B.: First report on friction experiments, *Proc. Inst. Mech. Engrs.*, (a) 1883, 632-659.
- [205] Tsou F., Sparrow E.M., Goldstein R.: Flow and heat transfer in the boundary layer on a continuous moving surface, *Int. J. Heat Mass Transfer*, **10** (1967), 219-235.
- [206] Wang L.: A new algorithm for solving classical Blasius equation, *Appl. Math. Comput.*, **157** (2004), 1-9.
- [207] Weidman P.D., Kubitschek D.G., Brown S.N.: Boundary layer similarity flow driven by power law shear, *Acta Mechanica*, **120** (1997), 199-215.
- [208] Weidman P.D., Magyari E.: Generalized Crane flow induced by continuous surfaces stretching with arbitrary velocities, *Acta Mechanica*, **209** (2010), 353-362. DOI: 10.1007/s00707-009-0186-z
- [209] Weinstein S.J., Ruschak K.J.: Coating flows, *Annu. Rev. Fluid. Mech.*, **36** (2004), 29-53. doi: 10.1146/annurev.fluid.36.050802.122049
- [210] White F.M.: *Viscous Fluid Flow*, McGraw-Hill, New York 1974.
- [211] Williams P. D., Symmons G. R.: Analysis of hydrodynamic journal bearings lubricated with non-Newtonian fluids, *Tribology International*, **20** (1987), 119-124.

BIBLIOGRAPHY

---

- [212] Weyl H.: On the differential equations of the simplest boundary-layer problems, *Ann. of Math.*, **43** (1942), 381-407.
- [213] Wilkinson W.L.: *Non-Newtonian Fluids*, Pergamon Press, New York-London-Oxford-Paris 1960.
- [214] Wong W., Tian T., Smedley G., Moughon L., Takata R., Jocsak J.: Low-engine-friction technology for advanced natural-gas reciprocating engines, Technical Report, MIT 2007.
- [215] Wu Z., Zhao J., Yin J., Li H.: *Nonlinear Diffusion Equations*, World Scientific 2001.
- [216] Wu B., Chen S.: Simulation of non-Newtonian fluid flow in anaerobic digesters, *Biotechnology and Bioengineering*, **99** (2008), 700-711.
- [217] Yacob N.A., Ishak A.: Stagnation point flow towards a stretching/shrinking sheet in a micropolar fluid with a convective surface boundary condition, *The Canadian Journal of Chemical Engineering*, (2011) DOI: 10.1002/cjce.20517
- [218] Yacob N.A., Ishak A., Pop I.: Boundary layer flow past a stretching/shrinking surface beneath an external uniform shear flow with a convective surface boundary condition in a nanofluid, *Nanoscale Research Letters*, **6** (2011), pp. 314, DOI: 10.1186/1556-276X-6-314
- [219] Yang S.P., Xia Z.W., Lu Y.J.: Theoretical and experimental investigation on a semi-active magneto-rheological isolation system, *International Journal of Nonlinear Sciences and Numerical Simulation*, **9** (2008), 167-174.
- [220] Yildirm A.: Exact solutions of nonlinear differential-difference equations by He's homotopy perturbation method, *International Journal of Nonlinear Sciences and Numerical Simulation*, **9** (2008), 111-114.
- [221] Zhang Y., Zheng L., Wang X., Song G.: Analysis of Marangoni convection of non-Newtonian power law fluids with linear temperature distribution, *Thermal Science*, **15** (2011), S45-S52.
- [222] Zheng L.C., Chen X.H., Zhang X.X., He J.C.: An approximately analytical solution for the Marangoni convection in an In-Ga-Sb system, *Chin. Phys. Lett.*, **21** (2004), 1983-1985.
- [223] Zheng L., Zhang X., Gao Y.: Analytical solution for Marangoni convection over a liquid-vapor surface due to an imposed temperature gradient, *Math. Comput. Modelling*, **48** (2008), 1787-1795.
- [224] Zheng L., Zhang X., He J.: Existence and estimate of positive solutions to a nonlinear singular boundary value problem in the theory of dilatant non-Newtonian fluids, *Mathematical and Computer Modelling*, **45** (2007), 387-393.

BIBLIOGRAPHY

---

- [225] Zheng L., Zhang X., He J.: Suitable heat transfer model for self-similar laminar boundary layer in power law fluids, *J. Thermal Science*, **13** (2004), 150-154.
- [226] Zohdi T.I.: On the reduction of heat generation in lubricants using microscale additives, *International Journal of Engineering Science*, **62** (2013), 84-89.